University of Natural Resources
and Life Sciences, Vienna

Master Thesis

Recombinant expression of B-Cell CD19 fusion proteins in Chinese hamster ovary cells

submitted by

Brunner Dominik, BSc

Vienna, May 2018

Supervisor: Univ. Prof. Dipl.Ing. Dr. Renate Kunert

Co-Supervisor: Dipl. Ing. Patrick Mayrhofer, PhD

Department of Biotechnology

University of Natural Resources and Life Sciences, Vienna

1. Acknowledgements

First of all, I would like to thank Prof. Renate Kunert for giving me the opportunity to conduct my master thesis in her research group at the Department of Biotechnology as well as for her supervision and knowledge input into my thesis.

I would also like to thank Patrick Mayrhofer for his excellent guidance, help and contribution surrounding this project and my work in the lab.

Furthermore, I would like to thank Willibald Steinfellner and Anna Wachernig for their assistance and help in the lab as well as their contribution to this thesis.

Additionally, I would like to thank Prof. Johannes Huppa for the opportunity to conduct experiments at his lab at the Medical University of Vienna as well as Venugopal Gudipati for his assistance during the experiments.

I also thank Julia Hennicke, Linda Schwaigerlehner, Philipp Mundsperger, Lukas Damjanovic, David Reinhart and Florian Wiederstein for their help and for the exceptional work environment.

Last but not least, I would like to thank my parents and friends for their everlasting support during my work on this thesis and during the times of my study.

2. Abstract

The aim of this thesis was to recombinantly express fusion proteins of the extracellular portion of CD19 in Chinese hamster ovary cells (CHO). CD19 is a transmembrane protein found on B lymphocytes and is a promising target of CAR-T cell therapy for Non-Hodgkin-Lymphomas. For the expression in CHO-K1 cells, cloning steps were performed to prepare the plasmid expression vectors for the stable transfection using PEI. Cells were cultivated in a batch culture in 50 ml cultivation tube, selection was induced via G418/neoR and quantification of CD19 constructs was performed via sandwich ELISA. Additional flow cytometric analyses were conducted for intracellular product content and cell population homogeneity. Titers between 50-100 ng/ml for CD19-Fc, 100-200 ng/ml for CD19-HSAD2 and 200-500 ng/ml for CD19/CD21mutFc could be obtained. For the CD19-HSAD2 construct, the ELISA was successfully optimized. No CD19 was found in the final producing clones of CD19/CD21mutFc, indicating that the corresponding titers are derived from CD21mutFc only. Additionally, pseudoperfusion cultivations were performed with CHOK1/CD19-Fc, showing an advantage in terms of amount of product produced compared to the routine cultures. Moreover, CD19-Fc was successfully purified via protein A affinity chromatography and IMAC and one of the purified CD19-Fc samples was found to be binding to anti-CD19 CAR-T-Cells in a cell based flow cytometric assay. Further analyses via SDS-Page and Western Blot revealed that some proteolytic activity between the Fc-domain and the CD19 might be occurring and that CD19-Fc and CD19-HSAD2 both tend to aggregate to some extent.

2. Zusammenfassung

Ziel dieser Arbeit war es, Fusionsproteine des extrazellulären Teils von CD19 in Chinese Hamster Ovary Zellen (CHO) rekombinant zu exprimieren. CD19 ist ein Transmembranprotein, das auf B-Lymphozyten vorgefunden wird und ist dadurch ein vielversprechendes Ziel der CAR-T-Zelltherapie für Non-Hodgkin-Lymphome. Für die Expression in CHO-K1-Zellen wurden Klonierungsschritte durchgeführt, um die Plasmid-Expressionsvektoren für die stabile Transfektion unter Verwendung von PEI herzustellen. Die Zellen wurden in einer Batch-Kultur in einem 50 ml-Kultivierungsröhrchen kultiviert, die Selektion wurde über G418/neoR induziert und die Quantifizierung von CD19-Konstrukten wurde mittels ELISA durchgeführt. Zusätzliche durchflusszytometrische Analysen wurden für den intrazellulären Produktgehalt und die Zellpopulationshomogenität durchgeführt. Titer zwischen 50-100 ng/ml für CD19-Fc, 100-200 ng/ml für CD19-HSAD2 und 200-500 ng/ml für CD19/CD21mutFc konnten erzielt werden. Kein CD19 wurde in den final produzierenden Klonen von CD19/CD21mutFc gefunden, was bedeuten könnte, dass der entsprechende Titer nur auf CD21mutFc zurückzuführen ist. Zusätzlich wurden Pseudoperfusionskultivierungen mit CHO-K1/CD19-Fc durchgeführt, wodurch eine Verbesserung in Bezug auf die produzierte Produktmenge im Vergleich zu den Routinekulturen erreicht wurde. Darüber hinaus wurde CD19-Fc erfolgreich über Protein-A-Affinitätschromatographie und IMAC gereinigt. Ein Teil des aufgereinigten CD19-Fc konnte an anti-CD19 CAR-T-Zellen in einem zellbasierten Durchflusszytometrie-Assay binden. Weitere Analysen mittels SDS-Page und Western Blot zeigten, dass eine gewisse proteolytische Aktivität zwischen der Fc-Domäne und dem CD19 auftreten könnte und dass CD19-Fc und CD19-HSAD2 dazu neigen, zu einem gewissen Grad zu aggregieren.

3. Table of contents

4. Abbreviations

Abbreviations

µ	specific growth rate [d-1]
amp	ampicillin
ampR	ampicillin resistance gene
BAC	bacterial artificial chromosome
BCIP	5-bromo-4-chloro-3-indolyl-phosphate
BIS-TRIS	2-[Bis(2-hydroxyethyl)amino]-2-(hydroxymethyl)propane-1,3-diol
bp	base pairs
BSA	bovine serum albumin
BT	biotin
BX	bromphenolblue - Xylencyanol
CAR	chimeric antigen receptor
CB	CellBoost
CD	chemically defined
CHO	Chinese hamster ovary
DMSO	dimethyl sulfoxide
dNTP	deoxynucleoside triphosphates
DTT	Dithiothreitol
E. coli	*Escherichia coli*
ECL	enhanced chemiluminescence
EDTA	Ethylenediaminetetraacetic acid
ELISA	enzyme linked immunosorbent assay
EtBr	Ethidium bromide
EtOH	Ethanol
FACS	fluorescence activated cell sorting
Fc	fragment crystallisable
FITC	Fluorescein isothiocyanate
FS	forward scatter
G418	geneticin
GFP	green fluorescent protein
HRP	horse-radish peroxidase
HSA	human serum albumin
IMAC	ionized metal affinity chromatography
LB	Luria-Bertani
LDS	lithium dodecyl sulphate
L-gln	L-glutamine
MTG	Monothioglycerol
NBT	nitro blue tetrazolium
neoR	neomycin resistance gene
NHL	non-Hodgkin lymphoma
ori	origin of replication
PAGE	polyamine gel electrophoresis
PBS	phosphate buffered saline
PBST	phosphate buffered saline + Tween
PCR	polymerase chain reaction
PE	phycoerythrin

PEI	polyethyleneimine
PVP	polyvinylpyrrolidone
qP	specific productivity [pg/cell/day]
RO	reverse osmosis
RT	room temperature
SA	strept-avidin
scFv	single-chain variable fragment
SDS	sodium dodecyl sulphate
SOC	super optimal catabolite
SS	side scatter
TAE	Tris Acetate-EDTA
TFF	tangential flow filtration
TMB	3,3',5,5'-Tetramethylbenzidine
trafe	transfection
TRIS	Tris(hydroxymethyl)-aminomethane
UV	ultra violet

Units

°C	degree Celsius
µF	microfarad
µg	microgram
µL	microliter
d	days
g	gram
h	hours
kDA	kilo Dalton [1000*g/mol]
L	litre
M	[mol/L]
mA	milliampere
mAU	milli absorption units
mg	milligram
min	minute(s)
mio	million
ml	millilitre
ng	nanogram
nm	nanometre
pg	picogram
rpm	revolutions per minute
V	volt
W	Watt
Ω	ohm

5. Introduction

Basic functions of CD19:

CD19 is a 95 kDa co-stimulatory transmembrane receptor protein [3] which is used by B lymphocytes to modulate receptor signalling as a response to foreign antigens. It has a well-documented enhancing effect when it comes to signalling through the B-cell receptor (BCR), which is caused by a rapid phosphorylation of CD19 after BCR ligation that ultimately results in the recruitment of secondary effector molecules such as phosphoinositide 3-kinase (PI3K) and phospholipase C. These effector molecules are important for BCR-induced intracellular calcium flux and activation of mitogen-activated protein kinases (MAP kinases). Moreover, the co-ligation of CD19 and BCR results in an enhanced activation of three forms of MAP kinases. These enhancing effects are necessary since the B-cell receptors are low affinity receptors and therefore require additional signalling amplification upon antigen binding. However, there are not only positive functions of CD19 which causes an amplification of BCR signalling, but also some negative effects which are caused by cross-linking of CD19, which leads to a decrease of calcium release and/or proliferation following BCR ligation. The overexpression of human CD19 in transgenic mice even leads to a hindered development of immature B-cells in the bone marrow and a strongly decreased number of mature B cells in the periphery [1,2].
In terms of structure, the extracellular domain of CD19 exhibits an elongated β-sandwich formed by two immunoglobulin folds by swapping their C-terminal halves. This structural element was observed via crystal structure analysis and is different from the tandem of c-type immunoglobulin folds predicted from the amino acid sequence [3].

CD19 and the CAR-T cell therapy:

Non-Hodgkin lymphoma (NHL) is the most common hematologic malignancy with more than 385,000 cases per year worldwide and in recent years a new type of immunotherapeutic treatment emerged: the use of the CAR-T cell therapy. This new approach redirects T-cells against the tumour associated antigens (TAA) by transduction of T-cells with a chimeric antigen receptor (CAR) which is specific to antigen – in this case the CD19 receptor protein [4,5].
A CAR typically consists of three main components, namely the extracellular domain (containing a scFv and a hinge region) which binds to the TAA, a transmembrane domain and an intracellular domain. The intracellular domain is responsible intracellular signalling and is activated upon antigen binding to the extracellular domain. Depending on the number of intracellular domains there are three different types of CARs: the first generation has only one activating domain (CD3ζ), the second generation has two activating domains (CD3ζ plus either CD28 or 4-1BB) and the third generation with all three intracellular domains [4].
The most common (30%) NHL is the diffuse large B cell lymphoma (DLBCL) and patients with a relapsed or refractory DLBCL have a very poor prognosis for long term survival. Therefore, a second-generation CAR-T cell therapy was used in a trial for treatment of patients with this diagnosis. The extracellular domain of the CAR was targeting the CD19 receptor protein commonly found on malignant B-Cells and the intracellular domain consisted of CD3ζ and CD28. With a median follow up after 15.4 months, 40% of patients continued to be in “complete response” with overall survival of 52% and disease-free survival of 41% after 18 months. Based on the results of this trial the FDA approved axicabtagene ciloleucel (axi-cel, Yescarta^{TM}) for treatment of adults with relapsed refractory high-grade lymphoma, DLBCL, primary mediastinal B cell lymphoma, high grade B-cell lymphoma, and DLBCL arising from follicular lymphoma. Furthermore, another antiCD19-CAR-T cell therapy using a 4-1BB activating domain was approved by the FDA for paediatric and young adult patients (up to 25 years) with relapsed refractory B cell acute lymphocytic leukaemia [4].

However, therapies with CD19 targeted CAR modified T cells have also led to toxicities with high fevers, hypotension, and elevated pro-inflammatory serum cytokines. Highest cytokine elevations have been found in patients with a high tumour burden at the time of the CAR-T cell administration, which also had the largest number of CD19 CAR-T cells [6]. Concerning the difference between the two types second generation CAR-T cells (CD3ζ plus either CD28 or 4-1BB), a study showed that CD28 CAR-T and 4-1BB CAR-T both worked for response in treatment of relapsed or refractory acute lymphoblastic leukaemia (ALL) but they differed in response pattern (peak reaction time, reaction lasting time and reaction degree), adverse events, cytokine secretion and immune-suppressive factor level. Moreover, in prior studies, CAR-T containing CD28 persisted for 1–3 months in vivo while CAR-T containing 4-1BB persisted up to 5 years. In terms of adverse effects, again a correlation of tumour burden and severity could be observed [7].

Recombinant protein production in mammalian cells:

For the recombinant production of complex proteins like CD19, CD21, antibodies and many other biological therapeutics, suitable expression systems derived from mammalian cell lines are needed to fulfil the requirements of protein quality, biosynthetic complexity and post translational modification [8,10]. In academic research, those proteins are needed for functional analysis and structure determination to find new - or improve existing – therapeutics for treating human diseases. Furthermore, more and more blockbuster drugs are recombinant mammalian proteins (e.g. monoclonal antibodies) and therefore the industry relies on mammalian expression system to produce quantities in the range of milligrams per litre of culture [8].

While there are several different mammalian cell lines such as baby hamster kidney, mouse myeloma-derived NS0, human embryonic kidney HEK293, and the human retina-derived PerC6, Chinese hamster ovary cells (CHO) are the most commonly used host cell lines for producing biological therapeutics in the industry, producing about 70% of all recombinant proteins and reaching titers of more than 10 g/L [9]. The production capabilities of CHO are the result of its high adaptability, growth to high densities in suspension, and the adaptation to serum free media. This allowed for the application of chemically defined media which had a great impact on the growth performance of CHO. Furthermore, the absence of supplements like fetal calve serum provided increased safety regarding contaminations by viruses or prions as well as an easier downstream process due to reduced amount of protein present in the cultivation medium [8]. With the transition to protein and serum free media, the use of protein hydrolysates (peptones) became a viable option for supplying an abundance of amino acids to the medium without the need of time consuming optimization of media formulations. The single addition of tryptone N1 (casein peptone TN1) to the medium 24h after transfection showed a 2-fold increase in volumetric productivity which is comparable to supplementation with 4% (v/v) of serum. Furthermore, an accumulation of glycine, histidine, threonine, leucine, and valine was observed which are usually consumed in non-TN1-fed cultures. When looking at mRNA levels, it could be seen that the increased protein production is both a result of increased translational activity and transcription efficiency [21]. Other peptones include hydrolysates originating from plants like soy, rice and gluten which were also able to increase the specific productivity by 20-30% compared to peptone free media [22].

During cultivation, preventing or delaying cell death is an important factor for successful process development. Cell death can be caused by different factors like nutrient depletion, accumulation of toxic by-products, elevated osmolarity, and shear stress [9,12]. Means for increasing viable cell numbers in culture (and in turn product formation) include the overexpression of anti-apoptotic proteins like members of the bcl-2 family or inducing cell cycle arrest by using anti-mitotic agents [8,12]. Since apoptotic signalling strongly relies on signalling via caspase-cascade systems the

suppression of caspase activation is also a promising strategy [9]. Next to cell death regulating proteins, growth factors such as acidic Fibroblast Growth Factors (aFGF) or recombinant insulin-like growth factors can also improve cell densities and yields [8].
Since the accumulation of by-products also has a negative impact on production performance and cell viabilities, metabolic engineering approaches were used to reduce lactate formation in culture by disrupting genes for crucial enzymes like the lactate-dehydrogenase [13]. Another major waste product (of glutamine) is ammonia. To reduce the accumulation of ammonia in the medium, glutamate can be used as substrate instead of glutamine. This requires cells to be able to express glutamine synthase, which enables them to catalyse glutamate with ammonia to yield glutamine [8,13].
To further optimize production processes and optimize specific productivities, serval other methods have been developed, including protocols for increasing gene copy numbers within individual cells in hopes of achieving higher expression rates. An example is the dihydrofolate reductase (DHFR) selection system in combination with methotrexate (MTX), which requires the use of DHFR deficient cell lines. In the absence of hypoxanthine, thymidine and glycine these cell lines rely on the introduction of an exogenous DHFR gene through an expression vector which also carries the gene of interest. This makes sure that in a "selection medium" containing no hypoxanthine and thymidine, only cells which have been successfully transfected with the vector are able to proliferate. Furthermore, the addition of MTX causes an inhibition of DHFR and therefore only cells with enough gene copies of DHFR (and in turn more gene copies of the gene of interest) are able to overcome the inhibition of MTX and can continue to grow [8,11]. Another possibility is the use of the glutamine synthase (GS) system, which can be used in non-GS-producing NS0 cells as well as in GS expressing CHO cells. The enzyme is then inhibited by the application of methionine sulfoximine (MSX). With increasing concentrations of MSX, clones with a high copy number of the selection gene and flanking target gene are selected [8,11].
In terms of selection pressure, attenuated selection markers are a viable option to decrease the negative effects of high drug doses. As an example, a mutated variation of the neomycin phosphotransferase II (selection marker present on the gene vector) has lower affinities for the selection drug neomycin, which can therefore be used at lower concentrations in the medium, while still maintaining its ability for applying selection pressure [11].

Another major challenge in mammalian cell culture is the screening for clones with high specific productivities. After introducing the vector carrying the gene of interest into the cell, the integration into the host genome is a random event, thus, the locus in which the gene of interest is integrated might transcriptionally be inactive. Furthermore, it is not possible to tell *a priori* how many gene copy numbers are present within one cell. Due to these factors, the clones obtained are highly heterogenous and it is necessary to screen large cell populations. This is traditionally done by limiting dilution, which aims at obtaining cell populations derived from preferably one single cell by diluting the transfection pool. Since this is a very time-consuming process and additionally requires the screening via ELISA, other methods like fluorescence activated cell sorting (FACS) based screening have been used to rapidly screen and isolate the best producing clones from a population [8,9,11,14].
In an attempt to increase the expression of genes integrated into random loci of the host genome, sodium butyrate was added to the medium, which can be capable of altering the chromatin structure and therefore enhance the accessibility of the gene to the transcription machinery. This is mainly caused by the hyperacetylation of histones, originating from the inhibition effect of sodium butyrate on the histone-deacetylase enzyme [15,16]. In a transient gene expression setting, valproic acid provides a more cost-effective alternative to sodium butyrate, which also acts as a histone-deacetylase inhibitor. Additionally, valproic acid is also approved by the FDA for treating several medical conditions, including cancer [17].

To address the problem of random gene integration into the genome and to circumvent the low integration rates of the vector into the genome in general, methods have been developed to insert the gene into specific sites and thus allowing for a reproducible, stable and efficient development of clones. The gene of interest is therefore integrated into a so called “hot-spot”, a locus in the genome which is transcriptionally highly active, which makes the fast and efficient selection of high-producing stable clones possible [9]. The recombinase-mediated cassette exchange (RMCE) provides the tool for such site-specific integration by using a gene of interest which is flanked by two heterospecific recognition target sites such as Flp recognition target sites (FRT) or *lox*P which are recognized by the recombinase enzymes Flp and Cre respectively. Furthermore, an initial generation of a host cell lines is required which carries a marker gene such as GFP flanked by two heterospecific recognition target sites, corresponding to those flanking the gene of interest on the vector. The clones producing the most GFP are the ones which probably have the expression cassette in a hot-spot of their genome and are therefore used for the exchange of GFP with the gene of interest. This is achieved by recombinases which mediate the recombination between the homologue sequences of the host cell line and the vector carrying the gene of interest, thereby integrating the target gene (and possibly a new selectable marker) into the desired locus of the genome and removing the reporter gene. Using this procedure, a fixed gene copy number is present within one cell at a specific and transcriptionally highly active locus in the genome [8,9,11,18,19].

Bacterial artificial chromosomes (BAC) can be used as an expression vector in mammalian cell culture and can provide another option for chromatin structure independent expression of target genes. BACs are very large and can accommodate inserts up to 400 kB, allowing them to carry their own chromatin environment. If the gene of interest is placed in a transcriptionally active site of the BAC, very high expression rates can be achieved. Other improvements of the BAC system compared to traditional expression vectors are the gene expression independent of the chromatin structure of the host genome, which also allows for maintained expression over longer periods of time. Furthermore, it is possible to introduce higher gene copy numbers compared to RMCE, where usually only one gene copy is present within one cell, potentially reducing maximally achievable expression levels [20].

Finally, the use of secretion tags on recombinant proteins also provides a possibility to enhance secretion levels and titers. Those tags include the Fc part of immunoglobulins, albumin and bacterial maltose-binding protein (MBP) which are fused to the target proteins, thus creating so-called fusion proteins. The use of tags also allows for secretion of protein fragments, mutant proteins, intracellular or (trans-)membrane proteins into the culture supernatant which would normally be retained in or on the cell [23]. An example is shown by the Fc and the albumin tag which were used in this thesis to express and secrete the extracellular portion of the transmembrane protein CD19 as CD19-Fc and CD19-HSAD2 respectively. Moreover, since the expression of complex mammalian proteins usually requires sophisticated protein folding, the overexpression of chaperons – proteins in the endoplasmatic reticulum – which help in the folding process, can also have a positive effect on the secretion of proteins [9].

6. Objectives

The aim of this thesis was to recombinantly express fusion proteins of the extracellular portion of CD19 in Chinese hamster ovary cells (CHO). CD19 is a transmembrane protein found on B lymphocytes and is a promising target of CAR-T cell therapy for Non-Hodgkin-Lymphomas [4,5]. Used fusion proteins comprised CD19-Fc using the Fc tag of immunoglobulins, CD19-HSAD2 using the domain 2 of human serum albumin and CD19/CD21mutFc, which is a heterodimer consisting of CD19-Fc and CD21-Fc with a mutation in the Fc part to prevent homodimer formation. The recombinantly produced CD19 constructs was then used to see whether binding to anti CD19 CAR-T cells is possible (experiment performed at the Huppa Lab, Medical University of Vienna) which may allow to potentially study the underlying binding mechanisms, which could be used for further improvements of the CAR-T cell therapy.

If enough recombinant CD19 can be obtained, it is intended to be stained fluorescently by the Huppa Lab, which could be used determine the cell surface expression of anti-CD19 CAR on T-Cells and to manufacture glass-supported lipid bilayers to perform TIRF (Total Internal Reflection Fluorescence) microscopy experiments, which could allow to study the molecular dynamics of the recombinant CD19 binding to anti-CD19 CAR T-Cells as well as the resulting signalling events within the T-cell by observing the calcium response as well as the release of cytolytic granules.

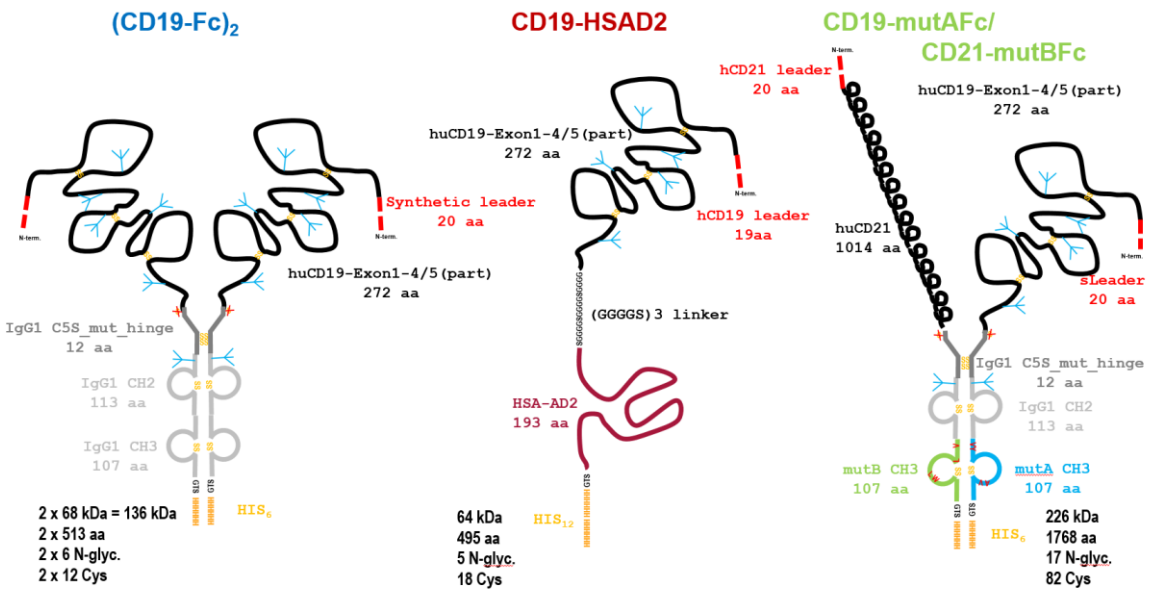

Figure 6.1.: The three different CD19 fusion proteins. ©Patrick Mayrhofer

Before the expression in CHO, cloning steps were performed to prepare the plasmid expression vectors for the stable transfection of CHO using PEI. Cells were cultivated in 50 ml cultivation tubes and passaged/monitored every 3-4 days. Additionally, pseudoperfusion cultivations were performed in order to try to obtain higher protein amounts.
Selection for the recombinant CD19 clones was performed via G418 (Geneticin) and the neomycin resistant gene present on the expression vector, whereas the quantification of CD19 in the culture supernatant was performed via qualitative (for screening after transfections or subcloning) and quantitative (for the routine cultures) sandwich ELISA, targeting either Fc or HSAD2. For the analysis of CD19-HSAD2, an optimization of the quantitative anti HSA ELISA was required.

Furthermore, subcloning by limiting dilution was used to obtain better producing clones from the initial clone pools and to further increase cell population homogeneity, which was analysed via flow cytometry by looking at the intracellular product content of the cells.

Some of the expressed CD19-Fc constructs were also purified via tangential flow filtration, protein A affinity and IMAC chromatography. Lastly, SDS-PAGEs and Western Blots were used for further product analysis of all three different fusion proteins.

7. Material and Methods

7.1 Material

7.1.1 Equipment

- Balance: Sartorius AW-4202
- Centrifuge: Thermo Scientific Heraeus Megafuge 16
- Diafiltration Membrane: Merck Pellicon™ XL Cassette, Biomax 30 kDa, Cat. No.: PXB030A50
- Electroporator
- Eppendorf® Centrifuge 5415 R
- Flow cytometer: Beckman Coulter® Gallios™
- FUSION-FX7 SPECTRA: ECL imaging device
- Gel electrophoresis chamber: BioRad
- Gel electrophoresis power supply: BioRad PowerPac™ Basic Power Supply
- Gel analyser: Gel Doc™ XR+
- IMAC column: 1 mL HiTrap Chelating HP (GE, Cat. 17040801)
- Incubator: Thermo Fisher Scientific Heracell 150i CO_2 incubator
- Laminar flow hood: Thermo Scientific MSC-Advantage
- Microplate reader: Tecan Infinite® M1000 Pro
- Microscope: Leica DMIL LED
- Millipore Labscale TFF System
- Multichannel pipettes:
    - Thermo Fisher Scientific Finpipette F2 30-300 µL
    - Integra Twelve Channel Evolve Manual Pipette. 20-200 µL, Cat. No.: 3036
- PCR cycler Bio-Rad C1000 Thermal cycler serial CC00873
- Photometer: NanoDrop™ 1000
- Pipet boy: Pipethelp Accumax, Matrix CellMate II®
- Pipettes:
    - 20 – 200 µL pipette: pipetman neo® P200N
    - 2 – 20 µL pipette: pipetman neo® P200N
    - 100 – 1000 µL pipette: Gilson pipetman neo® P1000N
    - 10 – 100 µL pipette: Gilson pipetman neo® P100N
- Plate Washer: Tecan 96 Plate Washer
- Protein A affinity chromatography column: GE Healthcare, HiTrap MabSelect SuRe 1 mL, Cat. No.: 29-0491-04
- Thermoblock: Eppendorf Thermomixer comfort
- Vortex: Scientific Industries Vortex-Genie® 2
- Äkta Start chromatography system

7.1.2 Reagents, chemicals:

- BSA (Bovine serum albumin): Sigma Aldrich® Cat. No.: A6283
- Albumin: Sigma Aldrich Cat. No. A7223 50 mg/mL
- DNA Ladder Thermo Scientific GeneRuler™ DNA Ladder Mix, Cat. No. SM033
- Ethidium bromide Sigma-Aldrich® Ethidium bromide E1510
- Nucleotides: dNTPs, KAPA Biosystems 10 mM, Cat. No. KN1009
- Glycerol: Merck, Cat. No.: 104201
- G418: Biochrom AG, Cat. No. A 2912
- Agarose: Fermentas TopVision™, Cat. No. R0499
- PEIMAX: Polyethylenimine (1 mg/ml) Polysciences, Cat No. 24765
- Tween® 20: Roth® Polyoxyethylene-20-sorbitan monolaurate Cat. No. 9127.2
- H_2SO_4: Roth® Sulphuric acide 25% Cat. No. 0967.1
- Formaldehyde 37% Sigma-Aldrich® Cat. No. 252549
- Glutaraldehyde Sigma-Aldrich® Cat. No. G5882
- ECL substrate: SuperSignal™ West Pico PLUS Chemiluminescent Substrate (Catalog number: 34580)
- BCIP (5-bromo-4-chloro-3-indolyl-phosphate) (50mg/ml) in 100% dimethylformamide
- NBT (nitro blue tetrazolium) (50mg/ml) in 70% dimethylformamide.
- Ethanol: Merck Emplura®, Cat. No.: 8.18760.2500
- TWEEN® 20: Roth®, Cat. No. 9127.2
- TMB: Invitrogen, Cat. No. SB02
- Transferrin: Merck®, Cat. No. 9701-10 20 mg/mL
- Valproic acid: Sigma Aldrich®, Cat. No.: P4543-10G
- Trypan blue: Sigma-Aldrich®: Cat. No. T8154-100
- Protein Ladder
    - Thermo Scientific PageRuler™ Pre-stained Protein Ladder, 10-180 kDa, Cat. No. 26616
    - Thermo Scientific PageRuler™ Plus Pre-stained Protein Ladder, Catalog number: 26619
- rEGF: Repligen Cat. No. 10-1021-1E 0.1 mg/mL
- Acetic acid: Sigma Aldrich®, Cat. No.: A6283
- NaCl: Roth®, Cat. No.: P029.3
- Sodium hydrogen carbonate: Merck®, Cat. No. 6329.1000
- Sodium carbonate: Roth®, Cat. No. A135.2
- TRIS: Merck®, Cat. No. A135.2
- Di-Sodium hydrogen phosphate - dihydrate: Roth®, Cat. No. 49843
- Potassium dihydrogen phosphate: Merck®, Cat. No. 104873
- Potassium chloride: Roth®, Cat. No. HN02.3
- Magnesium chloride: Merck®, Cat. No. 1.05833.1000
- Silver nitrate: Merck®, Cat. No. 101510

7.1.3 Disposables

- Microcentrifuge tubes: VWR®, Cat. No. 211-0015
- Serological pipettes: Corning® Costar® Stripette®
    - 2 mL: Cat. No.: 4486
    - 5 mL: Cat. No.: 4487
    - 10 mL: Cat. No.: 4488
    - 25 mL: Cat. No.: 4489
    - 50 mL: Cat. No.: 4490
- 10-200 µL pipette tips: Greiner Bio-One, Cat. No.: 73929
- 200-1000 µL pipette tips: Greiner Bio-One, Cat. No.: 740290
- Multichannel pipette tips: Integra Griptip tips. 300 µL, Cat. No.: 4431
- PCR tubes Quiagen 0.2 mL, Cat. No. 981005
- FACS tubes: Corning™ Falcon™ Round-Bottom, Cat. No.: 352054
- Cyro-vials: Thermo Scientific Nunc™ CryoTube, Cat. No. 375418
- Centrifuge tubes: Thermo Fisher Scientific Nunc™ 11 mL, Cat. No.: 347856
- Cell culture cultivation tubes: Corning® 50 mL Mini Bioreactor, Cat. No.: 431720
- T25 roux flask: Thermo Fisher Scientific Nunc™ Cat. No.: 163371
- 50 mL tubes: Greiner Bio-One CELLSTAR®, Cat. No.: 227261
- 96 well plates:
    - Thermo Fisher Scientific, Nunc™ MicroWell™ Cat. No.: 167008
    - Thermo Fisher Scientific, Nunc MaxiSorp™, Cat. No. 44-2404-21
- 384 well plates: Corning® 384-Well Clear Polystyrene, Cat. No.: 3701
- Cup filter: Stericup 500 mL, Millipore Express Plus, Cat. No.: SCGPU05RU
- Syringe filter: Millipore® Millex-GP, 0.22 µm, Cat. No.: SLGP033RS
- Merck® Amicon Ultra-4 and -15 Centrifugal Filter Units 10 kDa cutoff

7.1.4 Kits

- PEQLAB peqGOLD Plasmid Miniprep Kit I LOT 082214
- PEQLAB peqGOLD Gel Extraction Kit LOT 12-2500
- Macherey Nagel NucleoBond® Xtra Midi EF kit

7.1.5 Plasmids

- pCEP4_CD19HSAD2
- pL vector
- pL_CD19-HSAD2
- pL_CD19mutAFc
- pL_CD21mutBFc

7.1.6 Gels

- DNA electrophoresis agarose gels (1% w/v) in TAE buffer and 200 ng/ml EtBr
- SDS-PAGE gel: NuPAGE 4-12% Bis/Tris 1.0 mm 10-12 well gels

7.1.7 Solutions

- BX buffer: 0.25% w/v bromphenolblue, 0.25%-w/v xylencyanol, 30%-w/v glycerin
- CutSmart buffer: New England Biolabs, B7204S
- T4 ligase buffer: New England Biolabs, Cat. No. B0202S
- Phenol red solution 0.5% in PBS: Sigma® Life Science, Cat. No. P0290
- PCR buffer: Thermopol buffer (10x), New England Biolabs, Cat. No. B9004S
- TAE 50x: 0.5M Tris, Acetic acid, 50mM EDTA
- 10x PBS (5L: 57.5 g Na_2HPO_4, 10 g $KH_2PO_4 \cdot 2\ H_2O$, 10 g KCl, 400 g NaCl, filled up to 5000 ml with RO-H_2O)
- ELISA coating buffer (500 ml: 4.2 g $NaHCO_3$ 2.1 g Na_2CO_3, filled up to 500 ml with RO-H_2O, pH 9.5-9.8)
- ELISA washing buffer (1L: 100 g PBS 10x, filled up to 1000 g with RO-H_2O, 1 ml Tween 20)
- ELISA dilution buffer (100 ml: 0.1g BSA, 100 mL washing buffer)
- SDS loading buffer
- LDS loading buffer: Thermo Scientific NuPAGE® Cat. No. NP000
- MOPS Buffer (2L: 100 ml NuPAGE® MOPS SDS Running Buffer (20x) Cat. No.: NP0001 filled up to 2L with RO-H_2O)
- Tris/Acetate Buffer (2L: 100 ml NuPAGE™ Tris-Acetate SDS Running Buffer (20X) catalog number: LA0041 filled up to 2L with RO-H_2O
- Western blot transfer buffer (500 ml: 25 ml NuPAGE® Transfer Buffer (20X), 100 ml methanol, filled up to 500 ml with RO-H_2O)
- Alkaline phosphatase (AP) buffer (100 mM Tris-HCl [pH 9.0], 150 mM NaCl, 1 mM $MgCl_2$)
- Protein A affinity chromatography
    - Running buffer: 100 mM glycine, 100 mM NaCl pH 7.5
    - Elution buffer: 100 mM glycine, pH 2.5
- IMAC chromatography
    - Running buffer: 20 mM sodium phosphate, 0.4 M NaCl, 20 mM imidazole, pH 8
    - Elution buffer: 20 mM sodium phosphate, 0.5 M NaCl, 500 mM imidazole, pH 9.6
    - Charging solution: 0.1 M $NiCl_2$ in H_2O
    - Stripping solution: 20 mM sodium phosphate, pH 7.4 + 0.5 M NaCl + 5 mM EDTA
- TRIS “FACS buffer” (1L: 100 mM TRIS, 0.1% TRITON, 2 mM $MgCl_2$
- Silver staining
    - Fixation solution: 50% Ethanol / 10% Acetic Acid in RO-H_2O
    - Incubation solution: 150 ml Ethanol, 1.75g $Na_2S_2O_3$*$5H_2O$, 56.4g sodium acetate*$3H_2O$, filled up to 500 ml with H_2O, 62.5 µL glutaraldehyde / 25 ml added before use
    - Silver solution: 0.25 g $AgNO_3$ in 500 ml RO-H_2O, 5 µL formaldehyde / 25 ml added before use
    - Develop solution: 12.5 g Na_2CO_3 in 500 ml H_2O, 5 µL formaldehyde / 25 ml added before use

- Stop solution: 0.05 M EDTA in RO-H_2O

7.1.8 Antibodies

- Rabbit anti-CD19 antibody: Huppa Lab/Medical University of Vienna
- Mouse anti-CD21 antibody: Thermo Scientific MA5-11417
- Goat anti mouse IgG-HRP: Sigma Aldrich Cat. No. A8924
- Goat anti-rabbit IgG-AP: Thermo Fisher Scientific T2191
- Anti-rabbit IgG-HRP: Sigma Aldrich Cat. No. A0545
- Anti-rabbit IgG-FITC: Sigma Aldrich Cat. No. F0382
- Anti-mouse IgG-phycoerythrin: Thermo Fisher Scientific PA1-84395
- Mouse anti-HIS (HIS.H8) – biotin: Sigma Aldrich Cat. No. MA1-21315-BTIN
- Anti-human IgG gamma-chain 1 mg/mL, Sigma Aldrich Cat. No. 13382, (ELISA coating)
- Anti-human IgG gamma-chain-HRP 1 mg/mL, Sigma Aldrich Cat. No. A6029 (ELISA conj.)
- Anti-human IgG gamma-chain-FITC, Sigma Aldrich®, Cat. No.: F0132-1ML
- Goat anti-HSA antibody: 1 mg/mL Bethyl A80-129A
- Goat anti-HSA-HRP antibody: 1 mg/mL Bethyl A80-129P
- 6x-His tag antibody (1mg/mL) [invitrogen MA1-21315-BT]
- Strept-Avidin-Alexa647 (1mg/ml) [S21374]

7.1.9 Media

- CD-CHO medium: Gibco® by life technologies™, Cat. No. 10743-029
- CDM4HEK293.6E medium: HyClone™ CDM4HEK293™ Cat. No.: SH30858.02
- CDM4NS0: HyClone™ GE Healthcare Life Sciences Cat. No.: SH30579.02
- LB (Luria-Bertani) medium + ampicillin: 5 mg/mL yeast extract, 10 mg/mL peptone from casein, 10 mg/mL NaCl, 100/200 mg/L ampicillin
- SOC (Super optimal catabolite) medium: 20 mM glucose, 3 mM KCl, 10 mM $MgCl_2 \cdot 6\ H_2O$, 10 mM $MgSO_4 \cdot 7\ H_2O$, 10 mM NaCl, 0.5% (w/v) yeast extract, 2% (w/v) Tryptone
- Agar-agar: Merck, Cat.1.01614.1000,
- Agar plates: LB + amp + 16 g/L agar
- Trafe medium: CD-CHO medium (+ 8mM L-Gln + 15 mg/L phenol red)
- Selection medium: CD-CHO medium (+ 4 mM L-Gln + 15 mg/L phenol red + 0.5 mg/mL G418)
- Cellboost 1 - HyClone Cell Boost 1 Supplement
- Cellboost 3 - HyClone Cell Boost 3 Supplement
- Synth-a-freeze®: Gibco® by Life Technologies, Cat. No. A12542-01

7.1.10 Cell lines

- Top 10 electrocompetent *E.coli*
- *Escherichia coli (E. coli)*
- CHO-K1 cells (Chinese Hamster Ovary)
- anti-CD19-CAR-T cells provided by Huppa Lab/Medical University of Vienna
- anti-RORI-CAR-T cells provided by Huppa Lab/Medical University of Vienna

7.1.11 Enyzmes

- KAPA polymerase: KK1512 ROCHE
- AscI New England Biolabs Cat. No. R0630
- AvrII New England Biolabs Cat. No. R0174
- T4 ligase: New England Biolabs Cat. No. M0202S
- Taq polymerase: Promega GoTaq® DNA M300

7.2 Methods (expression vector preparation)

7.2.1 PCR

For the amplification of the open reading frame of the gene of interest from the pCEP4_CD19-HSAD2 template plasmid, which was needed for the upcoming cloning steps, a high-fidelity PCR was performed using a KAPA high-fidelity polymerase. The mixture of table 7.2.1.1 was transferred into PCR tubes and placed in the thermo-cycler. The conditions for the PCR can be seen in table 7.2.1.2. The polymerase was the last component to be added to the mix before starting the PCR. After the PCR procedure, the entire PCR product was subjected to a preparative agarose gel electrophoresis.

Table 7.2.1.1.: PCR assay for one reaction

Component	Volume (total 45 µL)	End-Concentration
HiFi-Buffer x10	4.5 µL	x1
dNTPs	1.5 µL	200 µM of each nucleotide
Forward primer (10 µM)	1.5 µL	0.33 µM
Reverse primer (10 µM)	1.5 µL	0.33 µM
Plasmid (42 ng/µL)	1 µL	0.93 ng/µL
KAPA polymerase (5 U/µL)	1 µL	0.11 U/µL
RO-H2O	33.5 µL	

Table 7.2.1.2.: PCR conditions for CD19-HSAD2 gene amplification

	Temperature	Time	Purpose
	95°C	5min	pre-denaturation
x20	98°C	20 sec	denaturation
	58°C	15 sec	annealing
	72°C	50 sec	elongation
	72°C	1 min 30 sec	Final elongation
	12°C	unlimited	storage

7.2.2 DNA Gel electrophoresis

PCR products were subjected to either a preparative (up to 60 µL) or an analytical (up to 15 µL) electrophoresis gel, depending on the amount of applied sample and whether or not the sample was intended for further use. Before the electrophoresis, the samples had to be treated with 5x BX buffer, which was diluted 1:5 with the sample solution. The gel was placed in TAE buffer and the samples were applied to the gel wells using a pipette. For the DNA ladder, 6-12 µL of GeneRuler DNA Ladder were used. The electrophoresis was then run with 130 V and stopped when the band of the BX buffer almost reached the end of the gel.

7.2.3 Gel elution

In order to extract a specific band from an agarose DNA electrophoresis, the band was excited with UV light via a gel analyser, cut out and the DNA then eluted from the gel using a peqGOLD Gel Extraction Kit according to the manufacturers manual. During the last step of the elution, the DNA was taken up in 50 µL of nuclease free water.

7.2.4 Restriction digest

DNA restriction digests were performed to either create sticky ends of the vector/insert for ligation or as a tool for quality control of entire plasmids to check for the correct fragment size and the absence of possible contaminations or unexpected restrictions. The restriction itself was done depending on the restrictions enzymes used and the respective recommendations of the manufacturer (i.e different temperatures, durations, buffers).

For the continuation of the pL_CD19-HSAD2 plasmid preparation, the eluted DNA of 7.2.3 was treated with 1 µL AscI restriction enzyme as well as 5 µL CutSmart buffer at 37°C over night. To stop the restriction, the assay was heated to 80°C for 20min and afterwards again subjected to the peqGOLD Gel Extraction Kit to remove the enzymes.

If the restriction digest was used as quality control, a negative control without a restriction enzyme present was performed additionally. Furthermore, if a plasmid was subjected to two enzymes, then additional controls with only one enzyme present at a time were used. Table 7.2.4.1 shows the setup of a restriction control performed with two restriction enzymes. Since the DNA fragments were not needed in future experiments, there was no need for enzyme inactivation and removal and the restriction assay was loaded onto an analytical agarose gel electrophoresis as described in 7.2.2.

Table 7.2.4.1.: Restriction digest with two enzymes for plasmid quality control.

	Negative control	Single enzyme	Single enzyme	Double enzyme
Plasmid (0.8 µg)	x µL	x µL	x µL	x µL
Buffer (e.g. CutSmart)	5 µL	5 µL	5 µL	5 µL
Enzyme 1 (e.g AvrII)	-	0.5 µL	-	0.5 µL
Enzyme 2 (e.g AsiSI)	-	-	0.5 µL	0.5 µL
RO-H_2O	ad 50 µL	ad 50 µL	ad 50 µL	ad 50 µL

7.2.5 Photometrical DNA quantification

To quantify the amount DNA after purification, approx. 1 µL of plasmid solution were applied to a photometer (Nanodrop) and the absorption at 260 nm and 280 nm (protein/aromatic amino acid absorption) was measured.

The DNA concentration was then calculated by the following equation:

Equation 7.1: $Absorbance_{260}$* 50 ng/µL = DNA concentration [ng/µL]

The purity coefficient provides information about possible protein impurities. It was calculated by

Equation 7.2: A_{260}/A_{280} = purity coefficient

Purity coefficients lower than 1.8-2.0 would indicate a significant protein contamination which leads to an overestimation of DNA content, since proteins also absorb at 260 nm to some extent.

7.2.6 Ligation

For the ligation of insert and vector, both had to be cut with the same sticky-end creating enzyme (e.g AscI for the pL vector and CD19-HSAD2 insert) as described in 7.2.4. To prevent re-ligation, the vector was treated with calf-intestine-phosphatase (CIP) after restriction.

The ligation was performed using 1 µL T4 ligase in combination with 2 µL T4 buffer in a total volume of 20 µL filled up with RO-H_2O after adding the insert and the vector. The insert and the vector were applied in a molar insert:vector ratio of 3:1 and 0:1 (negative control), which was calculated according to equation 7.3 with the length of the CD19-HSAD2 insert being 1615 bp, the length of the pL vector being 7125 bp and 30 ng of vector used. To achieve the desired ratio, 20.4 ng of insert DNA were needed, but since the insert solution contained 72 ng/µL of DNA and 0.5 µL were used, which equals 36 ng of insert DNA, a ratio of 5.3 : 1 was employed. The assay was then incubated for 15 min at room temperature and subsequently inactivated for 10 min at 65°C.

Equation 7.3.: $$amount\ of\ insert\ (ng) = \frac{amount\ of\ vector\ DNA\ (ng) * length\ of\ insert\ (bp) * 3}{length\ of\ vector\ (bp)}$$

7.2.7 *E. coli* transformation

To obtain enough plasmid material for the mammalian cell transfection, the ligated plasmid (7.2.6) was amplified in *E. coli,* which was transformed via electroporation using the ligation assay. For the transformation, 3 µL of the ligation assay (with and without insert as negative control) were added to 40 µL of TOP10 electrocompetent *E. coli*, vortexed, transferred into an electroporation cuvette, which was subjected to the electroporation device at 1800 V, 25 µF, 200 Ω. Afterwards, 500 µL of SOC medium were added, mixed and the cells recovered for 1h at 37°C. 50 µL of the transformed cell suspension were plated on 200 mg/L ampicillin containing agar plates and cultivated over night at 37°C. To calculate the transformation efficiency per ng of vector and evaluate whether the ligation and transformation were successful, the colonies of the negative control (ligation assay without insert) and the insert containing sample were counted and compared with each other. If the insert containing cells yielded significantly more colonies than the negative, then up to 12 colonies were checked via colony PCR for the insert and again cultivated on ampicillin containing agar plates over-night.

Equation 7.4 shows the calculation of the transformation efficiency based on the amount of vector used as shown in table 7.2.7.1 for the transformation of the CD19-HSAD2 insert and pL vector assay.

Table 7.2.7.1: Transformation of CD19-HSAD2 and pL ligation assay

Step	Assay	Volume [µL]	Vector DNA [ng]	
1	Ligation	20	30	3 µL for transformation
2	Transformation	543	4.5	50 µL for plating
3	Plating	50	0.414	

Equation 7.4.: transformation efficiency $= \frac{colony\ forming\ units\ (cfu)}{vector\ DNA\ [ng]} = \frac{13}{0.414\ ng} = 31.4 \frac{cfu}{ng\ vector}$

7.2.8 Colony PCR

The colony PCR uses a single bacterial colony instead of a pure DNA template and can therefore be used to screen single colonies for the desired insert after ligation and electroporation. Since no high-fidelity is required here, a Taq-polymerase was used instead of the high-fidelity KAPA polymerase.

Single colonies were picked via a pipette tip, partly transferred onto a new agar dish and then subjected to the PCR mix (table 7.2.8.1) by dropping the tip into the PCR vials. The tips were then removed and the PCR vials were placed in the thermo-cycler and the PCR was started under the conditions seen in table 7.2.8.2.

After finishing the PCR, the assays were treated with 5 µL of BX buffer and subjected to an analytical agarose gel electrophoresis. 1-2 clones with a positive result for the insert were chosen for starting an overnight culture with subsequent plasmid purification and cryostock preparation.

Table 7.2.8.1.: colony PCR mix for one reaction

Component	Volume (total 25 µL)	End-Concentration
Thermopol-Buffer x10	2.56 µL	x1
dNTPs (10 mM each)	0.56 µL	224 µM of each nucleotide
Forward primer (10 µM)	0.56 µL	0.224 µM
Reverse primer (10 µM)	0.56 µL	0.224 µM
Taq-polymerase (5 U/µL)	0.11 µL	22 U/mL
RO-H2O	20.67 µL	

Table 7.2.8.2.: PCR conditions for CD19-HSAD2 gene amplification

	Temperature	Time	Purpose
	95°C	5min	pre-denaturation
x30	95°C	20 sec	denaturation
	50°C	30 sec	annealing
	68°C	1min 50 sec	elongation
	68°C	5min	Final elongation
	12°C	unlimited	storage

7.2.9 Mini-scale plasmid purification

Isolation of plasmids from transformed *E. coli* was performed with peqGOLD plasmid miniprep kits. Beforehand, 10 ml of LB-amp medium were inoculated with an *E. coli* colony carrying the respective plasmid and incubated over night at 37°C/220 rpm. The purification itself was done according to the manufacturers manual after centrifuging the *E. coli* suspension for 10 min at 5000g. Ultimately, the plasmid DNA was eluted in 50 µL of nuclease free H_2O.

7.2.10 Cryostock preparation

In addition to the mini-scale plasmid purification, cryo-stocks were prepared from an aliquot of the overnight culture. Therefore, 625 µL of cell suspension were mixed with 375 µL of 80% glycerol in cryo-vials and then stored at -80°C.

7.2.11 DNA sequencing

Sequencing of plasmid inserts was performed by Microsynth with about 1200 ng of plasmid, 3 µL of 10 µM primer solution and the rest filled up to 15 µL with RO-H_2O.

7.2.12 Midi-scale plasmid purification

For midi-scale plasmid purifications, the NucleoBond® Xtra Midi EF kit was used. Before the purification a 2 ml LB-amp medium were inoculated from a cryostock using a pipette tip and incubated at 37°C/220rpm to create a starter culture. After 6h, 300 µl of starter culture were added to 150 ml of LB-amp medium and incubated at 37°C/220rpm overnight. The culture was then purified according to the manufacturers manual and eluted in 300 µL RO-H_2O.

7.3 Methods (cell culture)

7.3.1 PEI transfection of CHO-K1

For the transfection of CHO-K1 cells, the polyplex forming agent PEIMAX (polyethylenimine) was used in combination with the desired plasmid (e.g. pL_CD19-HSAD2). The positively charged PEIMAX binds the negatively charged DNA and therefore allows the uptake by the slightly negatively charged cell surface.

For the transfection procedure, 8 µg of plasmid DNA were transferred into 200 µL of transfection medium (CD-CHO, 8 mM L-glutamine, phenol red), vortexed and incubated for 3min at room temperature, while 16 µg of PEIMAX were incubated in 200 µL transfection medium for 3min at room temperature in parallel. After the incubation, the DNA and the PEIMAX solution were combined, vortexed and again incubated for 3min at room temperature to form polyplexes which were then, then added to $1*10^6$ CHO-K1 cells in 4 ml transfection medium. After 4h of incubation at 37°C and 220 rpm in 50 ml cultivation tubes, the cell suspension was centrifuged for 10 min at 180 g and 10 ml of fresh transfection medium were added to the cell pellet after removing the old medium. This step is necessary to remove the residual PEIMAX, which is toxic to cells if applied for a prolonged time.

After 2 days of incubation at 37°C/220 rpm/7% CO_2, selection pressure was applied by removing the old medium (10min/180g) and addition of 10 ml selection medium (CD-CHO, 4mM L-Gln, 0.5 mg/ml G418, 15 mg/L phenol red). After applying the selection pressure, the transfection pools were used to seed one 384 well plate with 1250-2500 cells/well in 50 µL and 1-2 96 well plates with 5000-10000 cells/well in 100 µL. On day 13 after the transfection, the cells were fed with 30 µL selection medium for the 384 well plate and 200 µL for the 96 well plate and on day 16 passaged 1:5 (50 µl cell suspension + 200 µL selection medium) into new 96 well plates. To this end, the 384 well plate was split into five 96 well plates to obtain enough cell suspension volume for the upcoming screening procedure.

For the co-transfection with pL-CD19mutAFc and pL_CD21mutBFc was performed the same way as described before, however, for the polyplex formation two approaches were used. 1) Polyplex formation with PEIMAX and both plasmids at once using 4 µg of each plasmid (=”CD1921”) and 16 µg of PEIMAX, which were added to 1 mio cell in trafe medium after incubation. 2) Polyplex formation with PEIMAX and only one plasmid at a time using 8 µg of each plasmid and 16 µg of PEIMAX. Therefore, in total 16 µg of plasmid DNA and 32 µg of PEIMAX were added to the 1 mio cells in trafe medium.

7.3.2 Screening and expansion of transfectants

Screening for product formation in the supernatant was performed on day 21 after transfection via a qualitative ELISA targeting either the HSAD2 or Fc part, depending on the produced CD19 construct. Furthermore, the transfection efficiency was calculated on that day based on the number of acidified (yellow) wells. The calculation of the transfection efficiency can be seen in equation 7.5. The 12 clone pools (i.e wells of the 96 well plates) with the highest product titer were transferred into a new 96 well plate by transferring 2x100 µL and addition of 200 µL selection medium to each well. On day 24 and 27 the cells were expanded in the 96 well plate by passaging them 1:2, until on day 29, they were transferred into 50 ml tubes (2ml cell suspension + 2 ml selection medium) and cultivated at 37°C/220rpm/7%CO_2.

Equation **7.5**: transfection efficiency = $\frac{number\ of\ yellow\ well * 100}{total\ number\ of\ wells\ (384\ or\ 96)}$

7.3.3 Cell passaging and cultivation

Cells were cultivated in 50 ml tubes at 37°C/7% CO_2/220 rpm in 10 ml CD-CHO selection medium (CD-CHO, 4mM L-Gln, 0.5 mg/ml G418, 15 mg/L phenol red). If more cell material was required (e.g. for starting a pseudoperfusion), volumes up to 30 ml were cultivated. Cells were passaged every 3-4 days to $2*10^5$ viable cells/ml and cell numbers/viabilities were determined via Vi-Cell™ XR Cell Counter by transferring an aliquot of 0.7 ml cell suspension into cups suited for the device. The Vi-Cell™ XR Cell Counter operates by adding Trypan blue to the cell suspension and then counting dead and living cells by evaluating fifty different images taken from the applied sample. For the passaging process, the entire cell suspension was transferred into a fresh tube and subsequently an aliquot was transferred back into the cultivation tube and the appropriate amount of selection medium was added to achieve a viable cell number of $2*10^5$ cells/ml.

For passaging of cells cultivated in 96 well plates, an approximate cell density was evaluated via microscopy and the passage ratio was chosen based on the assumption that cells double each day.

The specific growth rate µ was calculated according to equation 7.6**:**

Equation **7.6**: $\mu = \ln(x_2/x_1)/t$

µ…. Specific growth rate [d^{-1}]

x_2…. viable cell number on day “B” [cells/ml]

x_1…. viable cell number on day “A” [cells/ml]

t…. timer difference of day “A” and “B” [d]

Specific productivity q_P was calculated according to equation 7.7

Equation **7.7**: $qP = \frac{(titer2 - titer1) * \mu}{x2 - x1} * 1000$

qP…. Specific productivity [pg/cell/day]

titer2…. CD19 product titer on day B [ng/ml]

titer1…. CD19 product titer on day A after passaging [ng/ml]

x_2…. viable cell number on day "B" [cells/ml]

x_1…. viable cell number on day "A" after passaging [cells/ml]

7.3.4 Subcloning by limiting dilution

For the subcloning procedure, an aliquot of the cell suspension of the chosen clone pool was diluted in subcloning medium (selection medium + 1 mg/ml HSA, 20 µg/ml transferrin, 25 ng/ml rEGF) to achieve a final concentration of 1-3 cells/well/40-50 µL for a 384 well and 3 cells/well/120 µL for a 96 well plate. For CHOK1/CD19HSAD2 clone pools, HSA was not added to the subcloning medium, which would have distorted the result of the screening procedure via anti-HSA ELISA. 17-20 days after seeding, the subcloning efficiency was evaluated by counting the acidified (yellow) wells, which were then transferred into new 96 well plates by taking 30-40 µL cell suspension and adding 70-120 µL selection medium. The calculation of the subcloning efficiency was calculated in the same way as the transfection efficiency in equation 7.5. 20-25 days after subcloning, 150-200 µL selection medium were added to the cells in the 96 well plates. To find the best subclones, a qualitative ELISA targeting either the HSAD2 or Fc part, depending on the produced CD19 construct, was performed with the supernatant of the 96 well plates when the wells acidified again (approx. 24-27 days after subcloning). Based on the product titer in the supernatant, the 12 best clones (i.e wells on the 96 well plate) were chosen for transfer into a new 96 well plate by using 100-150 µL of cell suspension plus 150-200 µL selection medium. Subsequently the cells were expanded in the 96 well plate for one week by passaging them twice with a passage ratio of 1:2. After the expansion the subclones were transferred into 50 ml tubes (~2ml cell suspension + 2 ml selection medium) and cultivated at 37°C/220rpm/7%CO_2.

7.3.5 Pseudoperfusion cultivation

To produce larger amounts of product, the CHOK1/CD19-Fc/H21 subclone 1G4 was cultivated in a pseudoperfusion cultivation, which should allow for obtaining very high cell density and in turn more product formation. It was therefore necessary to exchange the medium on a daily basis by removing the medium by centrifugation (180g, 10min) and adding 30 ml of fresh medium to the cell pellet. The removed medium was stored at 4°C and later on used for purification via tangential flow filtration and protein A affinity chromatography. All cultivations were performed in 50 ml tubes at 37°C/220rpm/7%CO_2. In addition to the medium exchange, 1 ml of sample were taken each day to determine cell numbers and viabilities via Vi-Cell™ XR Cell Counter as well as to perform a flow cytometric analysis on the cells. Since the Vi-Cell™ XR Cell Counter can only determine cell numbers up to $10*10^6$ cells/ml, cell suspensions had to be diluted 1:4-1:10 with PBS during the later phases of

the cultivation. For the flow cytometric analysis, the cell pellet of 0.4-0.9 ml was treated with 1-2 ml ethanol on every second day of the cultivation.

For starting the pseudoperfusion cultivation, the cells were first grown in a typical batch culture for three days, starting with 0.3-0.5*10^6 cells/ml in 30 ml medium. For the first pseudoperfusion experiment CD-CHO medium and CDM4-medium (both with 8 mM L-Gln, 0.5 mg/ml G418 and 15 mg/L phenol red) were used. The second experiment was performed with CDM4NS0 medium (8mM L-Gln, 0.5 mg/ml G418, 15mg/L phenol red, + 16.5 g/L glucose) and CDM4NS0+CB1/3 medium (8mM L-Gln, 0.5 mg/ml G418, 15mg/L phenol red + 11.1% Cellboost 1 and 19.7% Cellboost 3) and furthermore, a cell-bleeding approach was applied from day 5 onward, removing 20% (= 6 ml) of the cell suspension each day. The removed cell suspension was also used as a sample for the ViCell measurement and the ethanol fixation for the flow cytometric analysis.

7.3.6 Cryo-preservation stock establishment

For creating cryo-preservation stocks, an aliquot of cell suspension containing 5 mio cells (per cryostock) was centrifuged at 180 g for 10 min. The supernatant was removed and the cell pellet was taken up in 1 ml (per cryostock of cryopreservation) synth-a-freeze medium containing DMSO after breaking it up by dragging the centrifuge tube over a rack. Subsequently cryovials were filled with 1 ml of synth-a-freeze medium containing 5 mio cells and cooled at -1°C/min to -80°C, stored at least overnight and ultimately transferred to liquid nitrogen at -196°C.

In order to start a new culture from cryostocks, a vial was thawed in the hand and its content was transferred into 8 ml of cool culture medium. After centrifuging for 10 min/180g the medium was removed and the cell pellet dissolved in 5 ml fresh selection medium and transferred into a cultivation tube containing 5 ml of selection medium as well which was prepared beforehand.

7.4 Methods (analysis)

7.4.1 Product quantification via ELISA

The ELISA analysis was performed to determine the titer of CD19 constructs in the supernatant of cultured CHO-K1 clones. Therefore, a 1 mL aliquot of the cell suspension was taken on each passage day and the cells were removed by centrifugation at 180g/10min. The supernatants were then stored at -20°C until the day of the analysis via quantitative ELISA. Furthermore, a qualitative ELISA was used to screen new transfectants and subclones in 96 well plates for the best clones/well by removing 50 µL of supernatant from the top of the well and transferring it into a new 96 well plate (dilution plate). The ELISA was performed in a sandwich setup and it was therefore required to first coat Nunc MaxiSorp™ 96 well plates with the coating antibody diluted between 1:500-1:2000 in coating buffer and 100 µL per well for 2h at room temperature and 200 rpm or at 4°C over night. Sample, standard and blank dilutions were prepared on separate Nunc 96 well plates (without MaxiSorp™) with dilutions buffer according to the schemes in figure 7.4.1.1 and 7.4.1.2 and subsequently 50 µl were transferred to each well of the already incubated coating plates which were washed three times with washing buffer by the Tecan 96 Plate Washer beforehand. After incubation of at least 1h at room temperature and 200 rpm, the plates were again washed three times with washing buffer and 50 µL of conjugation antibody with HRP (in the desired dilution between 1:1000-1:2000 prepared in dilution buffer) were applied to each well. The plates were again incubated for 1h/RT/200rpm and washed three times. As substrate for the HRP labelled conjugation antibody, 100 µL of TMB were added to each well and the resulting colorimetric reaction was stopped with 100 µL 2.5 M H_2SO_4 when the well(s) of the 1:128 diluted standard turned light blue. The absorption of the wells was then analysed at 450 nm with a Tecan plate reader and the product concentration calculated by the MAGELLAN software.

	H	G	F	E	D	C	B	A	
1									Blank
2	pre-diluted	1:2	1:4	1:8	1:16	1:32	1:64	1:128	Standard
3	pre-diluted	1:2	1:4	1:8	1:16	1:32	1:64	1:128	Standard
4	pre-diluted	1:2	1:4	1:8	1:16	1:32	1:64	1:128	Sample 1
5	pre-diluted	1:2	1:4	1:8	1:16	1:32	1:64	1:128	Sample 2
6	pre-diluted	1:2	1:4	1:8	1:16	1:32	1:64	1:128	Sample 3
7	pre-diluted	1:2	1:4	1:8	1:16	1:32	1:64	1:128	Sample 4
8	pre-diluted	1:2	1:4	1:8	1:16	1:32	1:64	1:128	Sample 5
9	pre-diluted	1:2	1:4	1:8	1:16	1:32	1:64	1:128	Sample 6
10	pre-diluted	1:2	1:4	1:8	1:16	1:32	1:64	1:128	Sample 7
11	pre-diluted	1:2	1:4	1:8	1:16	1:32	1:64	1:128	Sample 8
12	pre-diluted	1:2	1:4	1:8	1:16	1:32	1:64	1:128	Sample 9

Figure 7.4.1.1.: Dilution scheme for a quantitative ELISA. Minimum dilution of the pre-dilution: 1:4

	H	G	F	E	D	C	B	A	
1									Blank
2	pre-diluted	1:2	1:4	1:8	1:16	1:32	1:64	1:128	Standard
3	1:4	1:4	1:4	1:4	1:4	1:4	1:4	1:4	Samples
4	1:4	1:4	1:4	1:4	1:4	1:4	1:4	1:4	
5	1:4	1:4	1:4	1:4	1:4	1:4	1:4	1:4	
6	1:4	1:4	1:4	1:4	1:4	1:4	1:4	1:4	
7	1:4	1:4	1:4	1:4	1:4	1:4	1:4	1:4	
8	1:4	1:4	1:4	1:4	1:4	1:4	1:4	1:4	
9	1:4	1:4	1:4	1:4	1:4	1:4	1:4	1:4	
10	1:4	1:4	1:4	1:4	1:4	1:4	1:4	1:4	
11	1:4	1:4	1:4	1:4	1:4	1:4	1:4	1:4	
12	1:4	1:4	1:4	1:4	1:4	1:4	1:4	1:4	
	Samples								

Figure 7.4.1.2.: Dilution scheme for a qualitative ELISA

Reducing anti-HSA ELISA:

The reducing quantitative anti-HSA ELISA was using the supernatant of the CHO-K1/CD19HSAD2/J16 subclone 2C12 to test different reducing agents and their effect on the behaviour of the dilution absorption curve of CD19-HSAD2 samples compared to the HSA standard. Used reducing agents were the following:

- **Dithiothreitol (DTT):** the sample was diluted 1:4 for the first well (column "H") by using 50 µL of sample + 150 µL dilution buffer including 5 mM DTT. After diluting, the sample was incubated for 15 min/RT and the 1:2 dilution steps were performed with dilution buffer + 5 mM DTT
- **L-cysteine:** the sample was diluted 1:4 for the first well (column "H") by using 50 µL of sample + 150 µL dilution buffer including 0.5 g/L L-cysteine. After diluting, the sample was incubated for 15 min/RT and the 1:2 dilution steps were performed with dilution buffer + 0.5 g/L L-cysteine
- **Alpha-MTG:** the sample was diluted 1:4 for the first well (column "H") by using 50 µL of sample + 150 µL dilution buffer including 0.5% alpha-MTG . After diluting, the sample was incubated for 15 min/RT and the 1:2 dilution steps were performed with dilution buffer + 0.5% alpha-MTG
- **Beta-mercaptoethanol:** the sample was diluted 1:4 for the first well (column "H") by using 50 µL of sample + 150 µL dilution buffer including 6.5 mM mercaptoethanol . After diluting, the sample was incubated for 15 min/RT and the 1:2 dilution steps were performed with dilution buffer + mercaptoethanol
- **DTT + iodoacetamide:** 50 µL of sample, 40 µL of dilution buffer and 10 µL of 1M DTT (100 mM DTT final concentration) were incubated for 25min/30°C. Afterwards 100 µL of 0.6M iodoacetamide in PBST were added and incubated for 45min/RT in the dark. The 1:2 dilution steps were performed with ordinary dilution buffer.

7.4.2 SDS-Page / Western blot / silver staining

SDS-PAGE:

For the SDS-PAGE analysis, approximately 60-300 ng of product, were applied to NuPAGE 4-12% Bis/Tris 1.0 mm 10-12 well gels in a volume of 15 µL plus 5µL of either 5x SDS or 5x LDS sample buffer. For a reducing SDS-PAGE, 1 µL of DTT were added to achieve a final concentration of 50 mM DTT and the samples were heated to 95°C for 5 min. Samples were either taken from chromatography purification or culture supernatant was concentrated approximately 1:8-1:40 (depending on the initial product concentration) with Amicon Ultra centrifuge filters with a cut-off of 10 kDA. Furthermore, 6µL of PageRuler Prestained Protein Ladder (10 to 180 kDa) were used and the SDS-PAGE was run for approximately 1h at 200V with either MOPS or TRIS/Acetate running buffer.

Silver staining:

In order to un-specifically stain proteins on the SDS-PAGE-gel, the gel was subjected to silver nitrate. After removing the gel from the SDS-PAGE device, it was treated with 25 ml "fixation solution" for 1h. Following 20 min of incubation in 25 ml of "incubation solution", the gel was washed three times with RO-H_2O and subsequently incubated in "silver solution" for 15 min and then again washed three times with RO-H_2O. The gel was ultimately developed by adding 25 ml of "develop solution" to the gel until bands became visible on the gel. The reaction was stopped with "stop solution" for 15 min to 1h.

Western blot:

For western blotting, the proteins of the SDS-PAGE gel were transferred onto a PVDF membrane which was activated in 20% methanol for 30 sec. The membrane/gel were imbedded between two cardboard pieces and additional sponges which were all soaked in transfer buffer before placing the stack in the western blot device, filling it up with transfer buffer and running the blotting procedure for 1h at 25V, 125 mA, 17W. After blotting, the membrane was blocked with 3 % casein in 0.1% PBST for 1h/RT and then incubated with the (primary) antibody solution (diluted 1:500-2000 in PBST) for 1h at 100 rpm. The membrane was then washed three times for 10 min in 0.1% PBST at 100 rpm and either incubated with a secondary antibody or developed by adding 0.8 ml enhanced chemiluminescence (ECL) substrate for HRP conjugated antibodies or 5 ml AP-buffer, 16.5 µL BCIP, 33 µL NBT for alkaline phosphatase conjugated antibodies (stopped by washing with RO-H_2O). For the ECL detection which is much more sensitive than the use alkaline phosphatase induced colorimetric reaction, SuperSignal™ West Pico PLUS Chemiluminescent Substrate (containing luminol and stable peroxide, which were mixed 1:1) was used. After applying the substrate to the membrane and incubating for 5 min in the dark, the membrane was analyzed in the FUSION-FX7 SPECTRA using the chemiluminescence setting with exposure times between 1-120 sec.

7.4.3 Chromatography purification

Before subjecting supernatant containing the CD19 constructs to chromatography purification, a tangential flow filtration (TFF) was performed to concentrate the product, remove residues below 30 kDa and exchange the medium to the respective running buffer for chromatography. For the filtration, the supernatant was first filtered at 0.22 µm using cup-filters, then applied to the Millipore Labscale TFF System mounted with a 30 kDa cut-off Diafiltration membrane, concentrated approximately 1:10 and exchanged to chromatography running buffer. The retentate of the TFF was again filtered at 0.22 µm using a syringe filter and then subjected to chromatography. Furthermore, all buffers and solutions were used at room temperature and filtered at 0.22 µm as well. The used columns and buffers for the protein A affinity as well as for the IMAC can be seen in table 7.4.3.1. For the chromatography procedure, an Äkta Start system was used and the volumes of all fraction (including the TFF) were determined gravimetrically. Additionally, titers were determined via ELISA, which – in combination with the respective volumes – allowed to set up a mass balance for the whole purification procedure.

Table 7.4.3.1.: Chromatography buffers and columns

	Protein A affinity	IMAC
Column	GE Healthcare, HiTrap MabSelect SuRe 1 mL	1 mL HiTrap Chelating HP (GE, Cat. 17040801)
Running buffer (A)	100 mM glycine, 100 mM NaCl pH 7.5	20 mM sodium phosphate, 0.4 M NaCl, 20 mM imidazole, pH 8
Elution buffer (B)	100 mM glycine, pH 2.5	20 mM sodium phosphate, 0.5 M NaCl, 500 mM imidazole, pH 9.6

Protein A affinity:

The Äkta start chromatography system as well as the protein A affinity column were stored in 20 % ethanol which was first removed by flushing with 5 ml RO-H_2O, 10 ml elution and 10 ml running buffer. The sample tube as well as the column were cleaned with 5 ml 0.5 M NaOH, and again flushed with elution and running buffer. The retentate of the TFF was then applied to the column and after washing the column with 5 ml running buffer, the sample was eluted with 100 % elution buffer until the recorded UV (280 nm) signal displayed a peak, which was collected in a separate “eluate” fraction. The acidic pH of the elution fraction was then adjusted to pH 7 with 0.1 M Tris/HCl (pH 9.5) and then again filtered with a 0.22 µm syringe filter.

IMAC (immobilized metal affinity chromatography):

The column for the IMAC was first manually washed with 10 ml RO-H_2O, 5 ml elution buffer, 10 ml RO-H_2O, 6 ml stripping solution (20 mM sodium phosphate, pH 7.4 + 0.5 M NaCl + 5 mM EDTA) and 10 ml RO-H_2O using a syringe. Afterwards, the column was charged with 0.5 ml charging solution (0.1 M NiCl2 in RO-H_2O) and finally washed with 10 ml RO-H_2O. The chromatography procedure itself was performed like the protein A affinity, except for the elution with was performed by increasing the elution buffer percentage by 10% every minute. After obtaining a peak from the 280 nm UV signal, the elution buffer percentage was set to 100 % and the peak fraction was collected. Since the pH of the elution buffer was not acidic, no TRIS/HCl was added to the elution fraction.

7.4.4 Flow cytometry

Flow cytometry for intracellular CD19 products:

For the determination of intracellular product content, a flow cytometric analysis was performed on the CD19 construct producing CHO-K1 cells. Therefore, the pellet of 1 ml cell suspension obtained by centrifugation for 10 min at 180g was treated with dropwise addition of ethanol while vortexing. Cells were then stored at 4°C until the day of the staining procedure. For staining, an aliquot containing 1.5 mio cells was taken from the ethanol fix cells and the ethanol was removed by centrifugation at 200g/10 min. To remove the residual ethanol, 1 ml of TRIS "FACS buffer" was added to the cell pellet which was broken up by dragging the micro centrifuge tube across the rack a few times beforehand. After vortexing, the cell suspension was again centrifuged for 10 min at 200g. The cell pellet was then resuspended in 100 µL FACS buffer including 20% fetal calve serum (FCS) and incubated for 30min at 37°C. Subsequently, 100 µL of antibody solution (diluted 1:50 in FACS+FCS buffer) aiming at the desired part of the CD19 construct (e.g. His-Tag, HSAD2, Fc, CD19, CD21..) were added, resulting in a final antibody dilution of 1:100. Following 30-60 min of incubation at 37°C, 0.8 ml of FACS buffer were added directly to the antibody solution and were then removed by centrifugation. The pellet was then either treated with 200 µL of a secondary/labelling antibody solution (diluted 1:100 in FACS+FCS buffer) or 200 µL of FACS buffer, which already allowed for analysis via the flow cytometer. If a secondary antibody was added, the antibody solution was again incubated at 37°C for at least 30 min, after which 0.8 ml of FACS buffer were added, removed by centrifugation. Ultimately, 200 µL of FACS buffer were added to the cell pellet, which was the last step before the flow cytometric analysis. The entire staining procedure was also performed with an untransfected CHO-K1 clone, which acted as a negative control.

For the measurement a Beckman Coulter® Gallios™ device was used, with laser channels/filters used according to fluorescent dye used for staining (e.g FL1 for FITC and FL6 for Alexafluor647). During the measurement the forward scatter (particle/cell size), the side scatter (granularity) as well as the respective fluorescence signal were recorded. The forward scatter (FS) and the side scatter (SS) were used to set a gate for single, intact cells (figure 7.4.4.1, (A)) which were then used for observing their fluorescence signal (figure 7.4.4.1, (B)). The evaluation of the recorded data was performed with Kaluza (acquisition software for Gallios).

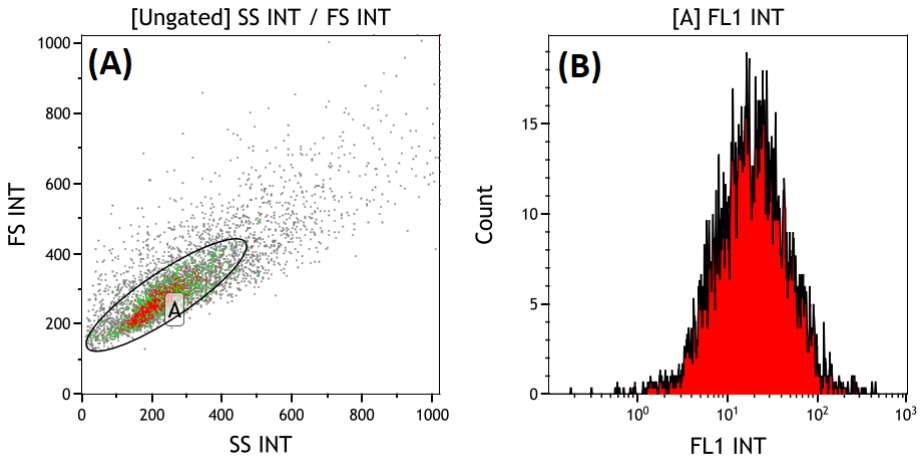

Figure 7.4.4.1.: (A) forward scatter (FS) and side scatter (SS) used for defining gate "A". (B) fluorescence signal of FITC recorded with FL1 of cells in gate "A" with the respective cell count on the y-axis.

Flow cytometry for the cell based CD19-CAR-T cell assay aiming at CD19-Fc:

For the CD19-CAR-T assay, chromatography purified samples which can be seen in table 7.4.4.2 were centrifuged for 5 min at 21000 g to remove debris and then concentrated using Amicon Ultra centrifuge filters with a 10 kDa cutoff at 4000 g. During the concentration procedure, the elution buffers of the samples were exchanged with PBS by washing three times. The washing procedure was performed by spinning the sample solution down to 50 µL and adding 1.5 ml PBS. After concentration, samples were concentrated between 1:5 and 1:10.

Table 7.4.4.1.: CD19-Fc samples used for the CAR-T assay

No.	Sample	initial concentration [µg/ml]	Buffer	final concentration in 40 µL PBS
1	CD19Fc Protein A affinity purified AM170427	4.0	PBS	26 µg/ml
2	CD19Fc Protein A affinity purified AW170830	3.6	protein A elution buffer	18 µg/ml
3	CD19Fc IMAC purified DB170608	2.3	IMAC elution buffer	23 µg/ml

A cell suspension containing $1*10^6$ cells/ml of anti-CD19-CAR-T cells was centrifuged for 3min/350g to remove the supernatant. Cells were washed once with 3 mL PBS and ultimately taken up in 300 µL of PBS (= 1 mio cells in 100 µL for the CD19 CAR-T cells).

For the staining procedure, 40 µL of the concentrated CD19-Fc samples were added to 10 µL of cell suspension (=10^5 cells) in FACS tubes and incubated for 20min on ice. For the washing procedure, 1 mL of FACS buffer (PBS + 1% BSA + 0.03% NaN3) was added, cells were then centrifuged for 3min/350g and the washing step repeated twice. After the washing, cells were contained in 100 µL of FACS buffer (PBS + 1% BSA + 0.03% NaN3), to which 1 µL (= dilution of ~1:100) of anti 6x-His-tag antibody or tEGFR antibody both conjugated with biotin was added. After incubation for 20 min on ice, cells were washed again three times like described before and subsequently 1 µL (= dilution of ~1:100) Strept-Avidin-Alexa Fluor 647 was added, followed by another incubation for 20 min on ice. The flow cytometric analysis was performed after washing the cells another three times. The forward scatter and side scatter were recorded and used for gating single, intact cells. Additionally, the fluorescence signal of Alexa Fluor 647 and GFP (present on the CAR-T Cells) was measured.

8 Results

8.1 Cloning of CD19-HSAD2 expression vector

To stably express the CD19-HSAD2 gene in CHO-K1, the insert from a pCEP4_CD19-HSAD2 plasmid needed to be transferred into a pL plasmid vector, which provided a selection marker (neomycin resistance) for transfected clones. The plasmid map of the entire pL_CD19-HSAD2 is shown in figure 8.1.1. The essential elements of the plasmid are described in table 8.1.1.

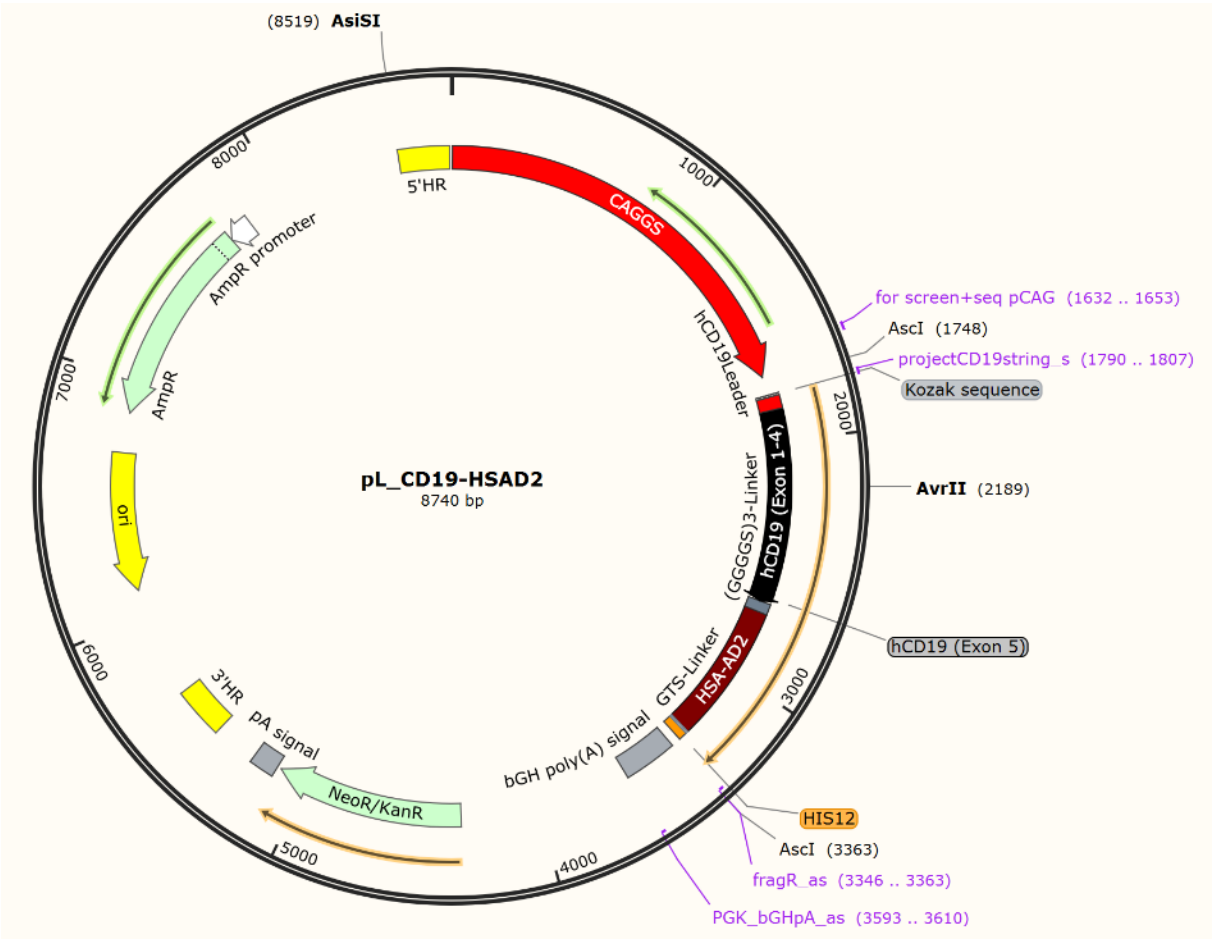

Figure 8.1.1.: Plasmid map of pL_CD19HSAD2

Table 8.1.1.: Sequence elements of the pL_CD19HSAD2 plasmid and their respective functions

Plasmid element	Function
5' HR	for integration into bacterial artificial chromosome (BAC) vectors via homologue recombination
CAGGS	synthetic promoter initiating transcription
AscI (1/2)	Restriction enzyme recognition site
Open reading frame encoding **1. Human CD19 leader** **2. hCD19 (exon1-4)** **3. HSAD2**	 leader of the native human CD19 protein Exon 1-4 of the human CD19 protein Domain 2 of the human serum albumin
AscI (2/2)	
bGH poly(A) signal	Provides signal for addition of poly(A) tail onto the 3' end of the mRNA of the gene of interest
NeoR/KanR	Confers resistance to neomycin (G418) and kanamycin and is used as selection marker
3' HR	for integration into bacterial artificial chromosome (BAC) vectors via homologue recombination
ori	Origin of replication in *E. coli*
ampR	Confers resistance to ampicillin in *E. coli*

8.1.1 CD19-HSAD2 insert amplification

The first step in the cloning procedure was to amplify the open reading frame of the gene of interest from the pCEP4_CD19-HSAD2 template plasmid via PCR. The PCR product was loaded onto a preparative agarose gel which can be seen in figure 8.1.1.1. The band between 1500 and 2000 base pairs was cut out and the DNA was eluted from the gel. After restriction with AscI to cut the 5' and 3' end of the amplicon and subsequent enzyme inactivation, the insert was quantified via a NanoDrop™ photometer yielding a concentration of 71.8 ng/µL and a purity coefficient of $A_{260/280}$ = 1.87, which lies within the desired range of 1.8-2.0.

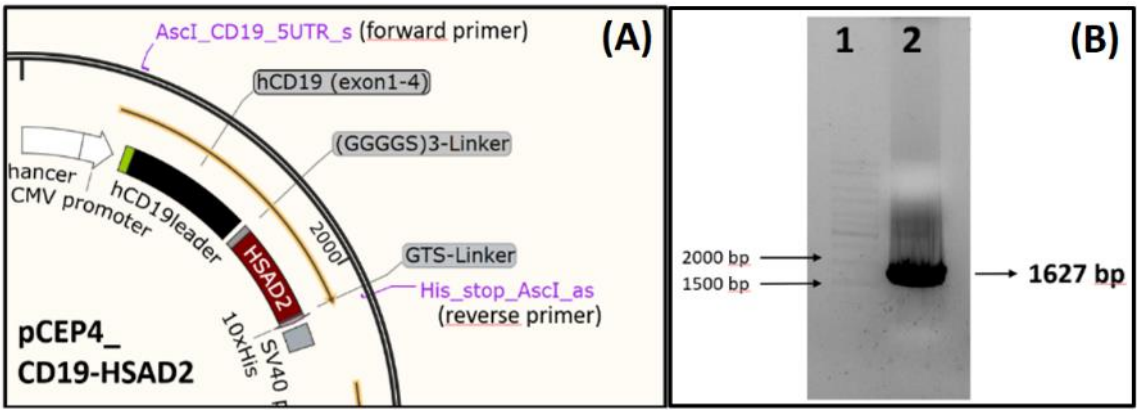

Figure 8.1.1.1.:
(A): partial segment of the pCEP4_CD19HSAD2 showing the forward and reverse primer used for PCR, as well as the gene of interest between them.
(B): Preparative agarose gel electrophoresis of the PCR product. Lane 1.: GeneRuler DNA Ladder. Lane 2: PCR product. PCR setup: HF-PCR: kappa polymerase, sample: pCEP4_CD19-HSAD2 (42 ng), forward-primer: AscI_CD19_5UTR_s, reverse-primer: HIS_stop_AscI_as, expected amplicon size: 1627 bp.
PCR conditions: pre-Denaturation: 95°C / 5min, [denaturation: 98°C / 20 sec, annealing: 58°C / 15 sec, elongation: 72°C / 50 sec] x20 cycles, final Elongation: 72°C / 1min30sec

8.1.2 Ligation with vector, *E. coli* transformation & colony PCR

The AscI-cut insert DNA (36 ng) was subjected to ligation with an pL plasmid vector linearized by AscI restriction followed by dephosphorylation of the DNA ends by calf intestine phosphatase (CIP). Ligation with T4 DNA ligase was performed in a molar insert:vector ratio of 3:1 and 0:1. After heat-inactivation of the ligase enzyme, the ligation mixtures containing 4.5 ng of vector DNA were used for *E. coli* transformation. The transformed *E. coli* were cultivated on ampicillin agar plates and ultimately 11 colonies were picked and checked for the insert via colony PCR. Additionally, the number of colonies on the agar plates was counted and the transformation efficiency (colony forming units per ng of vector DNA) was calculated.

Table 8.1.2.1.: Results of E. coli transformation with ligation assay of pL vector and CD19-HSAD2 insert

Ratio insert:vector	Colony forming units (cfu)	Transformation efficieny
3:1	13	31.70 cfu/ng vector DNA
0:1 (negative control)	1	2.44 cfu/ng vector DNA

Lane 1 to 11 of Figure 8.1.2.1 shows an analytical agarose gel for the different PCR products of the colony PCR with primers for_screen+seq_pCAG and fragR_as. The used primers were suitable to detect the presence of the gene of interest in the right orientation. Because of the band appearing between 1500 and 2000 base pairs (expected size = 1714 bp), colony 2 was picked for starting an overnight culture and subsequent mini-scale plasmid purification. For the positive control (expected size = 1771 bp) an already established pL_CD19Fc plasmid containing the same primer binding sequences was used to check if the PCR conditions were appropriate for the used primers.

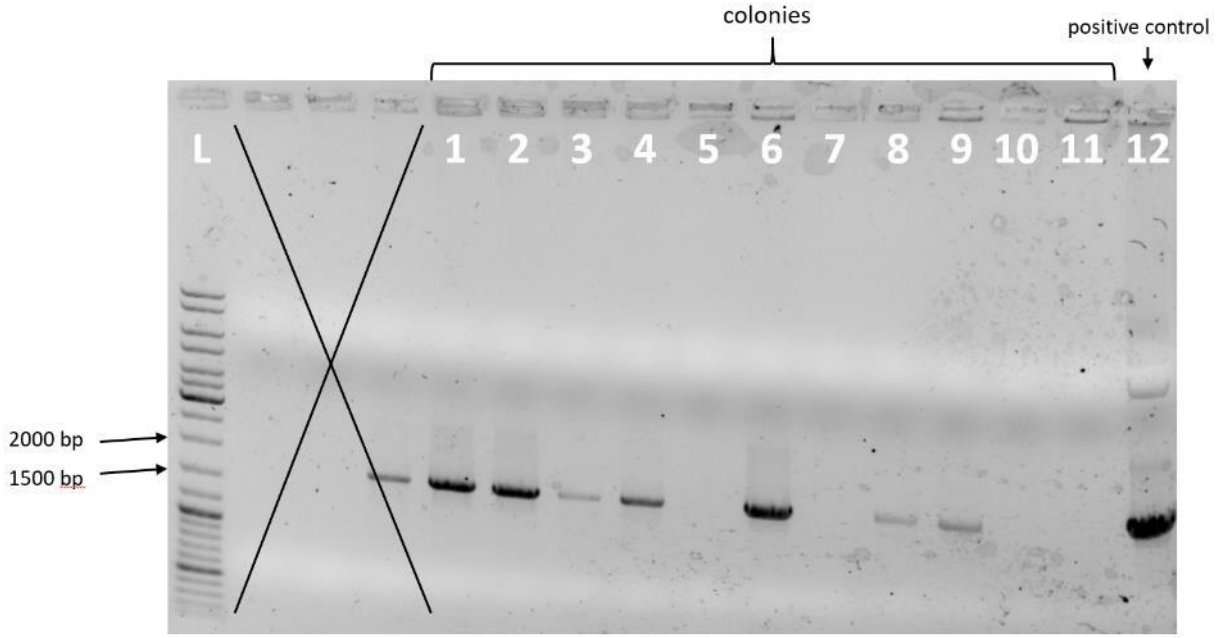

Figure 8.1.2.1.: Result of the colony PCR. L = GeneRuler Ladder, 1-11 = colonies, 12 = pL_CD19Fc plasmid (positive control), PCR setup: Taq-polymerase, expected amplicon size: 1614 bp, forward primer: for_screen+seq_pCAG. reverse primer: fragR_as PCR conditions: pre-Denaturation: 95°C / 5min, [denaturation: 95°C / 20 sec, annealing: 50°C / 30 sec, elongation: 68°C / 1min50 sec] x30 cycles, final Elongation: 68°C / 5min.

8.1.3 Quantification and sequencing of mini-scale plasmid purification

Positive *E. coli* transformants were used for an over-night culture for mini-scale plasmid purification and establishment of a cryostock. The purified plasmid solution was quantified photometrically (179 ng/µL, A260/280 = 1.87, 955 ng plasmid /ml of culture) and sequenced by Microsynth with "for_screen+seq pCAG" and "projectCD19string_s" as forward primers and "PGK_bGHpA_as" and "fragR_as" as reverse primers. The results of the gene sequencing were compared with the sequence found on the plasmid map (figure 8.1.1) and no mutation in the sequenced gene was observed.

8.1.4 Midi-scale plasmid preparation, quantification and restriction

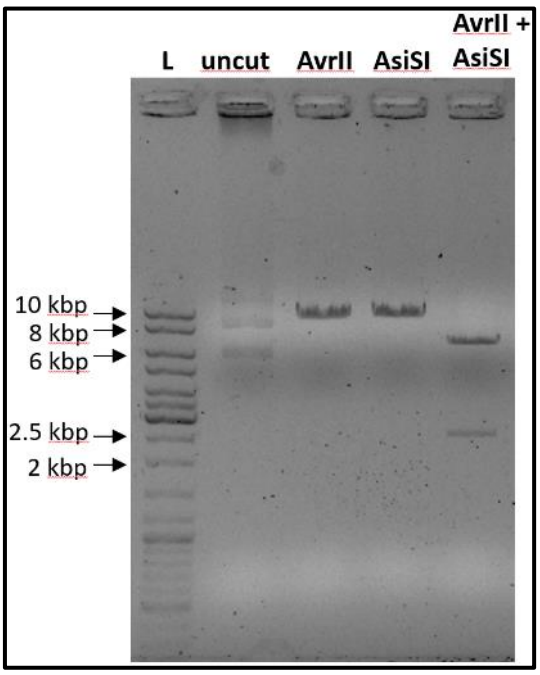

pL_CD19-HSAD2. L = GeneRuler Ladder, uncut = no enzyme, AvrII = cut with AvrII, AsiSi = cut with AsiSi, AvrII + AsiSi = cut with both enzymes

To obtain enough plasmid DNA material for the transfection (8 µg per reaction), it was necessary to perform a midi-scale plasmid purification before the stable transfection of CHO-K1. The purified plasmid solution was again quantified photometrically (1892 ng/µL, A260/280 = 1.89, 1892 ng plasmid DNA/ml of culture) and a restriction control was performed with the restriction enzymes AvrII and AsiSI.

Figure 8.1.4.1 shows the result of the single AvrII or AsiSI or AvrII/AsiSI double- digest on an analytical agarose gel (200 ng per lane) with the linearized AvrII or AsiSI plasmid at the expected positions of 8740 bp or the two fragments at 6330 bp and 2410 bp for the double-digest, respectively. The lane with the uncut plasmid displays three bands which represent the nicked, open-circular and supercoiled (from top to bottom) form of the plasmid. Furthermore, no unexpected bands and no impurities could be observed on the gel.

8.2 Recombinant cell line development for CHO-K1/CD19-HSAD2

8.2.1 PEI-transfection of CHO-K1 host cells with pL_CD19-HSAD2

The sequenced pL_CD19-HSAD2 plasmid which was obtained by the midi-scale plasmid purification, was used for the stable transfection of CHO-K1 cells.2 Days after transfection selection pressure was started with 500 µg/mL G418 followed by seeding the transfection pools into one 384 well plate (2500 cells/well in 50 µL) as well as two 96 well plates (10000 cells/well in 100 µL). On day 21 after the transfection, the transfection efficiency was calculated based on the acidification (and in turn the yellow colouring of phenol red) of the wells.

Table 8.2.1.1.: Transfection efficiency of stable transfection of CHO-K1 with CD19-HSAD2 on day 21

Plate:	Transfection efficiency:
96 well plate 1	90%
96 well plate 2	94%
384 well plate	82%
Negative control	0%

8.2.2 Screening and expansion of initial CD19-HSAD2 transfectant pools after limiting dilution subcloning

To screen the best CD19-HSAD2 producing pools in microtiter plates, a qualitative ELISA analysis specific for HSA was performed from the supernatants of all three seeded plates on day 21 after transfection. Prior to the ELISA analysis, the cells were passaged into new 96 well plates on day 16 (384 plate split into 5x96 well plates).

Figure 8.2.2.1 shows the result of the qualitative anti-HSA ELISA. The green dots represent the individual clone pools of the 384 well plate, whereas the red dots represent the 96 well plate clone pools. Clone pools with the highest titers can be found at the top, lowest titers at the bottom. J16, O12, P15, M4, M5, B15, C5, B1, B3 were best producing clone pools on the 384 well plate with a maximum titer of 39.48 ng/ml achieved by J16. A9 and F1 were the best producing clone pools on the first 96 well plate, G9 on the second 96 well plate. The highest titer of the two 96 well plates could be obtained by the A9 clone with 17.33 ng/ml. Those 12 clone pools were picked for expansion in a 96 well plate and further cultivation in cultivation tubes. The combination of letters and numbers of the clone pool designation refers to position on the 384 or 96 well plate respectively.

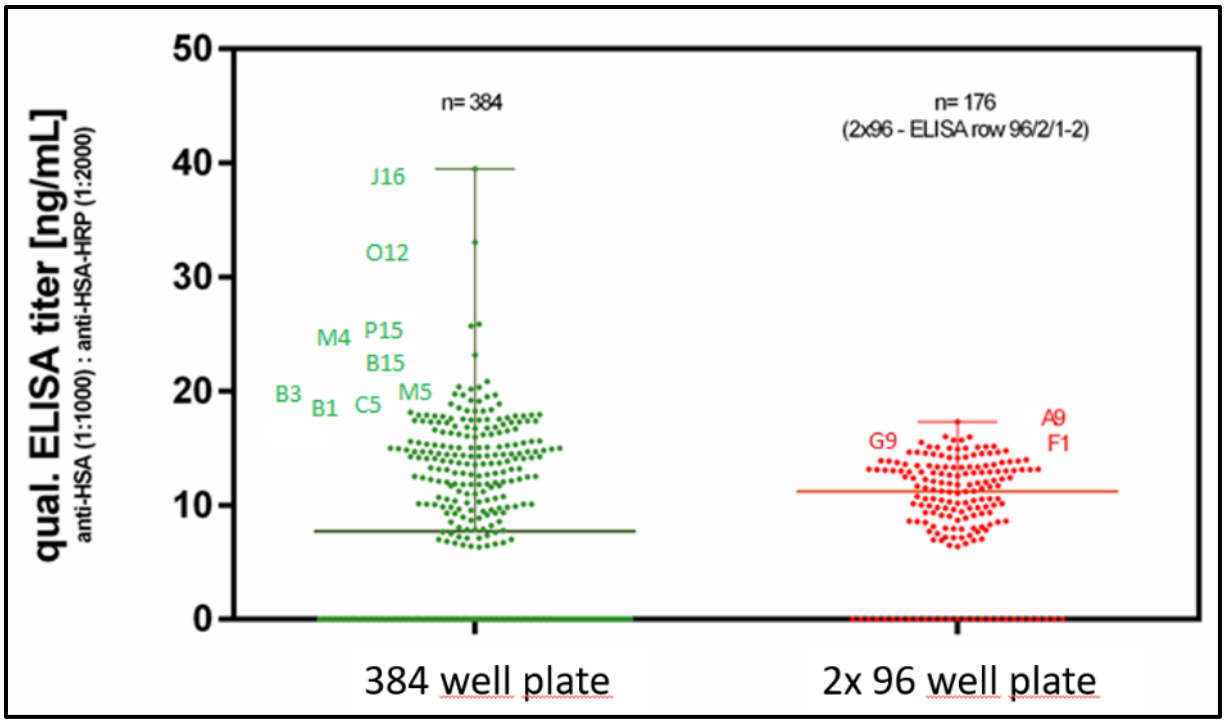

Figure 8.2.2.1.: Result of the qualitative anti-HSA ELISA. Coating antibody dilution: 1:1000, conjugating antibody dilution: 1:2000, sample dilution 1:4, standard: 200 ng/mL HSA.

After screening and expansion, the clone pools were cultivated in cultivation tubes for an extended amount of time by passaging them every 3-4 days into fresh CD-CHO "selection" medium. This allows to further pick the best performing subclones by observing their growth and productivity over several passages.

Figure 8.2.2.2-8.2.2.4 show the results of the viable cell number, growth rates and viabilities of the individual clone pools during the cultivation.

Passaging after 3 days yielded lower cell numbers compared to passaging after 4 days, which is why cell numbers vary from passage to passage. On passage number 7, cells were passaged after only 2 days, resulting in much lower cell numbers than usual.

After 3 passages, the J16, P15, B1, B3 were chosen for further cultivation and sub-cloning (based on CD19-HSAD2 titer, productivity and growth rate). After 9 passages only J16 was kept in culture for another 9 passages.

In general, viable cell numbers up to $8.36*10^6$ cells/ml could be obtained by the best growing clones (i.e J16 and P15), with an average cell number of $5.66*10^6$ cells/ml among all clone pools (from passage 4 to 9). Growth rates were ranging from 0.65 – 1.14 d^{-1}, averaging 0.90 d^{-1}. Viabilities never dropped below 85%, and an average viability of 96.0% could be observed.

Furthermore, the clones J16, P15, B3 and B1 were selected based on their CD19-HSAD2 titers and specific productivities on passage number 2 for subcloning and then subcloned on passage number 3. Additionally, two cryopreservation stocks of each clone were established on that day.

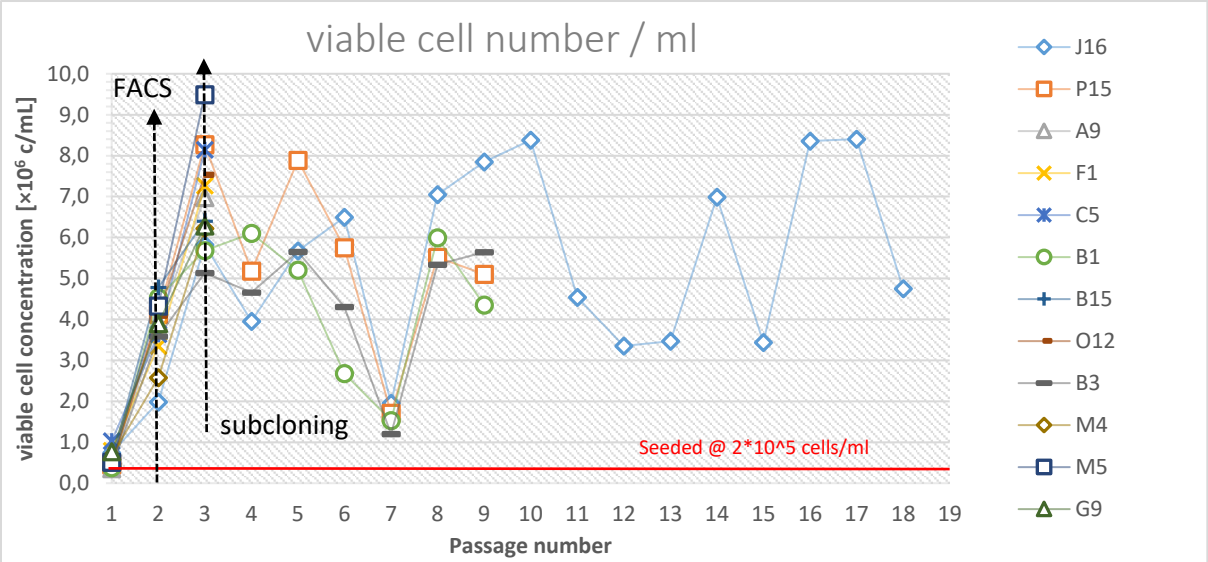

Figure 8.2.2.2.: Viable cell numbers of CHO-K1/CD19-HSAD2 clone pools cultured in CD-CHO selection medium containing 0.5 mg/mL G418.

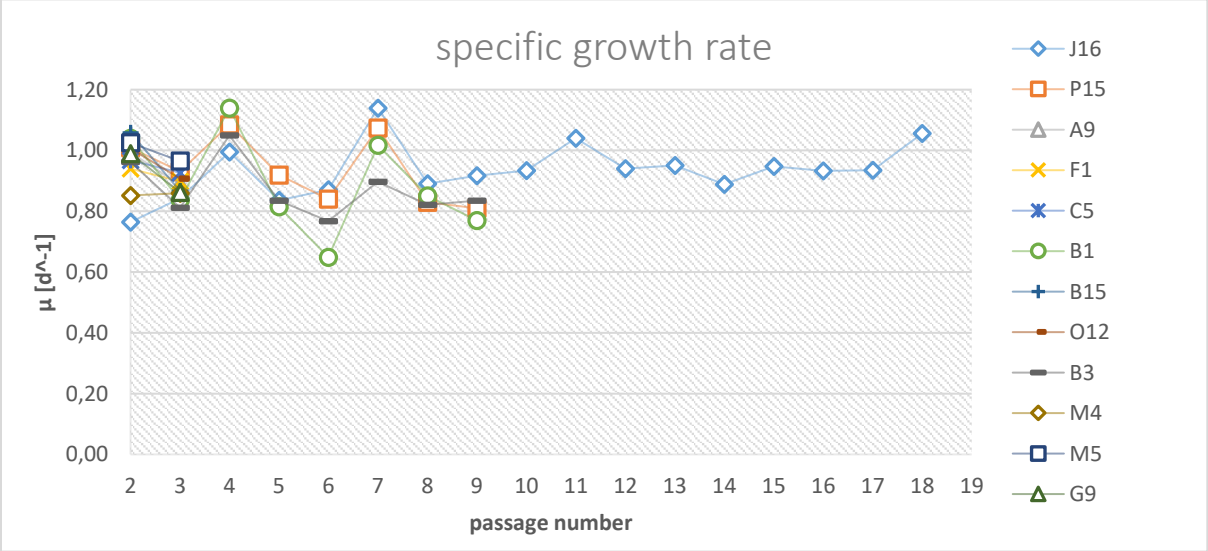

Figure 8.2.2.3.: specific growth rates [μ] of CHO-K1/CD19-HSAD2 clone pools cultured in CD-CHO selection medium containing 0.5 mg/mL G418

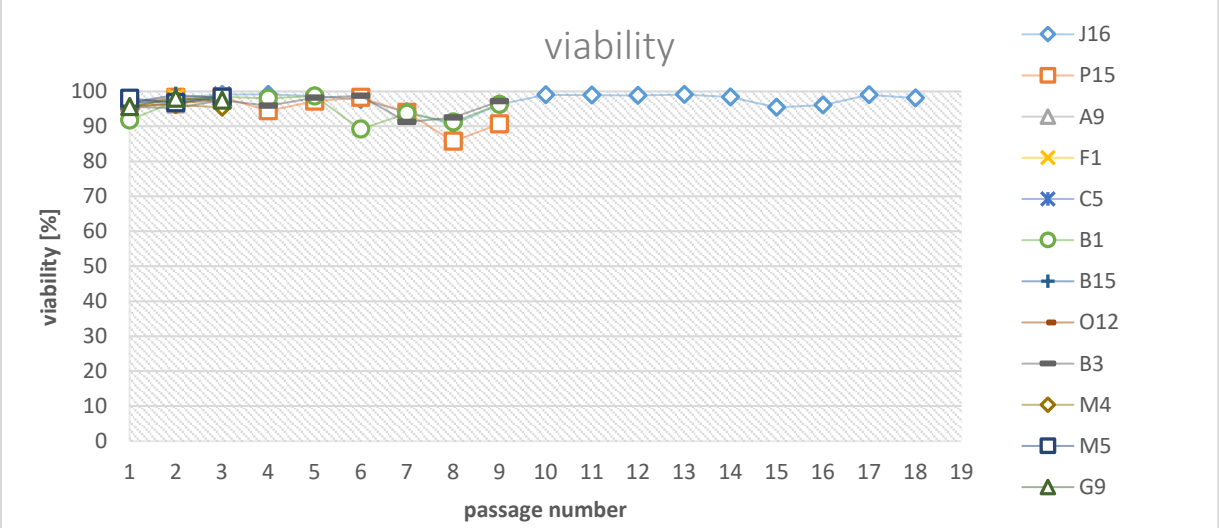

Figure 8.2.2.4.: Viabilities of CHO-K1/CD19-HSAD2 clone pools cultured in CD-CHO selection medium containing 0.5 mg/mL G418

During the analysis of the CD19-HSAD2 titer in the supernatant via ELISA, it was noticed that the samples did not behave like the standard curve when looking at the absorption at the lower dilutions (figure 8.2.2.5 & 8.2.2.6), which led to high titer deviations in the different dilution wells.

The first approach was to incubate the samples with different reducing agents before the analysis and add the reducing agents to the dilution buffer (except for DTT + iodoacetamide) in order to inhibit aggregate formation at higher concentrations of CD19-HSAD2. The result of this "reducing" ELISA can be seen in figure 8.2.2.5 and 8.2.2.6, with CD19HSAD2 coming from the 2C12 sub-clone and a negative control with the CD19/CD21mutFc clone pool 10C10. The samples were also tested without reducing agents present which can be seen in yellow and grey respectively. The standard curves of the standard are displayed in orange and light blue. A slight improvement compared to the untreated samples could be observed when using the combination of DTT and iodoacetamide, which can be seen in figure 8.2.2.6 in brown. The reason for this might be that iodoacetamide alkylates the cysteine residues reduced by DTT and therefore inhibits reformation of cysteine bonds. However, none of the reducing agents seemed to greatly improve the behavior of the dilution curve of the samples. The use of aMTG seemed to even weaken the binding of the antibodies and/or sample (figure 8.2.2.5, brown). Therefore, the next approach was to try different standard concentration, sample dilutions, coating and conjugating antibody dilutions.

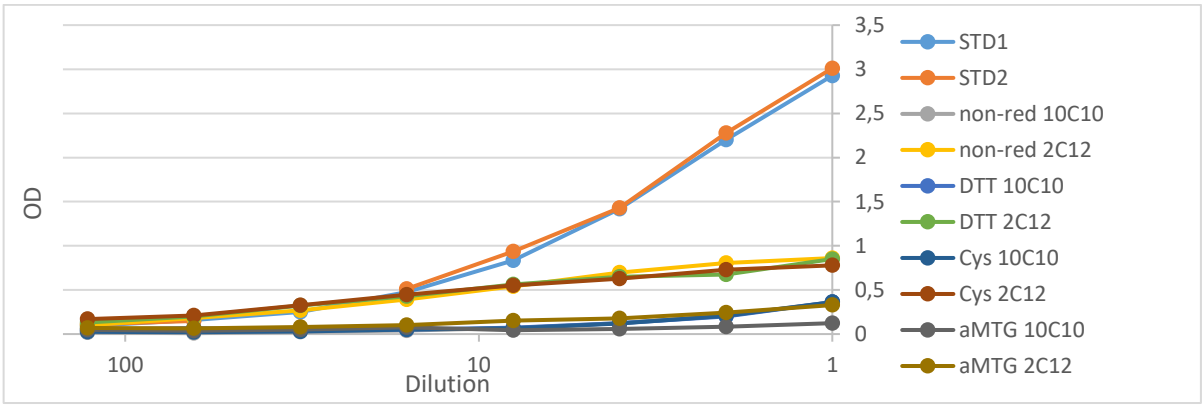

Figure 8.2.2.5.: HSA ELISA (coating antibody 1:2000, conjugation antibody 1:2000) of reduced CD19-HSAD2 from the 2C12 subclone on passage number 3. STD 1 & 2 = HSA standard 40 ng/ml. DTT = Dithiothreitol 5 mM, Cys = L-Cystein 0.5 g/L, aMTG = α-monothiol-glycerol 0.5%, non-red = non-reduced samples.

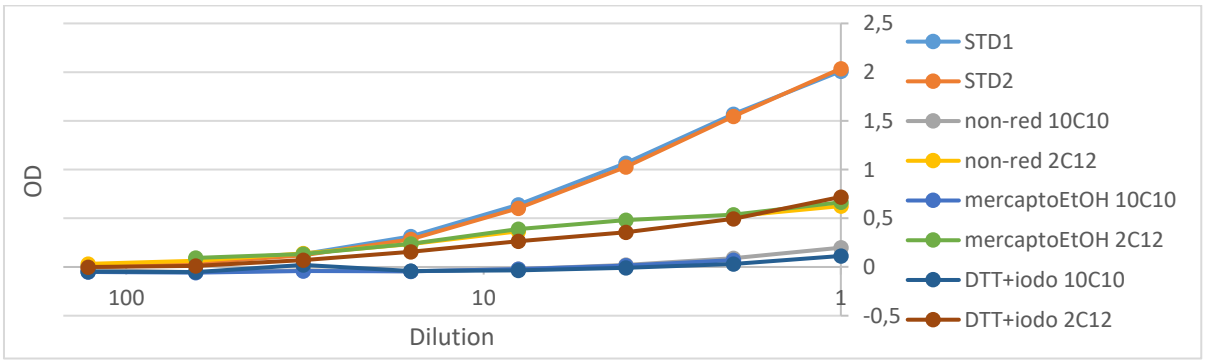

Figure 8.2.2.6: HSA ELISA (coating antibody 1:2000, conjugation antibody 1:2000) of reduced CD19-HSAD2 from the 2C12 subclone on passage number 3. STD 1 & 2 = HSA standard 40 ng/ml, mercaptoEtOH = mercaptoethanol 6.5 mM, DTT + iodo = dithiothreitol 100 mM + iodoacetamide 0.6 M, non-red = non-reduced samples.

Figures 8.2.2.7-8.2.2.10 show the results of different HSA ELISA setups with different standard concentrations, sample dilutions of 2C12, coating antibody dilutions and conjugation antibody dilutions. In figure 8.2.2.7 and 8.2.2.8 samples which have been diluted 1:20 (blue and green) in the first well of the dilution plate mimic the standard curve better than samples which started out with a 1:4 dilution (yellow and grey). Another major change was the coating antibody dilution to only 1:500, which gave better results than the analysis of 8.2.2.5 and 8.2.2.6. This phenomenon can again be seen in figures 8.2.2.9 and 8.2.2.10, where the only alternating parameter was the coating antibody dilution. The ELISA which used a coating antibody dilution of 1:1000 produced significantly worse results than the 1:500 dilution, although all samples were diluted 1:20.

It can therefore be concluded, that for a relying quantification of CD19-HSAD2 via ELISA, it is important to use a 1:500 dilution of the anti-HSA coating antibody and an initial sample dilution of 1:20 for the first well on the dilution plate. The standard concentration seemed not to have significant impact on the result; however, with a sample dilution of 1:20 and titer of approximately 230 ng/ml, a starting concentration of 20 ng/ml of the HSA standard seemed to work best. It should further be noted, that 2 % PVP was used in the dilution buffer instead of the typically used BSA.

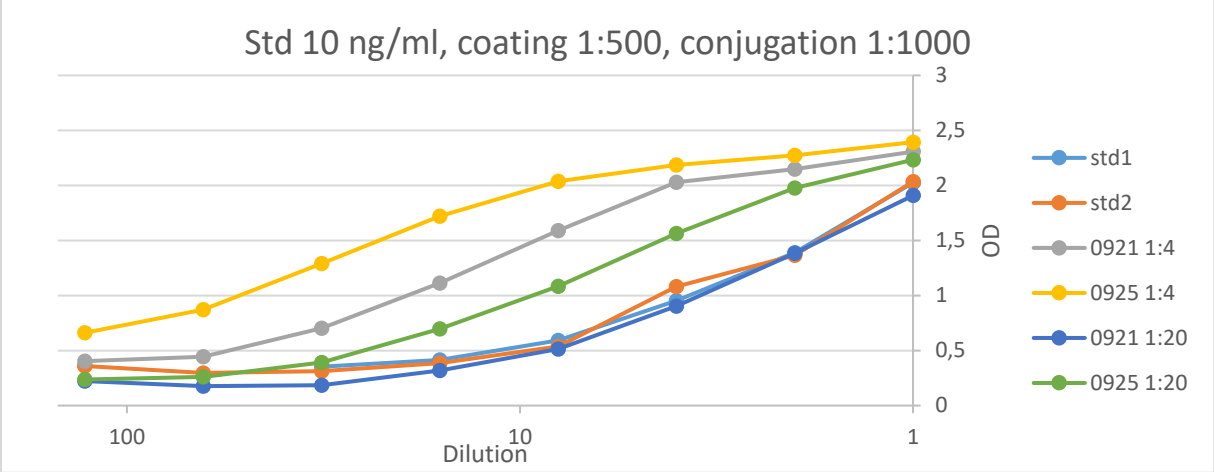

Figure 8.2.2.7.: HSA ELISA, Standard: 10 ng/ml HSA (blue, orange). 2C12 subclone passage number 1 (0921) and passage number 2 (0925) diluted 1:4 and 1:20. ***Coating antibody: 1:500****, conjugation antibody 1:1000*

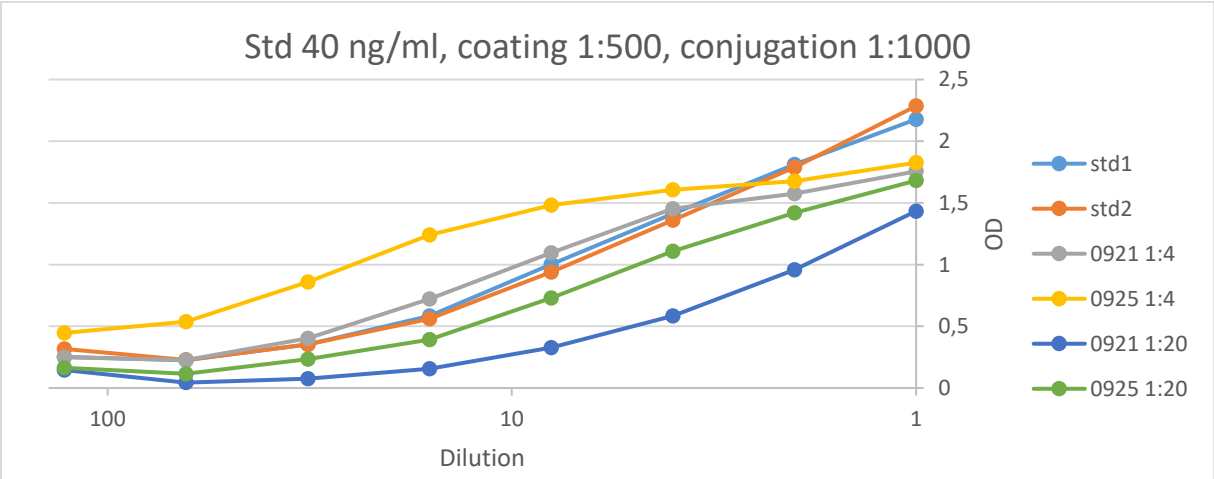

Figure 8.2.2.8.: HSA ELISA, Standard: 40 ng/ml HSA (blue, orange). 2C12 subclone passage number 1 (0921) and passage number 2 (0925) diluted 1:4 and 1:20. ***Coating antibody: 1:500****, conjugation antibody 1:1000*

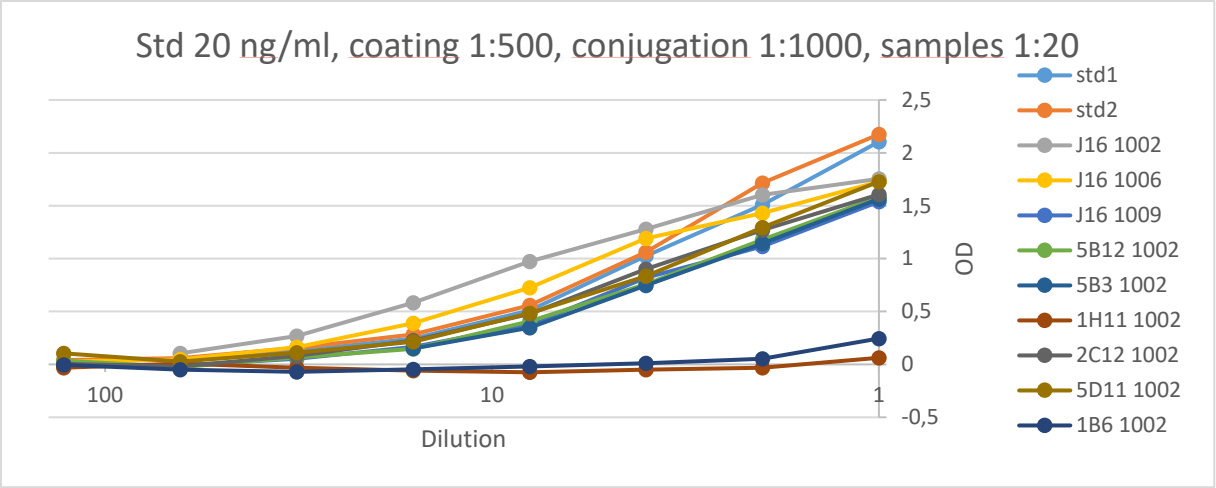

*Figure 8.2.2.9.: HSA ELISA of CD19-HSAD2 parental clone J16 and different CD19-HSAD2 subclones. Standard (orange, blue) HSA 20 ng/ml, **coating antibody: 1:500**, conjugation antibody 1:1000, sample dilutions 1:20*

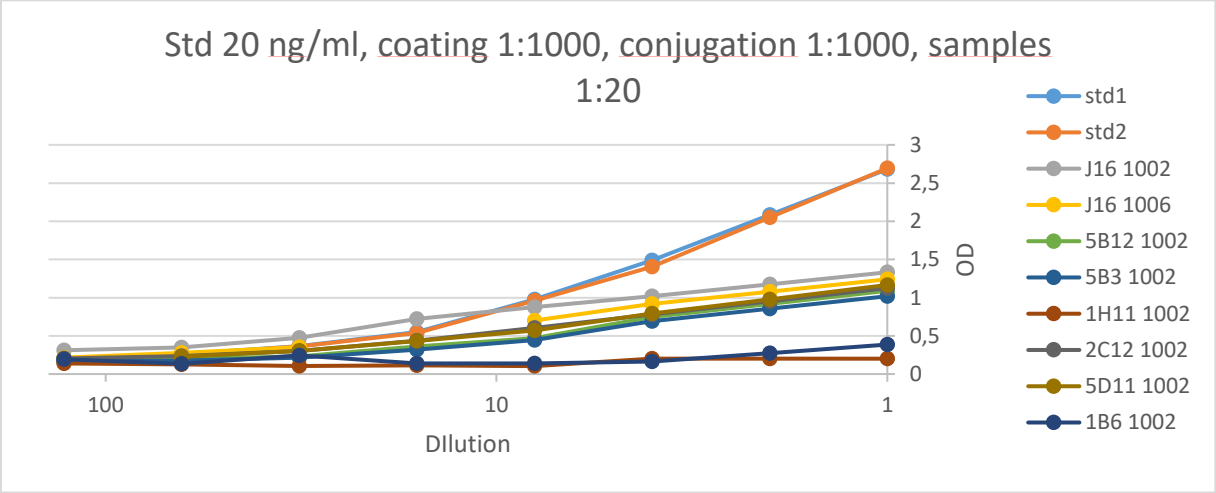

*Figure 8.2.2.10.: HSA ELISA of CD19-HSAD2 parental clone J16 and different CD19-HSAD2 subclones. Standard (orange, blue) HSA 20 ng/ml, **coating antibody: 1:1000**, conjugation antibody 1:1000, sample dilutions 1:20*

During the passaging process, samples of the supernatant were taken to determine the concentration of CD19-HSAD2 via a quantitative anti-HSA ELISA.

Figures 8.2.2.11 and 8.2.2.12 show the titers and the specific productivity of CD19-HSAD2. Since there have been some problems with establishing the antiHSA-antiHSA ELISA in the beginning (samples did not behave like the standard curve in lower dilutions - see anti-HSA ELISA establishment 8.9) and different antibody/sample/standard dilutions have been tested on samples from different passages, only titer values with the same ELISA setup can be compared with each other. Detailed analysis conditions of each passage can be found table 8.2.2.1.

For the best CD19-HSAD2 producing clone pool J16, titers were usually ranging between 100 and 200 ng/ml, with a significant increase on passage number 16 up to 600 ng/ml. This could either be explained by the different ELISA conditions for passages number 16-19 and an operator change for passaging and sample taking on passage number 15. Another outstanding titer was achieved by M5 on passage number 3 with concentrations of almost 500 ng/ml. Unfortunately, those values were measured after the clone pools had been removed from culture and could therefore not be cultivated further.

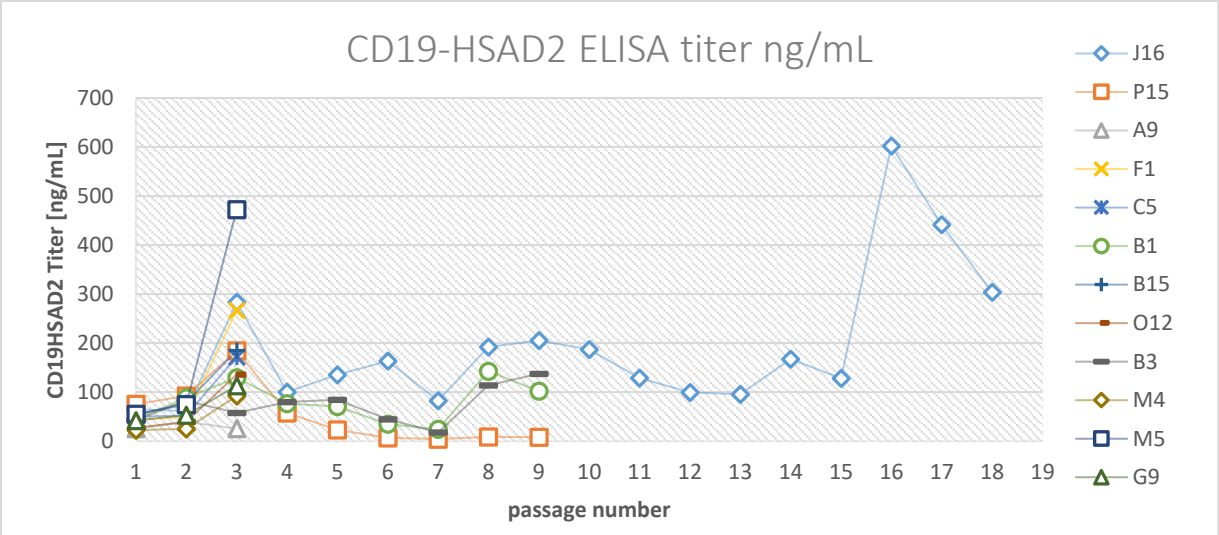

Figure 8.2.2.11.: CD19-HSAD2 titer in the supernatant of CHOK1/CD19-HSAD2 clone pools. Coating antibody: goat anti-HSA antibody. Conjugating antibody: goat anti-HSA-HRP antibody. Standard: HAS. For details see table 8.2.2.1.

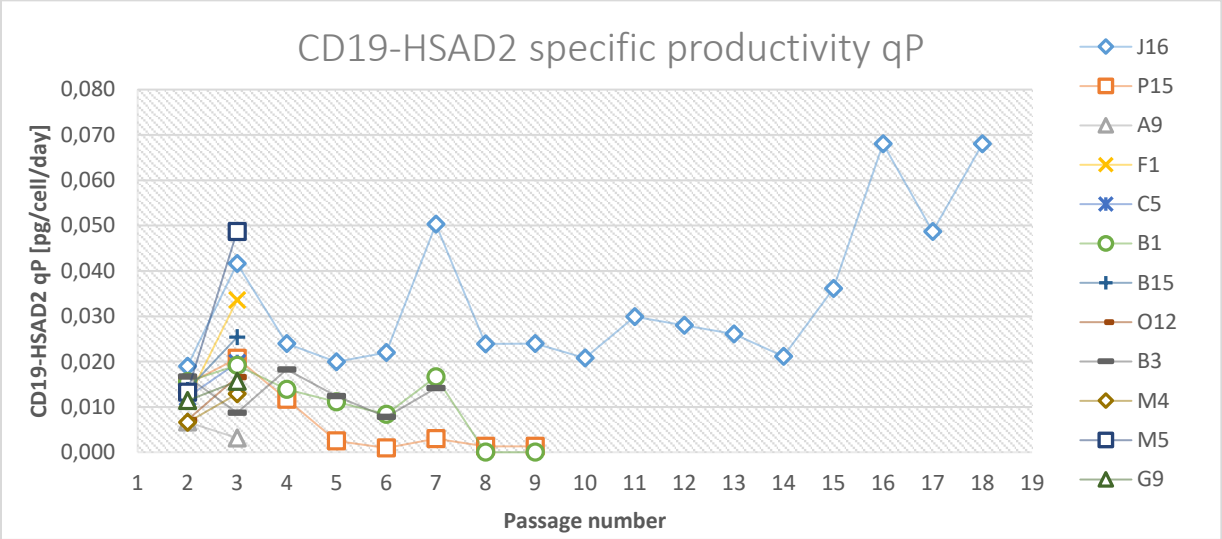

Figure 8.2.2.12.: Specific productivity of CD19-HSAD2

Table 8.2.2.1.: ELISA conditions for individual passages of CHOK1/CD19-HSAD2 clone pools

ELISA setup	Passage number
Coating antibody dilution: 1:1000 **Conjugating antibody dilution: 1:2000** **Sample dilution: 1:4** **Standard: 100 ng/ml**	1, 2
Coating antibody dilution: 1:2000 **Conjugating antibody dilution: 1:2000** **Sample dilution: 1:4** **Standard: 40 ng/ml**	4,5,6,7
Coating antibody dilution: 1:1000 **Conjugating antibody dilution: 1:2000** **Sample dilution: 1:4** **Standard: 40 ng/ml**	3,8,9,10,11,12,13,14,15
Coating antibody dilution: 1:500 **Conjugating antibody dilution: 1:1000** **Sample dilution: 1:20** **Standard: 20 ng/ml** **NOTE: 2% PVP was used instead of BSA in the dilution buffer**	16,17,18

Based on the titer and productivity of CD19-HSAD2 after 2 passages which can be seen in table 8.2.2.2, J16, P15, B1, B3 were chosen for subcloning on passage number 3.

Table 8.2.2.2.: Titers and specific productivities of CHO-K1/CD19-HSAD2 clones on passage number 2; clones chosen for subcloning are highlighted in green

Clone	Titer [ng/ml]	Specific productivity [pg/cell/day]
J16	61,65	0,019
O12	39,70	0,007
P15	92,32	0,015
M4	25,11	0,007
M5	74,84	0,013
B15	78,91	0,014
C5	52,86	0,012
B1	88,17	0,016
B3	82,34	0,017
A9	39,34	0,007
F1	49,42	0,011
G9	53,47	0,011

To determine the homogeneity of the clone pools after transfection, a flow cytometric analysis was performed by staining for intracellular CD19-HSAD2 product.

Figure 8.2.2.13 and 8.2.2.14 show the results of the flow cytometric analysis of the twelve transfected clone poola that were fixed with ethanol on passage number 2 and stained for intracellular CD19-HSAD2. In figure 8.2.2.13, B1 (light green) displays a distinct peak, which indicates a homogenous cell population and furthermore, has one of the highest fluorescence signals among all clone pools. B3 (dark blue) shows a more uneven peak distribution and thus a lower homogeneity. Due to the CD19-HSAD2 titer in the supernatant (table 8.2.2.2), this clone pool was still chosen for further cultivation and subcloning. The same applies to the P15 in figure 8.2.2.14 (light blue), which displays a very heterogeneous population compared to the other clone pools. J16 (light green, figure 8.2.2.14) was the last clone pool to be chosen for continued cultivation and subcloning, which demonstrated the highest intracellular CD19-HSAD2 content.

The black curve represents the negative control with an untransfected CHO-K1 clone, whereas the grey curve is obtained by measuring a CD19-HSAD2 producing clone pool without the addition of a primary antibody. Since both curves are nearly identical, there is no unspecific binding of the secondary antibody to CD19-HSAD2.

The “pos.” line includes all cells with a fluorescence signal higher than the highest 0.5% of the negative control, which are therefore taken as “positive” in terms of intracellular CD19-HSAD2.

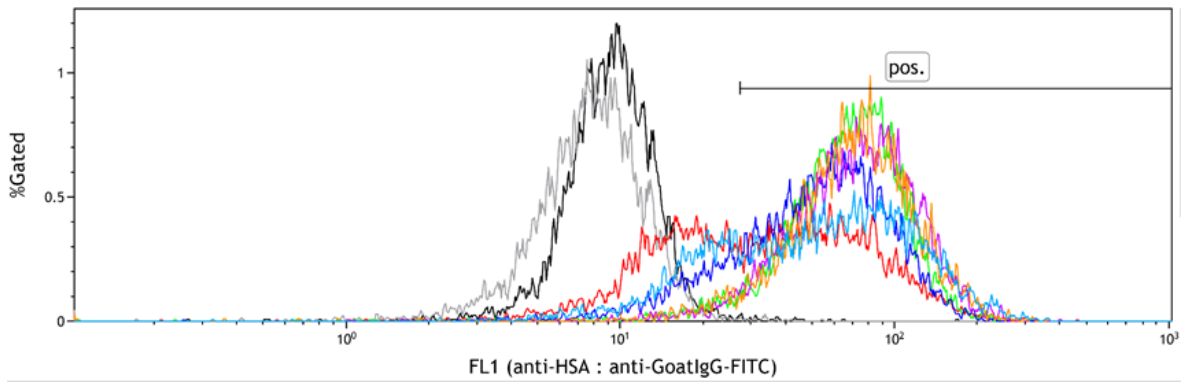

Marker	Number	%Gated	X-Med	X-Mode	X-GMean
All	5,270	100.00	54.63	88.67	46.16
All	3,444	100.00	72.13	80.32	65.00
All	5,122	100.00	73.49	72.75	67.94
All	6,834	100.00	53.55	59.16	46.27
All	5,585	100.00	69.38	89.48	62.72
All	7,224	100.00	34.38	57.58	30.56
All	4,628	100.00	7.96	7.61	7.37
All	4,038	100.00	9.34	9.62	9.00
pos.	3,888	73.78	73.02	88.67	70.83
pos.	3,256	94.54	74.47	80.32	72.95
pos.	4,892	95.51	75.59	72.75	73.12
pos.	5,578	81.62	61.43	59.16	60.57
pos.	5,297	94.84	71.29	89.48	68.93
pos.	4,172	57.75	57.86	57.58	58.68
pos.	15	0.32	33.34	27.29	33.54
pos.	22	0.54	35.43	27.29	37.60

170814 CD19HSAD2_F1 00091077 084 [A] FL1 INT
170814 CD19HSAD2_C5 00091078 085 [A] FL1 INT
170814 CD19HSAD2_B15 00091080 087 [A] FL1 INT
170814 CD19HSAD2_B3 00091082 089 [A] FL1 INT
170814 CD19HSAD2_B1 00091079 086 [A] FL1 INT
170814 CD19HSAD2_A9 00091076 083 [A] FL1 INT
170814 CD19HSAD2_B15_wo_prim 00091073 080 [A] FL1 INT
170814 CHOK1 00091072 079 [A] FL1 INT

Figure 8.2.2.13.: flow cytometric analysis of clone pools F1, C5, B15, B3, B1, A9. Intracellular CD19-HSAD2 labelled with goat anti HSA antibody (1:100) as primary antibody and anti-goat-FITC antibody (1:100) as secondary antibody.

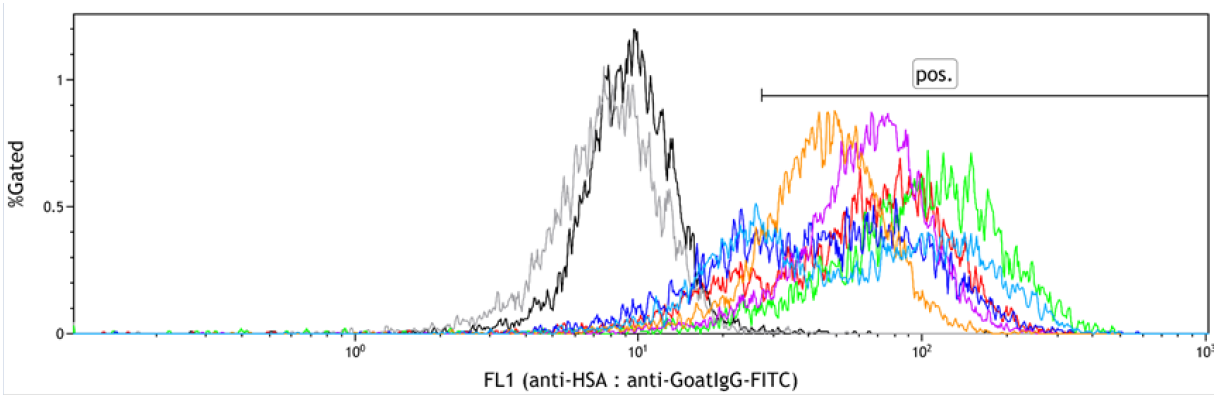

Marker	Number	%Gated	X-Med	X-Mode	X-GMean
All	6,770	100.00	54.97	25.86	49.89
All	6,686	100.00	45.89	46.40	42.62
All	7,229	100.00	65.38	66.50	59.25
All	4,891	100.00	45.48	63.57	40.79
All	3,281	100.00	100.74	146.74	83.17
All	5,552	100.00	64.16	59.69	51.67
All	4,628	100.00	7.96	7.61	7.37
All	4,038	100.00	9.34	9.62	9.00
pos.	4,848	71.61	87.28	27.29	80.18
pos.	5,745	85.93	49.58	46.40	50.19
pos.	6,706	92.77	68.01	66.50	66.23
pos.	3,416	69.84	65.07	63.57	64.73
pos.	3,074	93.69	105.72	146.74	100.27
pos.	4,460	80.33	76.03	59.69	73.05
pos.	15	0.32	33.34	27.29	33.54
pos.	22	0.54	35.43	27.29	37.60

170814 CD19HSAD2_P15 00091075 082 [A] FL1 INT
170814 CD19HSAD2_O12 00091081 088 [A] FL1 INT
170814 CD19HSAD2_M5 00091084 091 [A] FL1 INT
170814 CD19HSAD2_M4 00091083 090 [A] FL1 INT
170814 CD19HSAD2_J16 00091074 081 [A] FL1 INT
170814 CD19HSAD2_G9 00091085 092 [A] FL1 INT
170814 CD19HSAD2_B15_wo_prim 00091073 080 [A] FL1 INT
170814 CHOK1 00091072 079 [A] FL1 INT

Figure 8.2.2.14.: flow cytometric analysis of clone pools P15, O12, M5, M4, J16, G9. Intracellular CD19-HSAD2 labelled with goat anti HSA antibody (1:100) as primary antibody and anti-goat-FITC antibody (:100) as secondary antibody.

8.2.3 Single-cell subcloning of CHO-K1/CD19-HSAD2 pools by limiting dilution

On passage number 3, the 4 best clone pools of the initial transfection with pL_CD19-HSAD2 (= parental clone pools) were chosen for subcloning. The criteria for choosing the clone pools were mainly the CD19-HSAD2 titer in the supernatant, the growth rate as well as the flow cytometric result. For subcloning, each clone pool was diluted and seeded into one 384 well plate each to achieve an average number of 3 cells per well. The subcloning efficiency was determined on day 17 by counting the number of yellow wells and is shown in table 8.2.3.1. Additionally, the counted wells were transferred into 96 well plates for expansion and subsequent ELISA analysis (days of transfer can be seen in table 8.2.3.1). NOTE: wells of B1 were not transferred and therefore not used for the upcoming selection steps.

Table 8.2.3.1.: Subcloning efficiency of subcloning of CHO-K1/CD19-HSAD2 clones

Plate:	Subcloning efficiency (day 17):	Number of wells transferred:
P15	21%	80 (day 17)
J16	32%	124 (day 18)
B1	27%	106 (not transferred)
B3	29%	110 (day 20)

The best clones in terms of CD19-HSAD2 production were once again screened by performing a qualitative anti-HSA ELISA with the supernatant of the 96 well plates on day 24 after subcloning. The result of the ELISA analysis can be seen in table 8.2.3.2 (only the titers of the selected clones are shown). It is important to note that the titers of subclones coming from different parental clone pools can't be compared with each other since they were transferred from the 384 well plate to the 96 well plate on different days. The chosen clones were ultimately transferred into a fresh 96 well plate for expansion and then transferred into cultivation tubes.

Table 8.2.3.2.: Subclones of CHO-K1/CD19HSA-D2 selected by qualitative ELISA

Parental clone	Well position	CD19-HSAD2 [ng/ml]	Subclone code
P15	B6	8,64	1B6
P15	D8	8,50	1D8
P15	C10	8,44	1C10
P15	H11	11,42	1H11
J16	A3	13,47	2A3
J16	C12	13,13	2C12
J16	F7	30,06	3F7
J16	H11	19,61	3H11
B3	B3	11,29	5B3
B3	A11	11,40	5A11
B3	B12	11,46	5B12
B3	D11	10,49	5D11

8.2.4 Clone expansion and comparison of CHO-K1/CD19 HSAD2 subclones

After screening and expansion, the clones were cultivated in cultivation tubes for an extended amount of time by passaging them every 3-4 days into fresh CD-CHO “selection” medium.

Figures 8.2.4.1-8.2.4.2 show the results of the viable cell number, specific growth rates of the individual clones during the cultivation.
On passage number 5, a flow cytometric analysis was performed and the four best clones were chosen for continued cultivation (mainly based on CD19HSAD2 titer in the supernatant, specific productivity and growth rate).
Viable cell numbers up to ~9.5*10^6 could be achieved on passage number 4 by 5D11 and 1D8, with an average cell number of 6.16*10^6 among all clones through passage 3-7. Moreover, average growth rates of 0.94 d^{-1} with a maximum of 1.20 d^{-1} (1H11, passage number 2) were observed. Viabilities (not shown) never dropped below 90% and remained at a high average value of 98.5%.
After passage 7, clone 2C12 was chosen as main producer of CD19-HSAD2 based on its titer and specific productivity and was therefore kept in culture for another 12 passages (not shown in the graphs).
Additionally, 5 cryopreservation stocks of 2C12 were established on passage number 8.

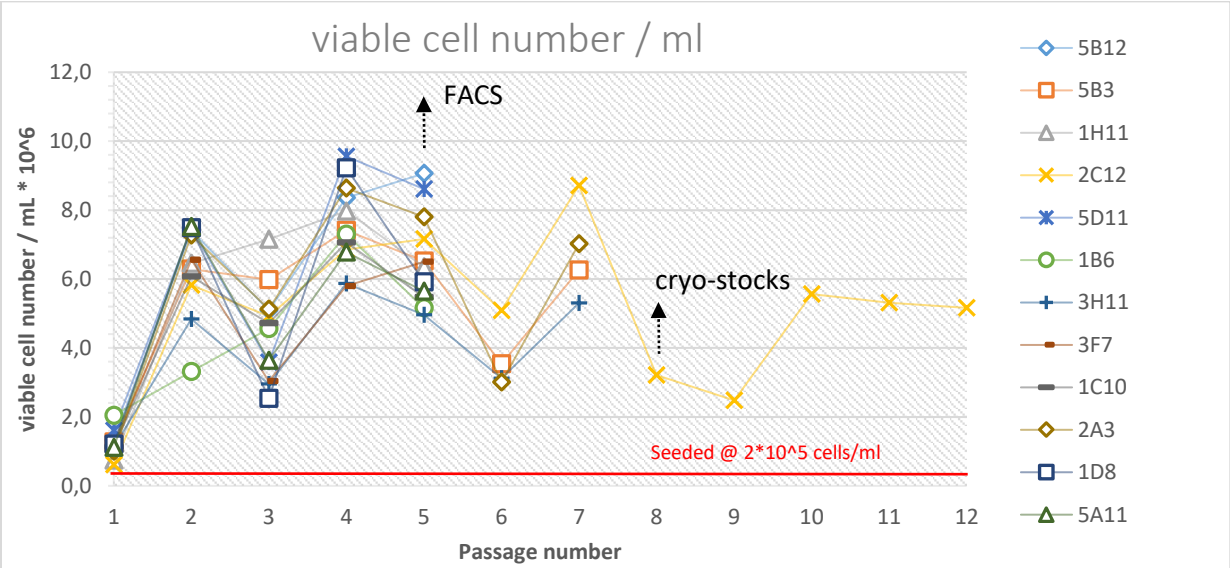

Figure 8.2.4.1.: viable cell numbers of CHO-K1/CD19-HSAD2 subclones cultured in CD-CHO selection medium containing 0.5 mg/mL G418

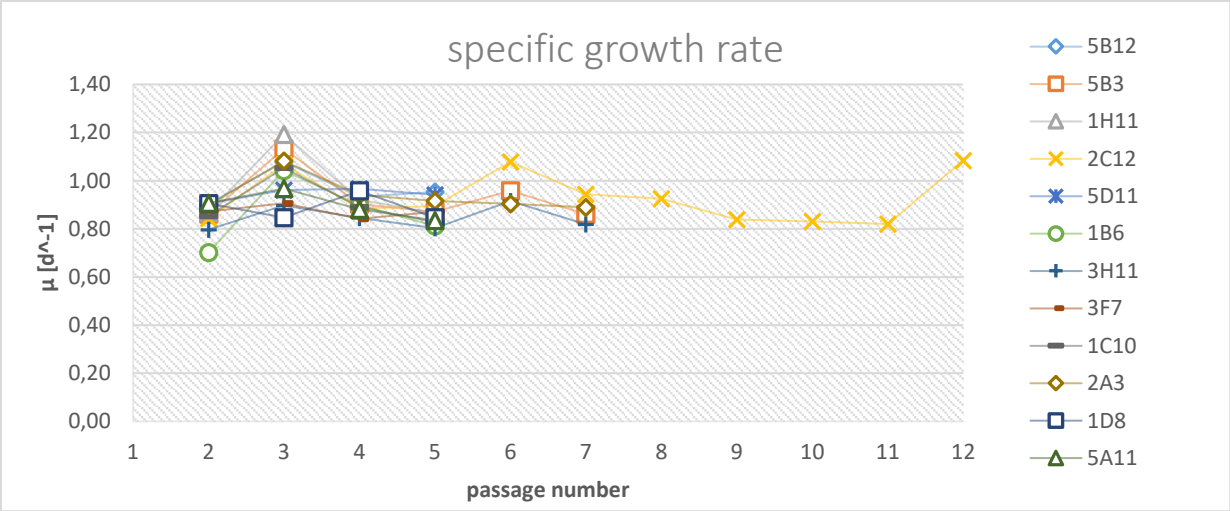

Figure 8.2.4.2.: specific growth rate of CHO-K1/CD19-HSAD2 subclones cultured in CD-CHO selection medium containing 0.5 mg/mL G418

During the passaging process, samples of the supernatant were taken to determine the concentration of CD19-HSAD2 via a quantitative anti-HSA ELISA; the results can be seen in figure 8.2.4.3 and 8.2.4.4

Passages 1-3 were analysed with the non-established ELISA and thus the titers cannot be compared with the values from passage 4 onward. Nonetheless, it could still be noticed that titers dropped during the first few passages until they settled in the range of 100 ng/ml (for the 2C12 clone), with specific productivities around 0.02 pg/cell/day. The conditions used for the ELISA can be seen in table 8.2.4.1.

Based on titers and specific productivities of CD19-HSAD2 on passage number 5, which can be seen in table 8.2.4.2, the 4 best clones (5B3, 2A3, 3H11, 2C12) were kept in culture and on passage number 7, 2C12 was ultimately chosen as the main CD19-HSAD2 producing clone.

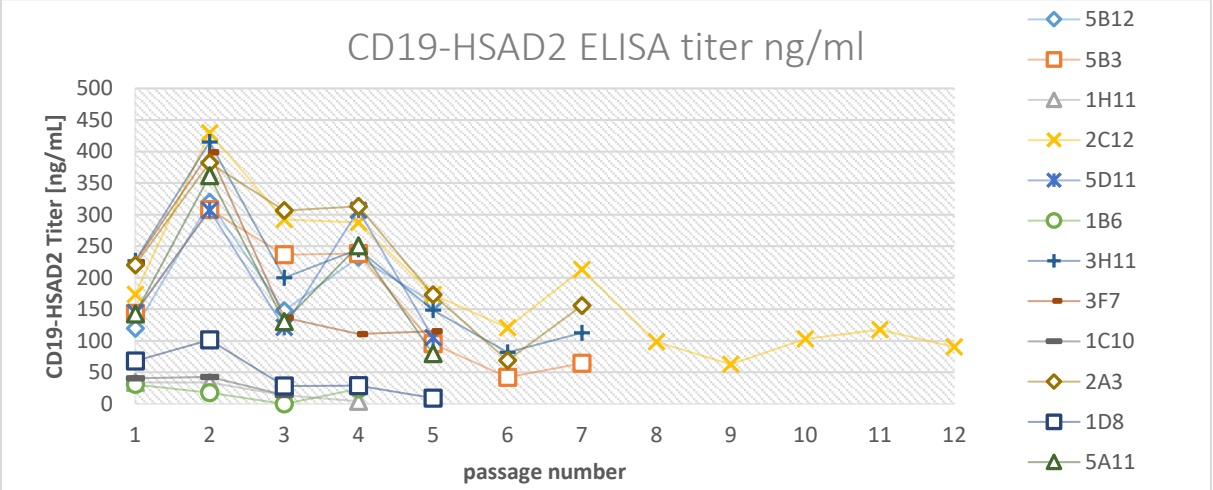

Figure 8.2.4.3.: CD19-HSAD2 titers from the supernatant of CHOK1/CD19HSAD2 subclones. Coating antibody: goat anti-HSA antibody. Conjugating antibody: goat anti-HSA-HRP antibody. Standard: HSA

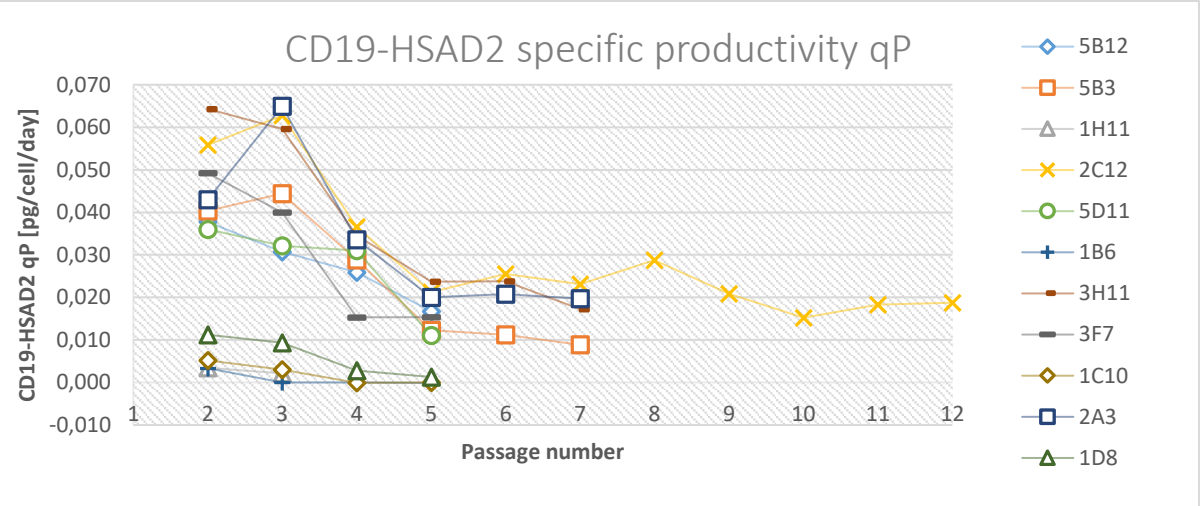

Figure 8.2.4.4.: specific productivity of CD19-HSAD2 of CHOK1/CD19-HSAD2 subclones

Table 8.2.4.1.: ELISA conditions for CHOK1/CD19-HSAD2 subclones

ELISA setup	Passage number
Coating antibody dilution: 1:1000 **Conjugating antibody dilution: 1:2000** **Sample dilution: 1:4** **Standard: 40 ng/ml**	1-3
Coating antibody dilution: 1:500 **Conjugating antibody dilution: 1:1000** **Sample dilution: 1:20** **Standard: 20 ng/ml** **NOTE: 2% PVP was used instead of BSA in the dilution buffer**	4-12

Table 8.2.4.2.: CD19-HSAD2 titers and productivities of subclone on passage number 5. Clones kept in culture are highlighted in green.

	CD19HSAD2 titer [ng/ml]	specific productivity [pg/cell/day]
5B12	161,02	0,017
5B3	95,35	0,012
1H11	<min	0,000
2C12	173,53	0,021
5D11	105,14	0,011
1B6	<min	0,000
3H11	148,80	0,024
3F7	114,92	0,015
1C10	<min	0,000
2A3	173,05	0,020
1D8	9,35	0,001
5A11	79,54	0,011

8.2.5 Intracellular HSA-D2 characterization by flow cytometry

In order to analyse the intracellular CD19-HSAD2 content as well as the homogeneity of the cell population, a flow cytometric analysis was performed on CD19-HSAD2 subclones which have been fixed with ethanol on passage number 5. Figure 8.2.5.1 shows the result of the analysis, with the negative control (untransfected CHO-K1) in orange as well as a sample (J16 parental clone) without a primary antibody in pink. Since both peaks are almost identical, the peak of the negative control is obscured by the pink colour of the sample without primary antibody. The “pos.” line includes all cells with a fluorescence signal higher than the highest 0.5% of the negative control which are therefore taken as “positive” in terms of intracellular CD19-HSAD2.

All samples display a very distinct peak with about the same fluorescence intensity (except for 5B3) which indicates that all clones consist of a very homogenous cell population and have the same amount of intracellular protein content. The parental clone pool J16 was also analysed with the subclone samples and shows the same homogeneity and intracellular product content as the subclones.

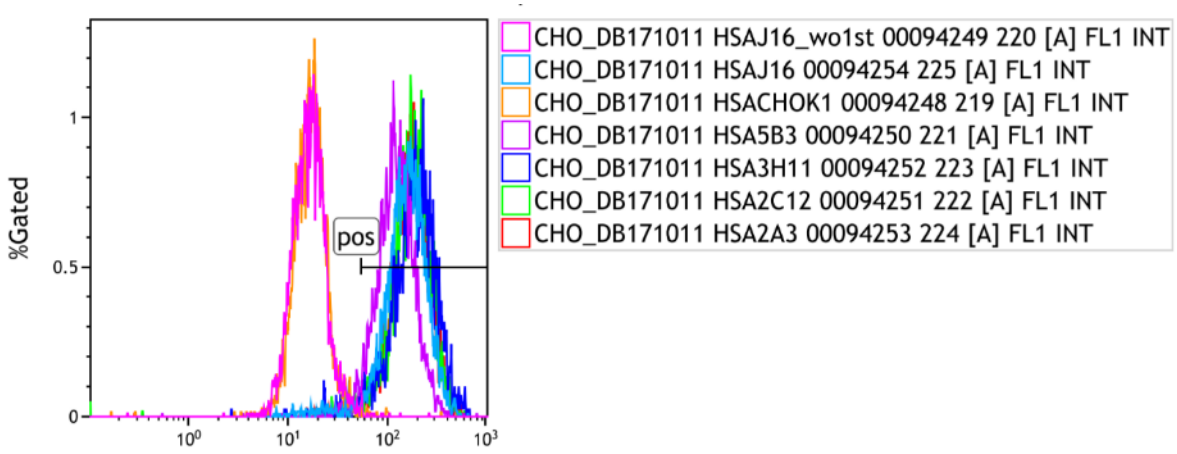

Marker	Number	%Gated	X-Med	X-Mode	X-GMean
All	3,050	100.00	16.38	16.20	16.02
All	3,831	100.00	158.59	162.00	144.61
All	2,316	100.00	16.94	18.21	16.45
All	3,791	100.00	122.38	116.14	118.19
All	1,376	100.00	190.96	183.74	175.01
All	1,981	100.00	177.60	217.98	163.19
All	3,290	100.00	173.70	185.40	163.77
pos	16	0.52	68.32	55.55	74.42
pos	3,677	95.98	162.02	162.00	158.18
pos	11	0.47	67.40	N/A	82.56
pos	3,651	96.31	125.00	116.14	124.13
pos	1,332	96.80	193.80	183.74	187.28
pos	1,934	97.63	180.12	217.98	175.47
pos	3,211	97.60	176.02	185.40	172.08

Figure 8.2.5.1.: Flow cytometric analysis of intracellular CD19HSAD2 in CHOK1/CD19HSAD2 subclones. Primary antibody: goat anti-HSA antibody (1:100). Secondary antibody: rabbit anti-goat-FITC antibody (1:100).

8.3 Recombinant cell line development for CHO-K1/CD19-Fc

8.3.1 Comparison of CHO-K1/CD19-Fc transfectant pools

CD19-Fc producing CHO-K1 clone pools have already been transfected, subcloned and selected previously. Here the resulting cell pools were monitored in shaking tubes for nine passages. In parallel, selected clone pools were also cultured in T25 Roux-flasks. Figures 8.1.3.1-8.1.3.3 show the viable cell numbers, the growth rates as well as the viabilities of these clone pools. Cells were passaged every 3-4 days into fresh CD-CHO "selection" medium.

Viable cell numbers up to $8*10^6$ cells/ml could be achieved for the N9 clone, with an average number of $3.95*10^6$ cells/ml among all clones (except for the T25 clones and CHOK1) during passage 2-9. The average specific growth rate was 0.8 d^{-1} and an average viability of 96.9% was achieved.

The untransfected CHO-K1 clone, displayed in red, shows similar growth behaviour compared to the best growing clone pool H21, however, the average viable cell number of $5.23*10^6$ and average growth rate of 0.94 d^{-1} were still higher than the average of the other transfected clone pools, probably due to the lack of stress induced by the recombinant protein production resulting in enhanced growth. In addition to the cultivation in tubes, the clone pools J5 and F1 were also grown in T25 Roux-Flasks, which are indicated by T25.J5 and T25.F1. With this cultivation method, much lower cell numbers and growth rates could be achieved (average viable cell number: $1.41*10^6$; average growth rates: 0.59 d^{-1}).

In the beginning, the F1 clone pools cultivated in tubes had some problems with growing properly compared to the other clone pools, which resulted in growth rates below 0.4 d^{-1} and cell numbers below $2*10^6$ cells/ml. On passage number 5, the growth rate increased to 0.74 d^{-1} and viable cell number increased to $3.81*10^6$ cell/ml.

On passage number number four, four cryopreservation stocks of K3, F1 and J5 were established and after passage 9, only N9 was kept in cultivation for another 10 passages which is not shown here; all the other clone pools except for the untransfected negative control CHO-K1 were removed from culture.

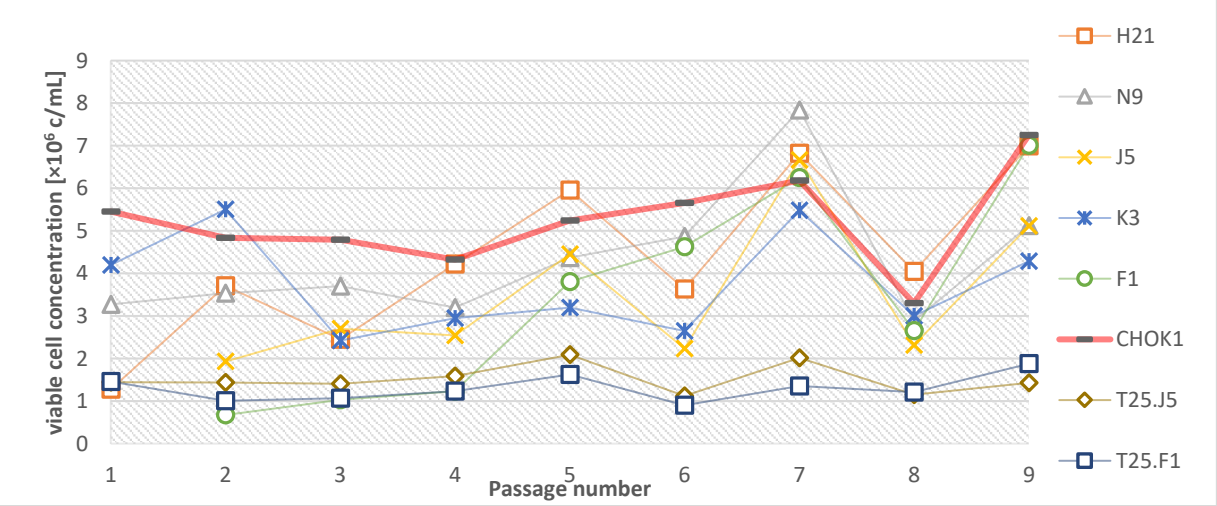

Figure 8.3.1.1.: Viable cell concentration of five CHO-K1/CD19-Fc clone pools cultured in CD-CHO selection medium containing 0.5 mg/mL G418.

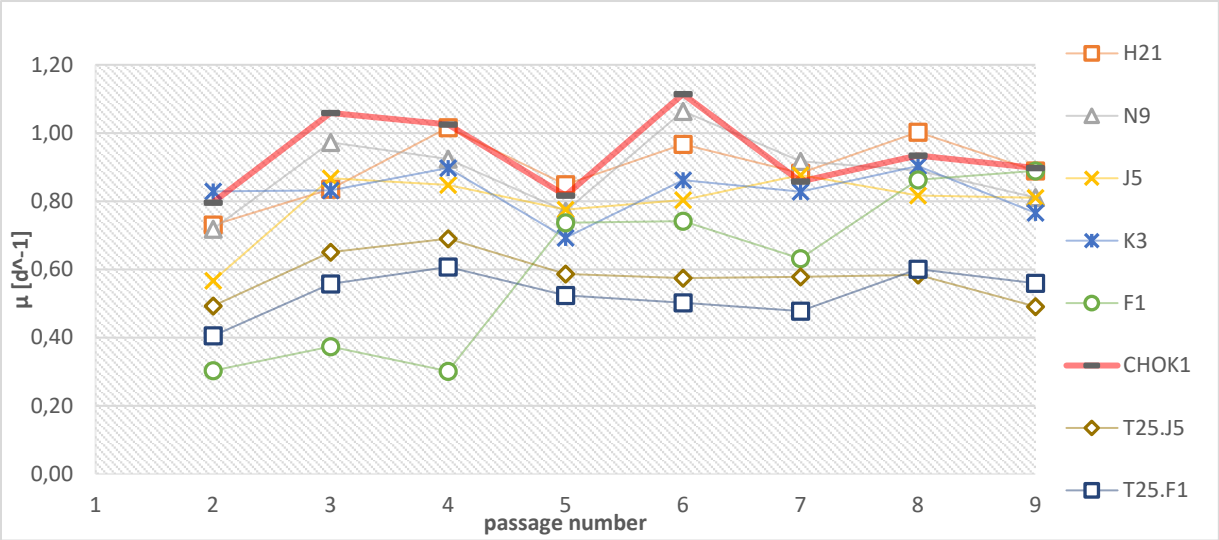

Figure 8.3.1.2.: specific growth rates of five CHO-K1/CD19-Fc clone pools cultured in CD-CHO selection medium containing 0.5 mg/mL G418

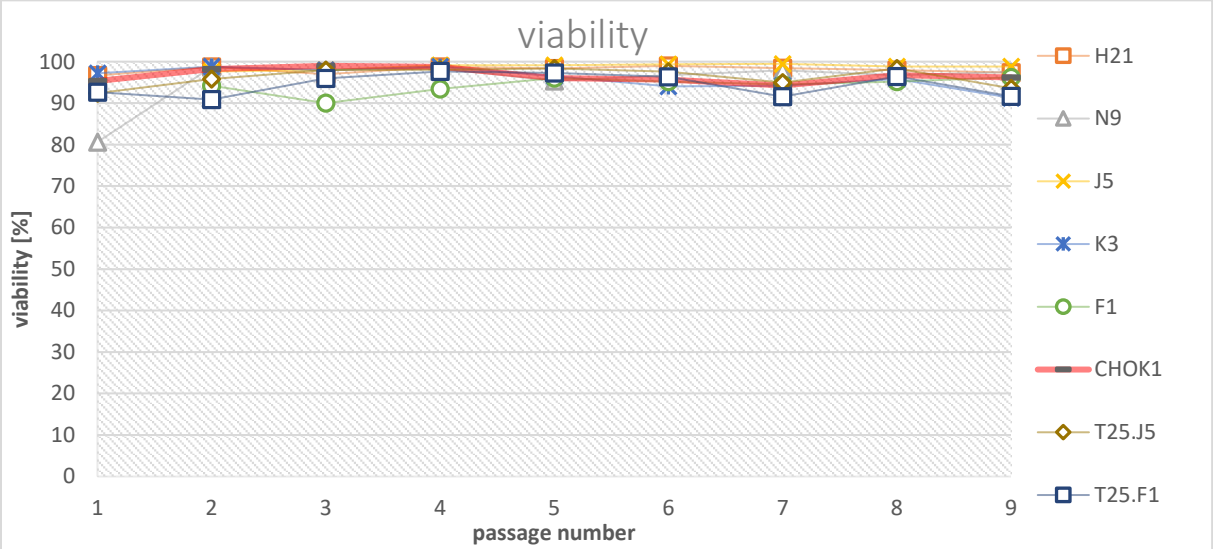

Figure 8.3.1.3 viabilities of five CHO-K1/CD19-Fc clone pools cultured in CD-CHO selection medium containing 0.5 mg/mL G418

During the passaging process, samples of the supernatant were taken to determine the concentration of CD19-Fc via an established quantitative anti-gamma-chain sandwich ELISA. The determined titers and calculated specific productivities are shown in figure 8.3.2.1 and 8.3.2.2 respectively.

Most clones achieved titers of about 50 ng/ml, with the exception of F1, which had a very steep increase in CD19-Fc production up to almost 290.67 ng/ml from passage 2-4 when growth was slow, followed by a drop down to 8.41 ng/ml until passage 9 with a concomitant increase in specific growth rate.

Specific productivities of about 0.01 pg/cell/day were calculated for most clones (figure 8.3.2.2). An exception is the T25.F1 clone which had lower growth rates, resulting in a higher specific productivity per cell (0.02-0.03 pg/cell/day from passage 2-5). Furthermore, the F1 clone cultivated in tubes could reach productivities up to 0.086 pg/cell/day due to the high titer and low cell number on passage number 4.

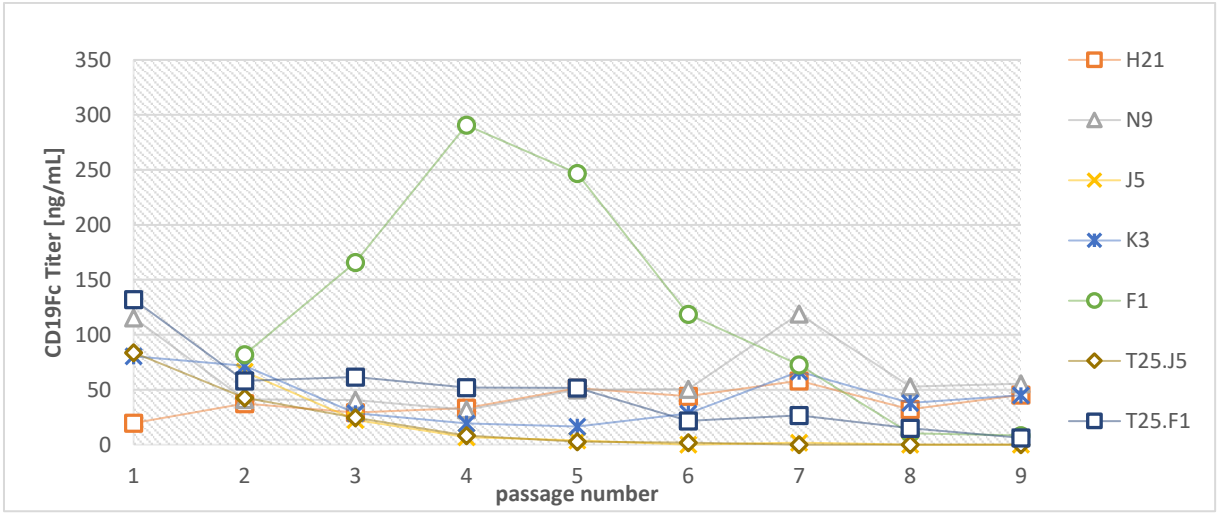

Figure 8.3.1.4..: CD19-Fc titers from the supernatant of five CHO-K1/CD19-Fc clone pools. Coating antibody: goat anti-human gamma chain antibody (1:2000). Conjugating antibody: goat anti-human gamma chain HRP antibody (1:2000). Standard: 3D6-scFv-Fc 40 ng/ml, samples diluted 1:4

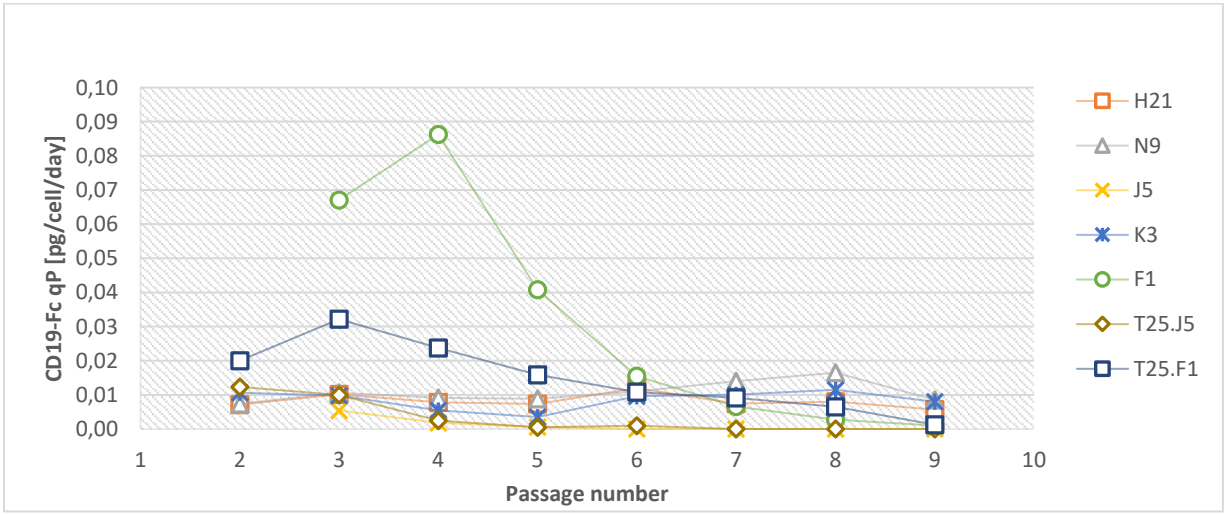

Figure 8.3.1.5.: specific productivity of five CD19-Fc of CHO-K1/CD19-Fc clone pools

During the later phases of the cultivation of N9, there was slow but steady decrease in viability of the N9 over 10 passages and a simultaneous increase in CD19-Fc titer which is shown in figure 8.3.2.3. The viability dropped from almost 100% on passage 9 down to about 50% on passage number 19, accompanied by a 3-fold increase in CD19-Fc titer at the same time. Furthermore, the specific productivity seen in figure 8.3.2.5 also increases from 0.01 pg/cell/day to 0.06 pg/cell/day.

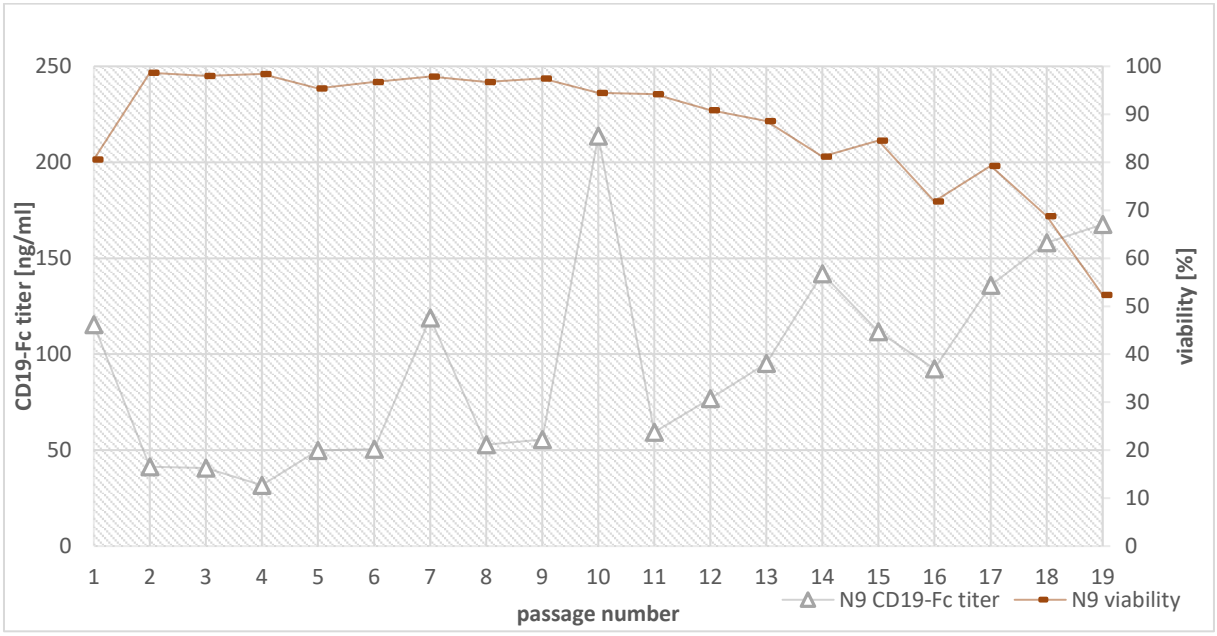

Figure 8.3.2.3.: CD19-Fc titer in relation to the viability of the N9 clone pools. CD19-Fc titer determined via ELISA: Coating antibody: goat anti-human gamma chain antibody (1:2000). Conjugating antibody: goat anti-human gamma chain HRP antibody (1:2000). Standard: 3D6-scFv-Fc 40 ng/ml, samples diluted 1:4 (passage 1-9 see also previous figure)

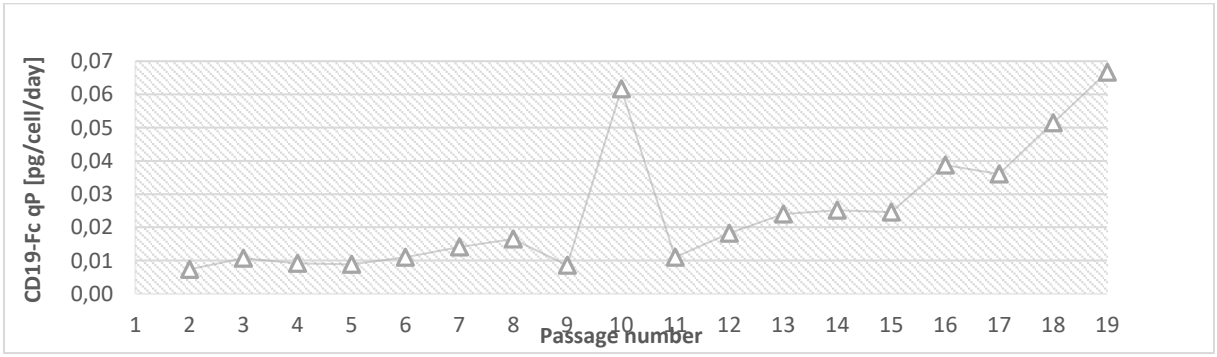

Figure 8.3.2.4.: CD19-Fc specific productivity of N9

8.3.2 Single-cell subcloning of CHO-K1/CD19-Fc/H21 pools by limiting dilution

Based on previous work, the H21 clone pool had already been chosen for subcloning by seeding two 384 well plates with 1 and 3 cells per well (on average). On day 19 after seeding, the subcloning efficiency was calculated for both 384 wells plates by counting the yellow wells that were subsequently transferred into a 96 well plate (plate 1) on the same day. A second 96 well plate (plate 2) was seeded from the 1cell/well on day 25.

Table 8.3.2.1.: Subcloning efficiency of H21 subcloning

Plate:	Subcloning efficiency (day 19):	Number of wells transferred:
H21 (1cell/well)	7%	28 (day 19) + 96 (day 25)
H21 (3cells/well)	16%	62 (day 19)

For the screening of the best H21 subclones, a qualitiative anti-gamma-chain sandwich ELISA was performed on day 7 after transfer of the clones to the 96 well plates. The result of the ELISA as well as the chosen subclones which are highlighted in green can be seen in table 8.3.2.2 for plate 1 and 8.3.2.3 for plate 2.

Table 8.3.2.2.: Result of the qualitative anti-gamma-chain ELISA of the 96 well plate seeded on day 19 (plate 1). Clones chosen for expansion are highlighted in green. Coating antibody: goat anti-human gamma chain antibody (1:2000). Conjugating antibody: goat anti-human gamma chain HRP antibody (1:2000). Standard: 3D6-scFv-Fc 40 ng/ml, samples diluted 1:10

ng/ml	1	2	3	4	5	6	7	8	9	10	11	12
A	<min	<min	<min	<min	<min	<min	<min	74,59	37,15	55,21	55,16	68,90
B	<min	52,42	34,43	40,83	<min	26,63	58,82	67,50	18,58	62,99	41,47	5,65
C	52,36	79,98	53,75	86,53	45,27	61,64	54,93	9,36	72,51	20,03	39,97	32,86
D	75,91	73,14	48,18	35,88	70,38	<min	73,01	62,95	65,56	70,55	38,94	65,82
E	57,30	10,07	57,78	75,18	35,99	22,15	47,62	69,67	55,07	6,39	36,90	82,90
F	18,84	42,84	60,95	55,46	4,85	54,54	43,39	74,86	19,43	29,76	56,46	15,78
G	74,64	30,39	68,62	73,01	64,45	16,82	15,77	69,00	23,98	61,92	77,70	89,68
H	28,10	16,16	44,05	58,76	17,76	27,09	46,29	42,13	49,63	41,81	54,83	27,98

Table 8.3.2.3.: Result of the qualitative ELISA of the 96 well plate seeded on day 25 (plate 2). Clones chosen for expansion are highlighted in green. Coating antibody: goat anti-human gamma chain antibody (1:2000). Conjugating antibody: goat anti-human gamma chain HRP antibody (1:2000). Standard: 3D6-scFv-Fc 40 ng/ml, samples diluted 1:10

ng/ml	1	2	3	4	5	6	7	8	9	10	11	12
A	24,13	82,47	<min	9,19	53,61	76,19	76,68	34,77	75,54	24,09	39,68	52,90
B	48,01	45,28	59,23	80,26	4,42	59,91	30,20	70,01	63,96	40,31	75,03	53,36
C	57,16	26,39	62,64	89,16	0,00	58,51	63,46	34,99	<min	44,02	78,20	51,55
D	45,67	36,83	4,59	77,02	46,21	31,03	52,39	39,83	51,59	29,19	61,18	50,87
E	27,24	21,80	20,53	35,45	56,42	<min	47,51	58,94	55,15	70,18	49,73	85,81
F	51,18	44,77	65,36	34,30	48,58	48,89	<min	48,38	55,54	33,13	50,94	30,06
G	34,42	42,63	56,22	31,74	<min	66,06	59,21	27,67	43,38	39,33	43,95	28,40
H	35,87	51,12	57,43	8,19	52,61	37,17	65,51	40,34	32,47	36,50	47,29	53,40

8.3.3 Clone expansion and comparison of CHO-K1/CD19-Fc/H21subclones

Clones chosen by the qualitative ELISA were transferred into a 96 well plate for expansion and afterwards cultivated in cultivation tubes for an extended time period by passaging them every 3-4 days into fresh CD-CHO “selection” medium.

Figure 8.3.3.1-8.3.3.3 show the results of the viable cell number, growth rates and viabilities of the two best subclones CHO-K1/CD19-Fc/H21/1G4 and -/1C9, chosen based on product titer, specific productivity and growth rate in comparison to their parental clone H21. The clones displayed here were all taken from the first subcloning plate of 8.3.2.

The cell numbers (8.3.3.1) of 1G4 and 1C9 were ranging between $2*10^6$ and $7*10^6$, with 1G4 usually achieving higher numbers than the 1C9 clone. The parental clone H21 grew to similar cell numbers. In terms of specific growth rate (8.3.3.2), 1G4 could reach the highest values up to 1.12 d^{-1} on passage number 9 and 1C9 dropped down to 0.62 d-1 on passage number 7. Most of the time growth rates were ranging between 0.8 d^{-1} and 1.0 d^{-1}, which lies in the same range as the parental clone H21. Viabilities (8.3.3.3) were above 90% for most of the time during the cultivation, except for 1G4 dropping down to 86% on passage number 11 and 1C9 having only 72% on passage number 10, which was the reason why 1G4 was chosen as the main final CD19-Fc clone at this timepoint.

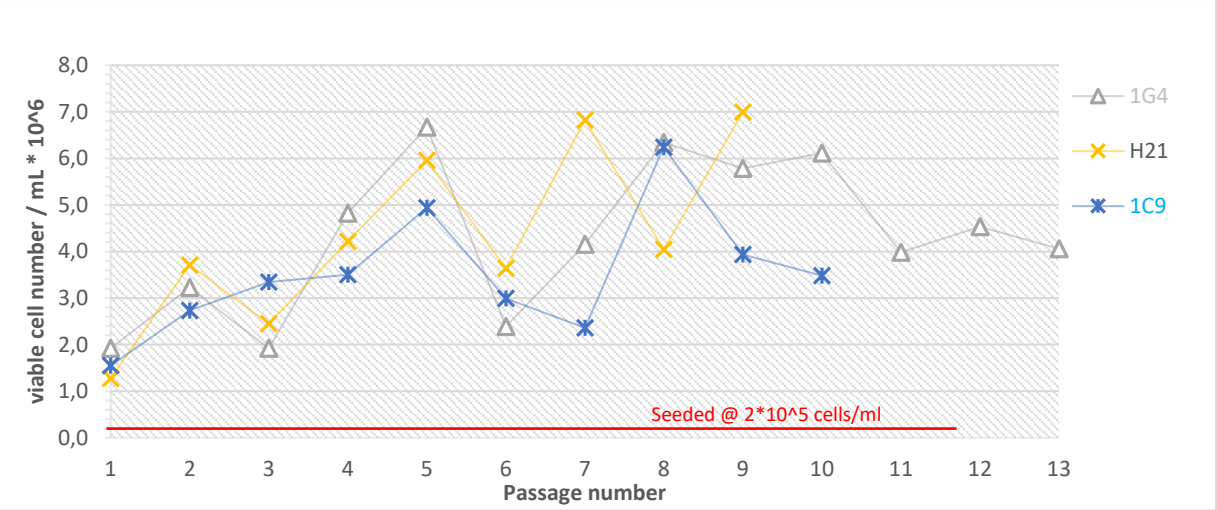

Figure 8.3.3.1.: Viable cell numbers of the CHO-K1/CD19-Fc/H21 subclones 1G4 and 1C9 was well as the parental clone H21 cultured in CD-CHO selection medium containing 0.5 mg/mL G418

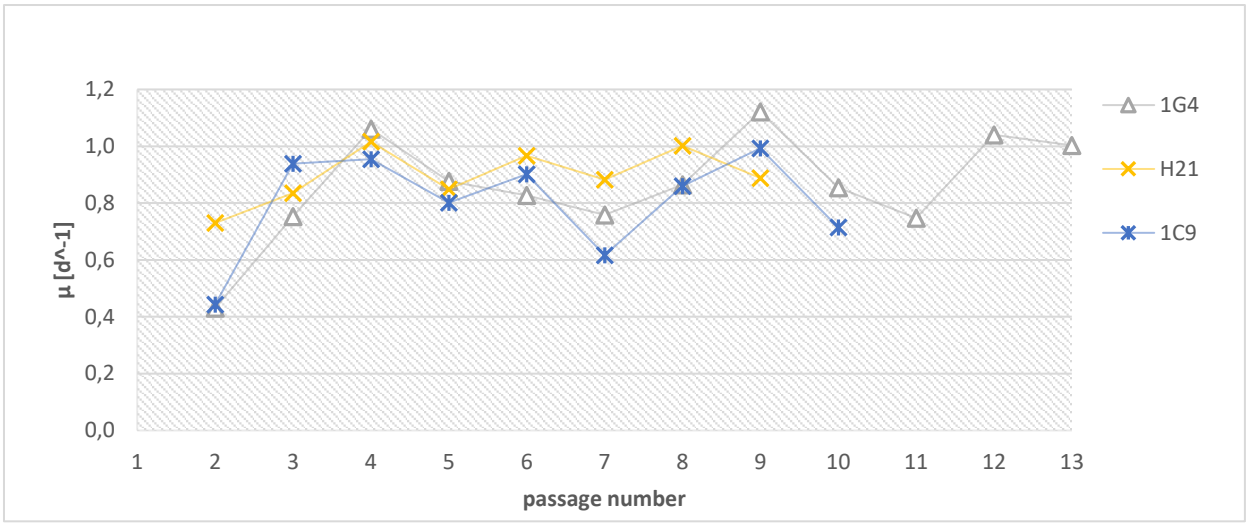

Figure 8.3.3.2.: Specific growth rate of the CHO-K1/CD19-Fc/H21 subclones 1G4 and 1C9 was well as the parental clone H21 cultured in CD-CHO selection medium containing 0.5 mg/mL G418

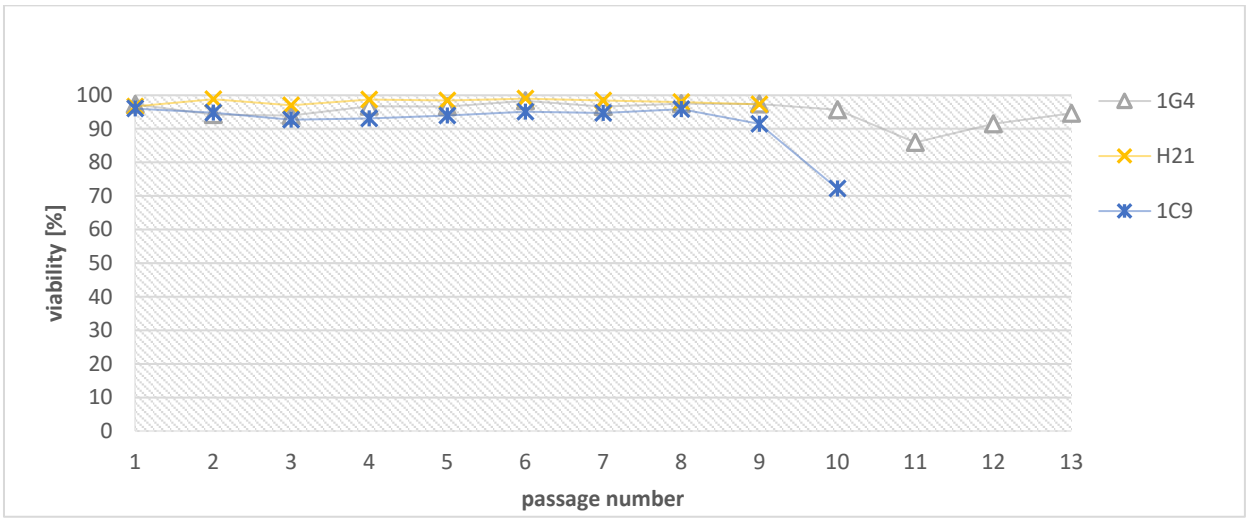

Figure 8.3.3.3.: Viabilities of the CHO-K1/CD19-Fc/H21 subclones 1G4 and 1C9 was well as the parental clone H21 cultured in CD-CHO selection medium containing 0.5 mg/mL G418

During the passaging process, samples of the supernatant of the two CD19-Fc producing subclones 1G4 and 1C9 were taken to determine the concentration of CD19-Fc via a quantitative anti-gamma-chain sandwich ELISA. The determined titers and calculated specific productivities are shown in figure 8.3.3.4 and 8.3.3.5 and are compared to the parental clone H21.

Titers were ranging between 100 ng/ml and 150 ng/ml at the beginning of the cultivation but were then dropping to 50-100 ng/ml for the 1G4 clone. Most of the time 1C9 could achieve higher titers than 1G4, which on the other hand had better growth properties. The parental clone pool H21 performed significantly worse, with titers never exceeding 58 ng/ml. Specific productivities of H21 were also lower with 0.01 pg/cell/day compared to 0.02-0.04 pg/cell/day of the subclones. Again, the 1C9 clone could outperform 1G4, but was still removed from culture on passage number 10 due to a significant drop in viability (figure 8.3.4.3).

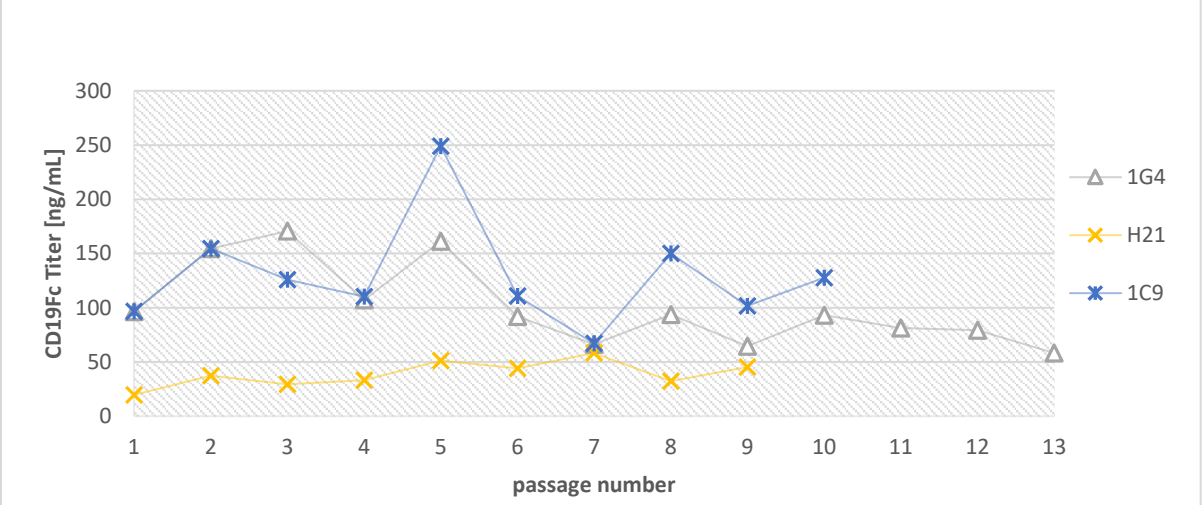

Figure 8.3.3.4.: CD19-Fc titer of the two best CHO-K1/CD19-Fc/H21 subclones 1C9 and 1G4. ELISA: Coating antibody: goat anti-human gamma chain antibody (1:2000). Conjugating antibody: goat anti-human gamma chain HRP antibody (1:2000). Standard: 3D6-scFv-Fc 40 ng/ml, samples diluted 1:4.

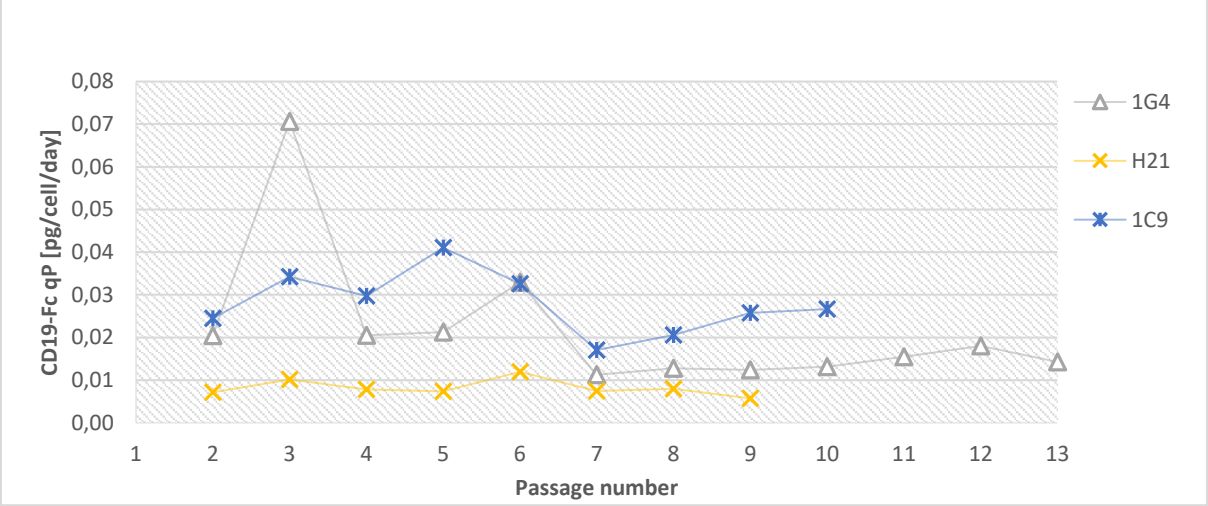

Figure 8.3.3.5.: CD19-Fc specific productivity of the two best CHO-K1/CD19-Fc/H21 subclones 1C9 and 1G4

8.3.4 Intracellular product content of CHOK1/CD19-Fc/H21 subclones 1C9 and 1G4 via flow cytometry

Figure 8.3.4.1 shows the result of the flow cytometric analysis of ethanol-fixed and stained CD19-Fc producing parental (H21) cells and derived subclone cells (1G4, 1C9), which allowed the comparison of intracellular product content as well as clone homogeneity. The green curve displays an untransfected but stained CHO-K1 as a negative control, with the "pos" marker gating the fluorescence signal in which only 0.5% of the CD19-Fc negative cells are included. In terms of homogeneity, the parental as well as the subclones displayed a very homogenous population indicated by the very narrow and symmetrical peaks, which is also indicated by similar mode, geometric mean and median values. For all staining procedures the same number of cells was used. H21 showed a lower intracellular product peak correlating with lower product secreted into the culture supernatant.

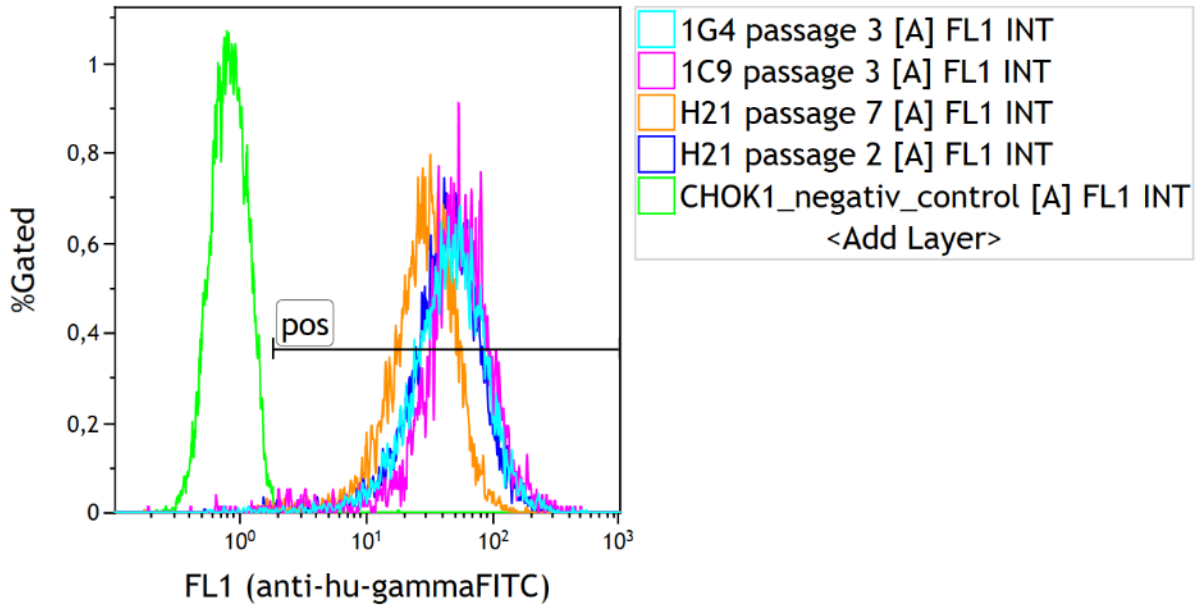

Marker	Number	%Gated	X-Med	X-Mode	X-GMean
All	7.181	100,00	46,54	67,10	43,62
All	2.594	100,00	53,62	54,07	49,07
All	6.565	100,00	29,52	25,86	27,55
All	4.970	100,00	44,19	41,66	41,79
All	7.090	100,00	0,83	0,75	0,82
pos	7.152	99,60	46,69	67,10	44,28
pos	2.574	99,23	53,80	54,07	50,60
pos	6.534	99,53	29,61	25,86	27,95
pos	4.957	99,74	44,28	41,66	42,16
pos	39	0,55	2,13	2,07	2,54

Figure 8.3.4.1.: Anti-gamma-FITC staining and flow cytometric analysis of parental CHO-K1/CD19-Fc/H21 and subclones 1G4 and 1C9

8.4 Pseudoperfusion cultivation of CHO-K1/CD19-Fc/H21/1G4

The aim of the pseudoperfusion cultivation experiments with the established main-producer of CD19-Fc (CHO-K1/CD19-Fc/H21/1G4), was to achieve very high cell numbers by daily media exchange, and in turn to produce higher amounts of CD19-Fc compared to traditional cell passaging every 3-4 days. For the experiment, different media as well as a "cell bleeding" approach were tested. 20% of the cells were removed each day in the bleeding strategy to prevent them from being in a real stationary phase, which may yield higher product titers by maintained productivities.

Figures 8.4.1.1-8.4.1.5 show the result of the pseudoperfusion using the CHO-K1/CD19-Fc/H21 1G4 subclone in either CDM4HEK293 medium or CD-CHO medium without any cell-bleed. During the first 3 days, no medium was exchanged and the cells were grown in a typical batch culture. The removed culture supernatant was collected each day and used for purification by protein A affinity chromatography.

Viable cell numbers up to $32.12*10^6$ cells/ml for the CDM4-HEK293 medium and $25.97*10^6$ cells/ml for the CD-CHO medium could be achieved on day 7, with growth rates of about 0.5 d^{-1}during the exponential growth phase from day 4-6. After day 7, a stationary state was reached and growth rates dropped to zero and below.

CD19-Fc titers also reached their maximum of 120-140 ng/ml on day 7, which correlates with the high cell numbers achieved on this day. Afterwards, titers dropped below 100 ng/ml, with titers being lower for cells grown in CDM4HEK293 compared to CD-CHO. Furthermore, it should be noted that these titers were achieved within one day of cultivation and therefore, a higher total amount of product (about 50 µg of CD19-Fc with both pseudoperfusions) could be produced in the same time period compared to cell passaging every 3-4 days.

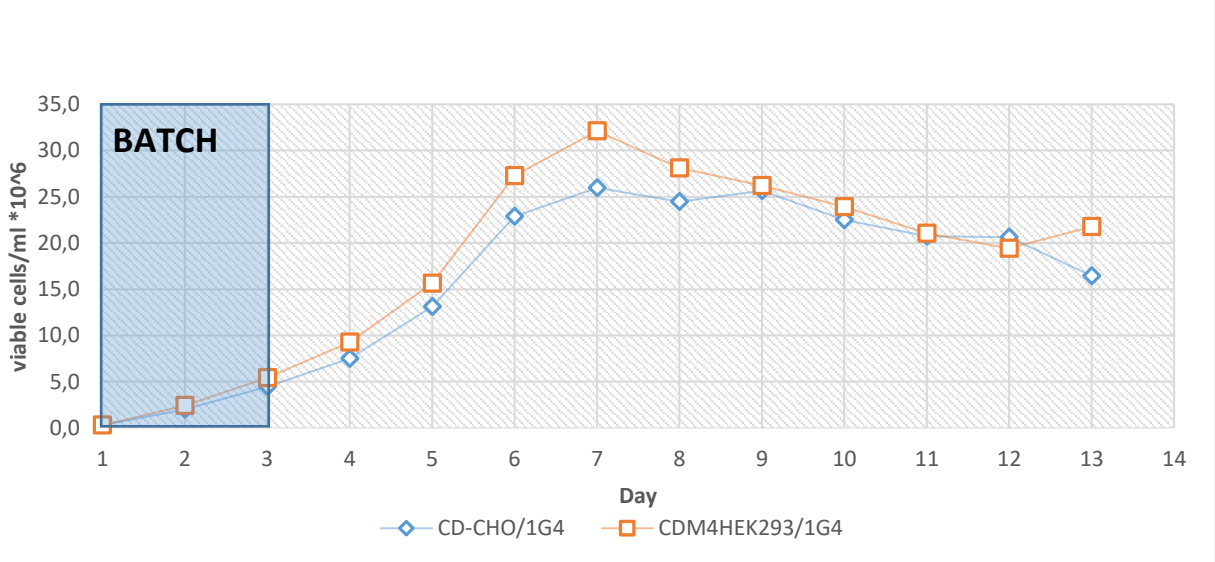

Figure 8.4.1.1.: viable cell numbers of pseudoperfusion in CD-CHO and CDM4HEK293 medium

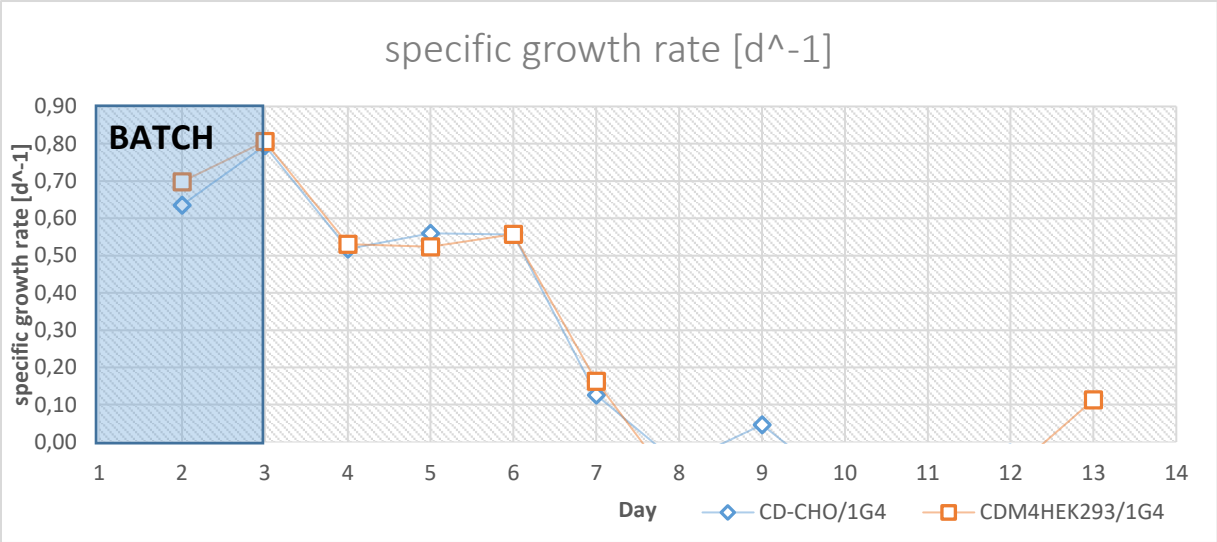

Figure 8.4.1.2.: specific growth rates of pseudoperfusion in CD-CHO and CDM4HEK293 medium

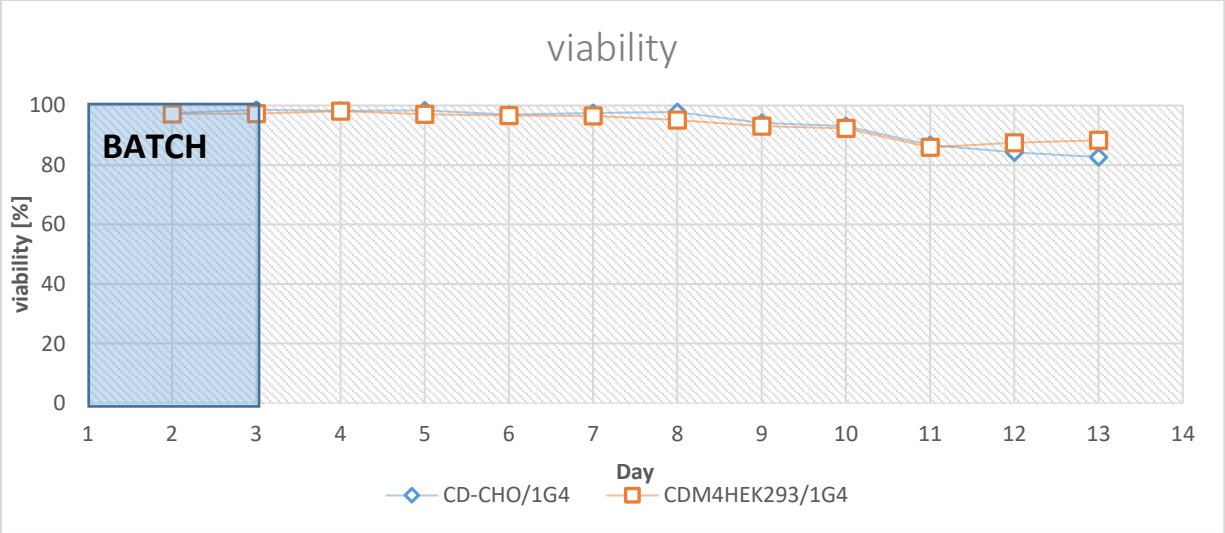

Figure 8.4.1.3.: viabilities of pseudoperfusion in CD-CHO and CDM4HEK293 medium

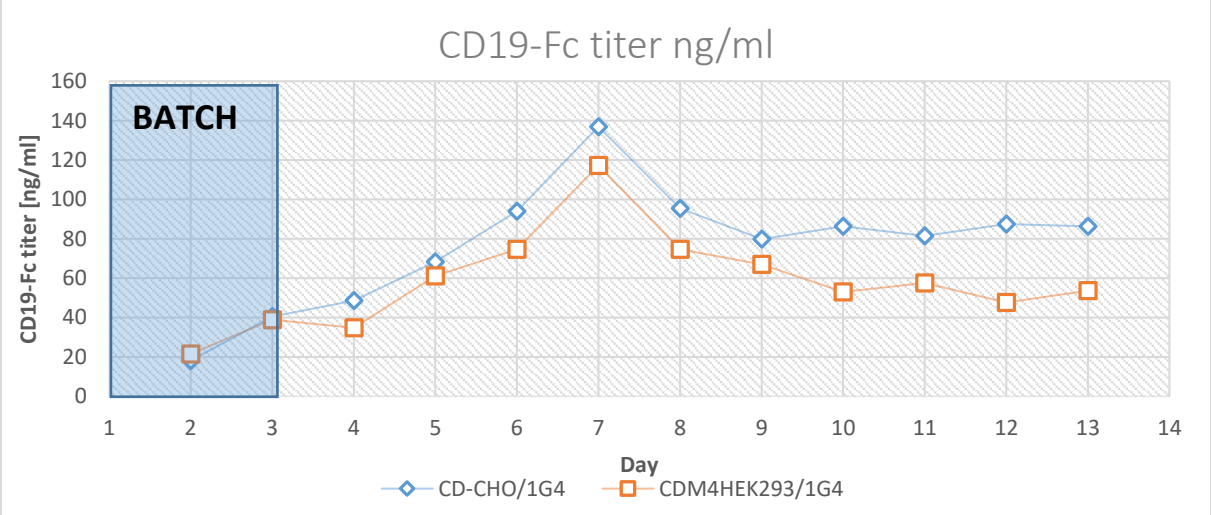

Figure 8.4.1.4 CD19-Fc titer of pseudoperfusion in CD-CHO and CDM4HEK293 medium. ELISA: Coating antibody: goat anti-human gamma chain antibody (1:2000). Conjugating antibody: goat anti-human gamma chain HRP antibody (1:2000). Standard: 3D6-scFv-Fc 40 ng/ml, samples diluted 1:4

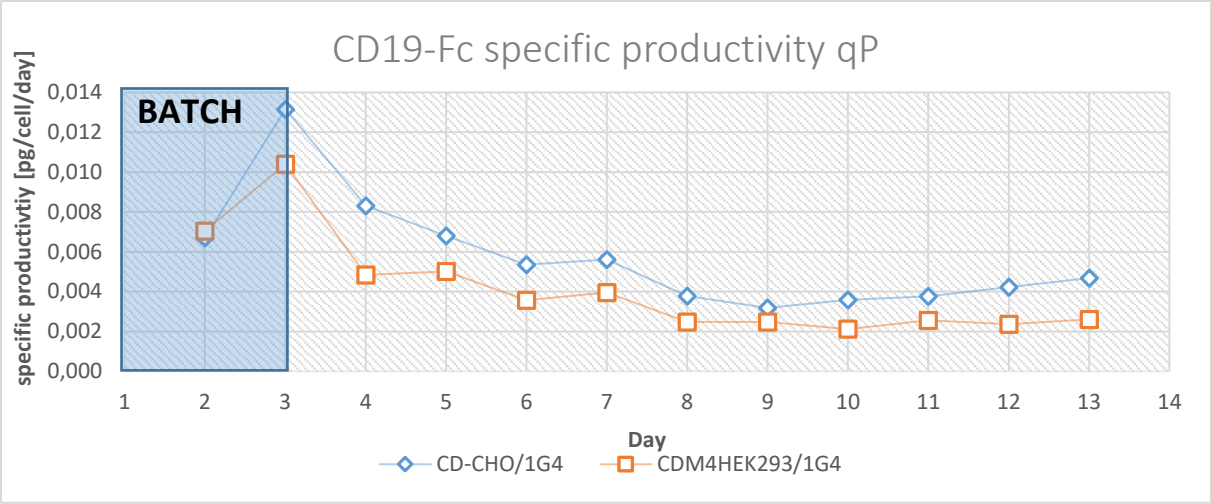

Figure 8.4.1.5 CD19-Fc specific productivity of pseudoperfusion in CD-CHO and CDM4HEK293 medium. ELISA: Coating antibody: goat anti-human gamma chain antibody (1:2000). Conjugating antibody: goat anti-human gamma chain HRP antibody (1:2000). Standard: 3D6-scFv-Fc 40 ng/ml, samples diluted 1:4

Figures 8.4.1.6-8.4.1.10 show the result of the pseudoperfusion using the 1G4 CD19-Fc subclone in either CDM4NS0 + 16.5 g/L glucose medium or CDM4NS0 + CB 1&3 medium with additional cell-bleeding (both with 4mM Gln, 0.5 mg/ml G418 and phenol red). During the first 3 days, no medium was exchanged and the cells were grown in a typical batch culture. The removed medium was again collected every day and later on used for protein A chromatography purification.

Starting on day 5, cell bleeding was applied and on day 7 the highest cell number of $26.55*10^6$ cells/ml was obtained. From then on, the cell number decreased by 20% every day, which indicates they were not able to re-grow by 20% until the next day. On day 14, cell numbers decreased to $6\text{-}7*10^6$ cells/ml, however viabilities never dropped below 90% during the entire experiment. After the exponential growth phase from day 3 to 7, the specific growth phase dropped from 0.5-0.7 d^{-1} to near zero, which again indicates a non-existent cell division after the exponential phase. However, an increase in average cell diameter from 16 µm to 19 µm can be seen from day 3 to 14, showing a slight growth in cell size.

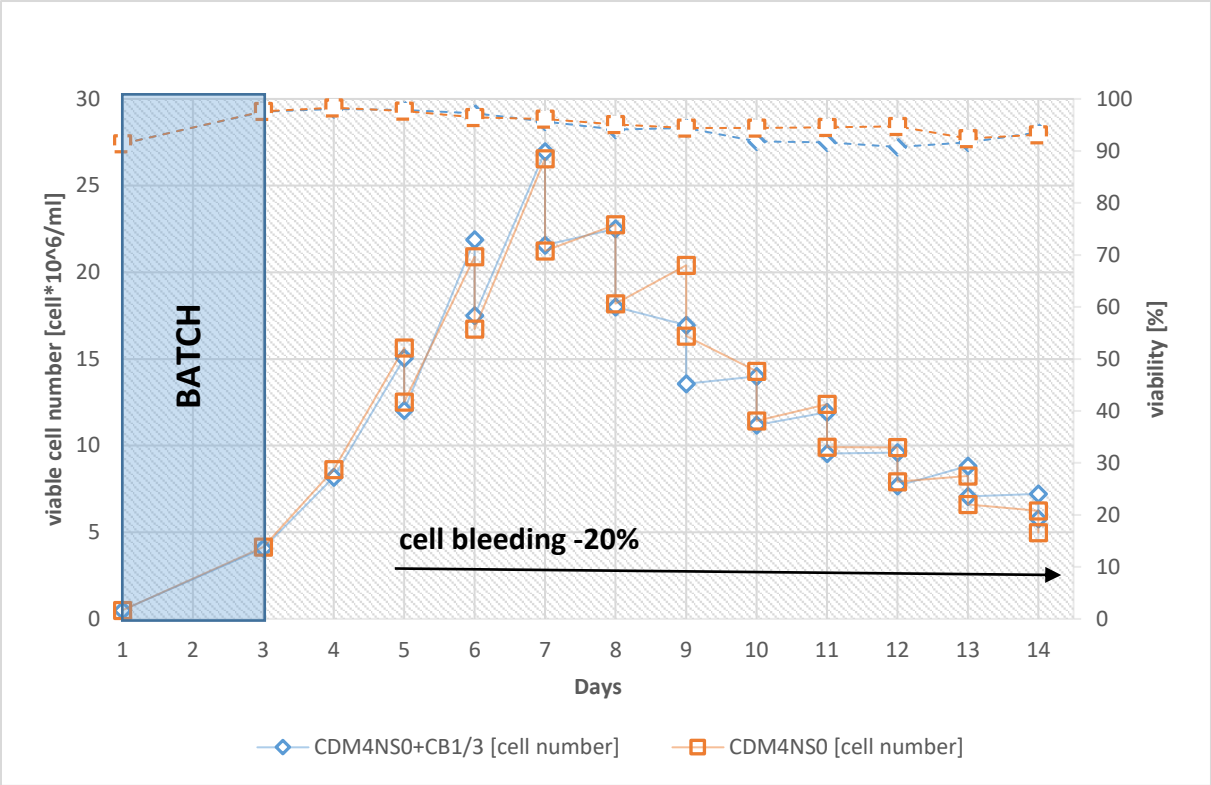

Figure 8.4.1.6.: viable cell number and viability of CD19-Fc/1G4 clones cultivated in pseudoperfusion with CDM4NS0 and CDM4NS0+CB1/3 medium.

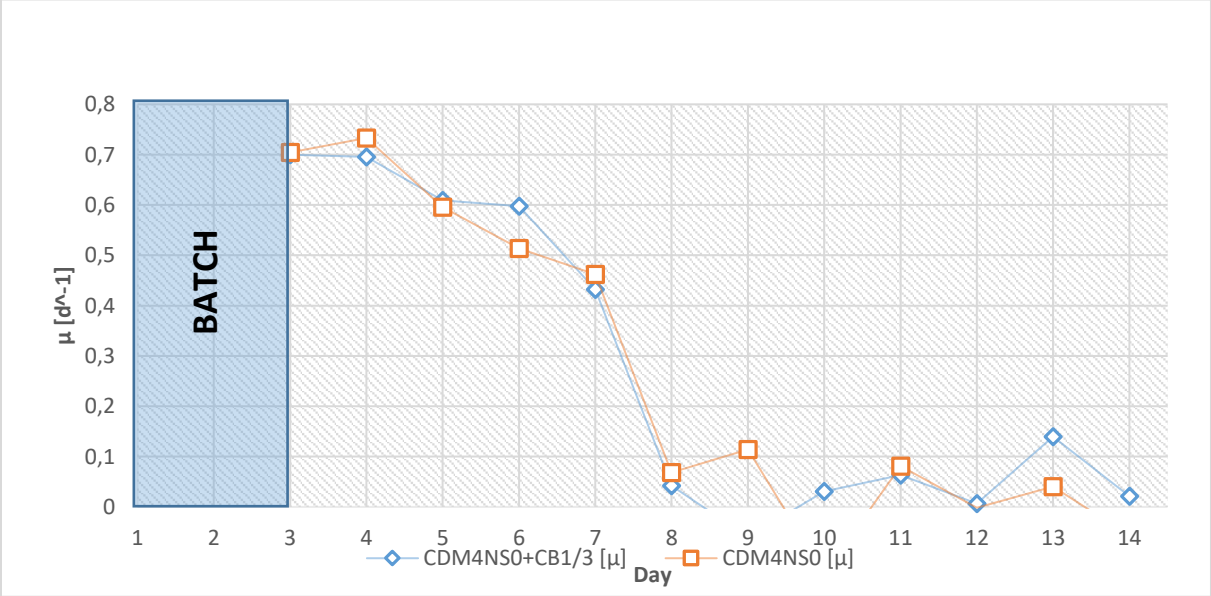

Figure 8.4.1.7.: specific growth rate of CD19-Fc/1G4 clones cultivated in pseudoperfusion with CDM4NS0 and CDM4NS0+CB1/3 medium

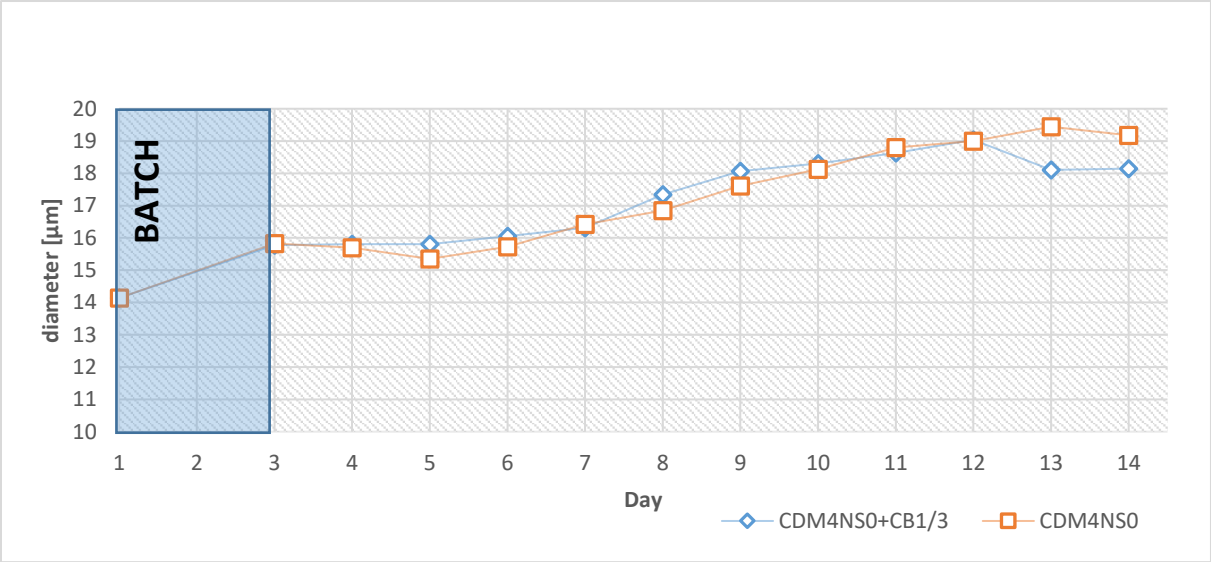

Figure 8.4.1.8.: average diameter of CD19-Fc/1G4 clones cultivated in pseudoperfusion with CDM4NS0 and CDM4NS0+CB1/3 medium. Measured via Vi-Cell™ XR Cell Counter

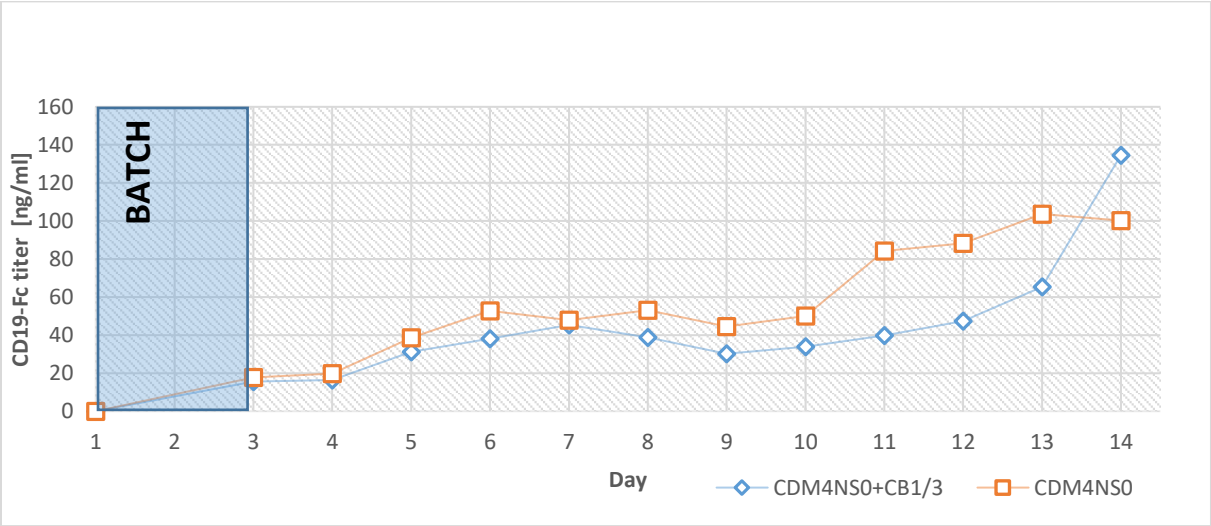

Figure 8.4.1.9.: CD19-Fc titer of CD19-Fc/1G4 clones cultivated in pseudoperfusion with CDM4NS0 and CDM4NS0+CB1/3 medium. ELISA: Coating antibody: goat anti-human gamma chain antibody (1:2000). Conjugating antibody: goat anti-human gamma chain HRP antibody (1:2000). Standard: 3D6-scFv-Fc 40 ng/ml, samples diluted 1:4

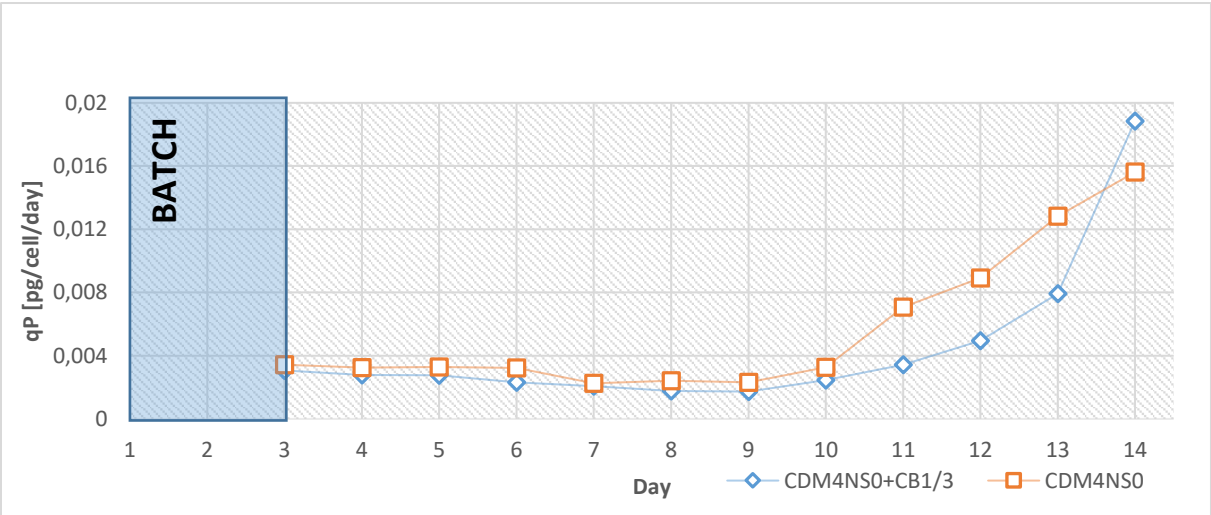

Figure 8.4.1.10.: CD19-Fc specific productivity of CD19-Fc/1G4 clones cultivated in pseudoperfusion with CDM4NS0 and CDM4NS0+CB1/3 medium

In order to check whether there was a change of intracellular CD19-Fc content or cell population homogeneity, a flow cytometric analysis was performed on every second day of the pseudoperfusion experiment in CDM4HEK293 and CD-CHO medium. Figure 8.4.2.1 shows the result of flow cytometric analysis with an untransfected negative control in green and the different days of cultivation in different colours. All the peaks display the same symmetrical shape and at about the same fluorescence intensity, indicating that there is no change in intracellular CD19-Fc content and cell population homogeneity (also indicated by similar mode, geometric mean and median values) throughout the cultivation.

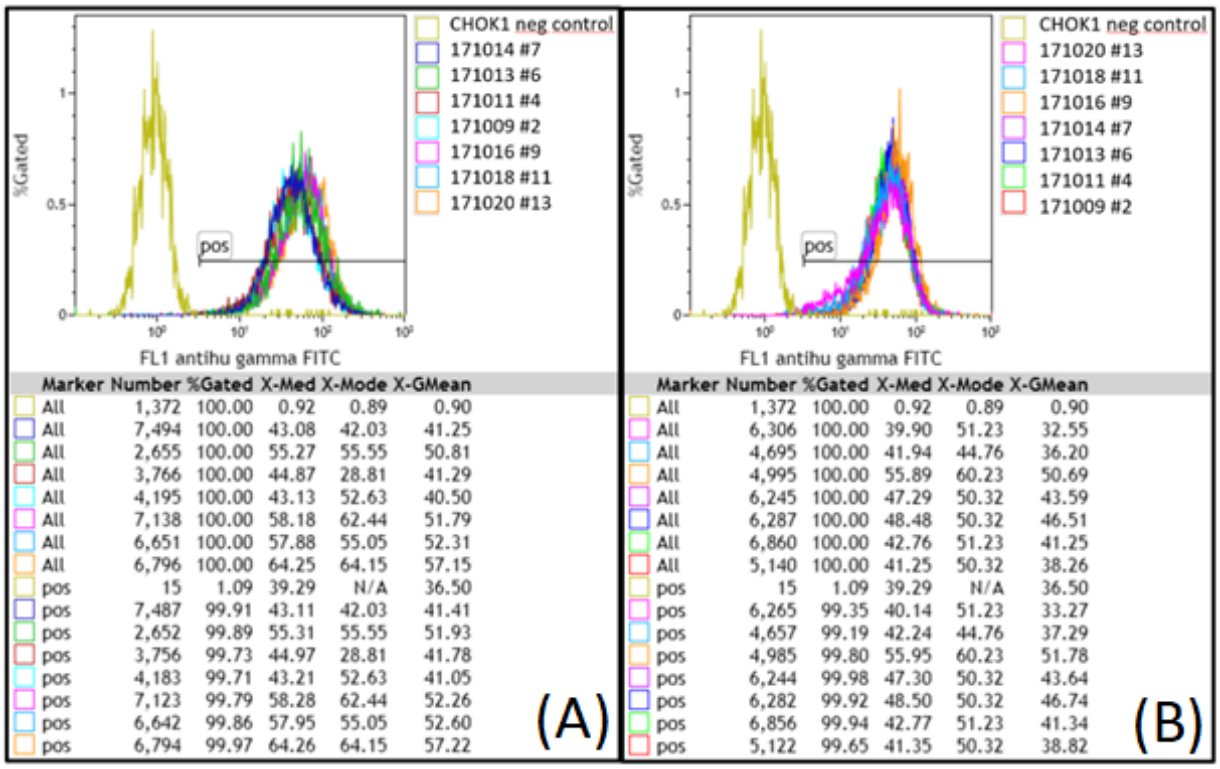

Figure 8.4.2.1.: Result of the flow cytometric analysis of the pseudoperfusion experiment in CD-CHO (B) and CDM4HEK293 (A). 1.5 mio cells fixed with ethanol and stained with anti-human-gamma-chain-FITC (1:100)

8.5 Affinity chromatography of CD19-Fc

For the purification of CD19-Fc from the culture supernatant (e.g. from the pseudoperfusion cultivation) the supernatants were first concentrated via crossflow filtration and then subjected to either protein A chromatography or Immobilized metal affinity chromatography (IMAC)chromatography, making use of the Fc-part or the His-tag of the protein, respectively.

8.5.1 Protein A affinity chromatography of pseudoperfusion cultivations

Tables 8.5.1.1-8.5.1.4 show the mass balances of the crossflow filtration steps as well as the protein A chromatography. The cross-flow filtration with a 30 kDa cutoff yielded concentrations factors of about 1:7 to 1:10, with losses up to 25% of CD19-Fc for the CDM4-HEK293 and CDM4NS0+CB purification and almost no losses for the CD-CHO and CDM4NS0 purification of the pseudoperfusion cultivations.

During the chromatography step, between 50-70% of CD19-Fc were lost with a total of 6-12 µg remaining in the eluate. The “flowthrough”, the “wash” and the “clean” fraction did only contain little to no CD19-Fc, and can therefore not be the reason for low yields in the protein A chromatography.

A typical chromatogram of a protein A chromatography is shown in figure 8.5.1.1, giving the CD19-Fc purification of the supernatant of the pseudoperfusion in CD-CHO medium (8.4) as an example (all other purifications had similar chromatograms). The blue curve shows the recorded UV absorption at 280 nm of aromatic amino acids, detecting all proteins present in the sample. During the loading of the sample onto the protein A column, the UV signal increased up to 325 mAU, representing all proteins in the sample that did not bind to the column. After washing the column with binding buffer the sample was eluted with elution buffer resulting in a small peak with about 80 mAU, which was collected in the elution fraction. The cleaning procedure (again with elution buffer) did not display any peaks. Since the conductivity of the elution buffer is lower than that of the binding buffer and the sample, a drop in the conductivity curve could be observed during the elution as well.

Table 8.5.1.1.: Massbalance of purification of supernatant from cultivation in CD-CHO medium

	fraction	CD19Fc [ng/ml]	volume [ml]	total [µg]	Mass balance total	Mass balance chromatography
Crossflow filtration	supernatant	73,32	286,54	21,01	100,00%	
	permeate	<min	397,99	n.a.	n.a.	
	retentate	632,66	35,34	22,36	106,42%	100,00%
Protein A chrom.	flow through	6,05	33,63	0,20	0,97%	0,91%
	clean	11,44	8,66	0,10	0,47%	0,44%
	wash	1,94	7,72	0,01	0,07%	0,07%
	eluate	5600,38	2,13	11,93	56,78%	53,35%

Table 8.5.1.2.: Massbalance of purification of supernatant from cultivation in CDM4-HEK293 medium

	fraction	CD19Fc [ng/ml]	volume [ml]	total [µg]	Mass balance total	Mass balance chromatography
Crossflow filtration	supernatant	110,37	287,75	31,76	100,00%	
	permeate	<min	399,01	n.a.	n.a.	
	retentate	766,45	31,12	23,85	75,10%	100,00%
Protein A chrom.	flow through	13,49	30,82	0,42	1,31%	1,74%
	clean	26,22	6,17	0,16	0,51%	0,68%
	wash	6,97	6,1	0,04	0,13%	0,18%
	eluate	3451,53	2,86	9,87	31,08%	41,39%

Table 8.5.1.3.: Massbalance of purification of supernatant from cultivation in CDM4SN0 medium

	fraction	CD19Fc [ng/ml]	volume [ml]	total [µg]	Mass balance total	Mass balance chromatography
Crossflow filtration	supernatant	75,26	323,49	24,35	100,00%	
	permeate	1,31	442,61	0,58	2,38%	
	retentate	784,88	28,66	22,49	92,39%	100,00%
Protein A chrom.	flow through	16,66	27,84	0,46	1,90%	2,06%
	clean	8,88	6,17	0,05	0,23%	0,24%
	wash	3,58	7,08	0,03	0,10%	0,11%
	eluate	1983,95	3,65	7,24	29,74%	32,19%

Table 8.5.1.3.: Massbalance of purification of supernatant from cultivation in CDM4SN0+CB medium

	fraction	CD19Fc [ng/ml]	volume [ml]	total [µg]	Mass balance total	Mass balance chromatography
Crossflow filtration	supernatant	50,58	304,1	15,38	100,00%	
	permeate	14,30	464,3	6,64	43,17%	
	retentate	386,84	29,68	11,48	74,65%	100,00%
Protein A chrom.	flow through	7,73	29,88	0,23	1,50%	2,01%
	clean	7,53	9,11	0,07	0,45%	0,60%
	wash	4,02	6,95	0,03	0,18%	0,24%
	eluate	1899,05	3,29	6,25	40,62%	54,42%

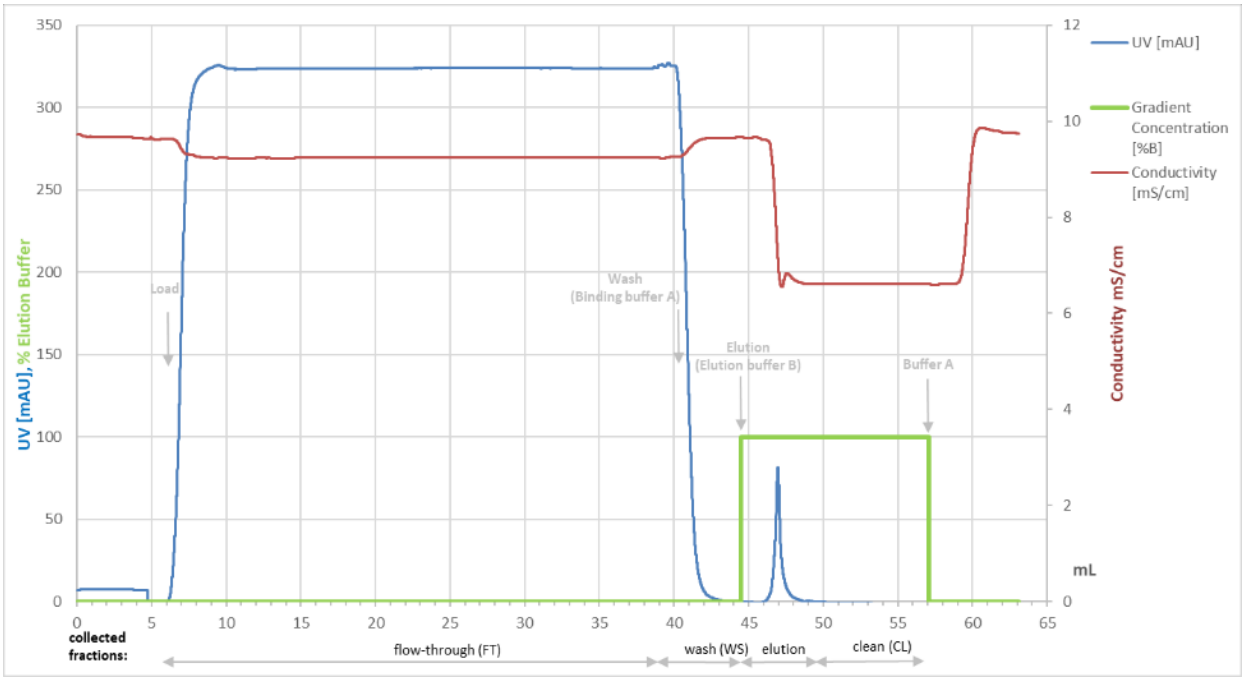

Figure 8.5.1.1.: Chromatogram of CD19-Fc purification from pseudoperfusion in CD-CHO medium. column: GE healthcare, HiTrap® MabSelect™ SuRe™ 29-0491-04, Running Buffer A (binding, wash): 100 mM glycine, 100 mM NaCl pH 7.5, Elution Buffer B (elution, clean): 100 mM glycine, pH 2.5

8.5.2 Immobilized metal affinity chromatography (IMAC) of CD19-Fc

Tables 8.5.2.1 shows the mass balances of the crossflow filtration steps as well as the IMAC of CD19-Fc transiently expressed in HEK-293 cells.

During the cross-flow filtration only 25% of the CD19-Fc could be recovered and essentially no concentration of the sample took place. However, the His-tag chromatography yielded 155% of CD19-Fc coming from the retentate of the crossflow filtration, indicating that maybe the quantification of CD19-Fc in the retentate was faulty. Furthermore, only very little CD19-Fc could be found in the permeate, therefore the low yield of the cross-flow filtration cannot be explained by the loss of protein through the membrane. In total, 22.5 µg of CD19-Fc could be recovered from the 56.4 µg found in the supernatant after the transient expression.

The chromatogram of the His-Tag purification can be seen in figure 8.5.2.1. The blue curve again shows the UV absorption at 280 nm, rising to about 600 mAU while loading the sample. The elution was performed with a step-wise increase of elution buffer, resulting in an elution peak after setting the elution buffer to 20 %. After setting the elution buffer to 100% another small peak occurred, which was also collected in the elution fraction. Furthermore, there was a shift in the UV baseline, which was caused by the higher imidazole concentration in the elution buffer, which also absorbs at 280 nm.

Table 8.5.2.1.: Mass balance of IMAC purification of CD19-Fc

	fraction	CD19Fc [ng/ml]	volume [ml]	total [µg]	Mass balance total	Mass balance chromatography
Crossflow filtration	supernatant	289,71	194,64	56,39	100,00%	
	permeate	4,23	289,99	1,23	2,18%	
	retentate	310,43	46,76	14,52	**25,74%**	100,00%
Protein A chrom.	flow through	76,31	33,8	2,58	4,57%	17,77%
	clean	43,40	7,84	0,34	0,60%	2,34%
	wash	38,12	12	0,46	0,81%	3,15%
	eluate	2282,52	9,85	22,48	39,87%	**154,88%**

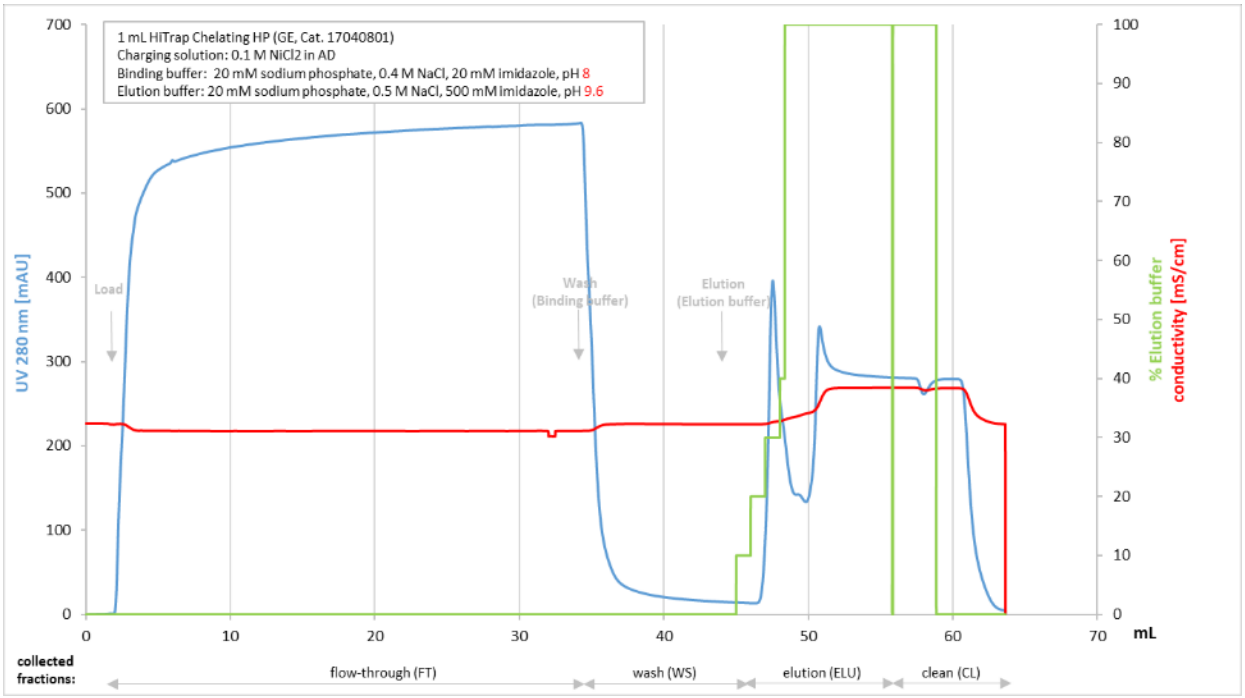

Figure 8.5.2.1.: chromatogram of the IMAC purification of CD19-Fc from the supernatant of a transient expression in HEK-293

8.6 Recombinant cell line development for CHO-K1/CD19mutAFc/CD21mutBFc

8.6.1 PEI-cotransfection of CHO-K1 host cells with pL_CD19mutAFc and pL_CD21mutBFc

To produce the heterodimeric protein CD19mutAFc/CD21mutBFc a pL_CD19mutAFc and a pLCD21mutBFc plasmid were used for the stable transfection of CHO-K1 cells (see methods). Both plasmids were established in the same way as the pL_CD19HSAD2 plasmid using PCR amplicification of the gene of interest followed by AscI restriciton and ligation into AscI-opend vector 'pL'. For the transfection, two approaches were used: 1) simultaneous polyplex formation with both plasmids ("CD1921" and 2) individual polyplex formation with each individual plasmid ("CD19+CD21") followed by co-transfection of the same cell suspension. After exchanging the medium to selection medium containing G418 and therefore applying selection pressure, the transfection pools were used to seed a 384 well plate (1250 cells/well/50 µL) as well as a 96 well plate (5000 cells/well/100 µL). On day 16 after the transfection the transfection efficiency was calculated based on the number of acidified (yellow) wells (table 8.6.1.1).

Table 8.6.1.1.: Transfection efficiency of stable transfection of CHO-K1 with CD19mutAFc and CD21mutBFc on day 16

Plate:	Transfection efficiency:
96 well plate "CD1921"	60%
96 well plate "CD19+CD21"	92%
384 well plate "CD1921"	17%
384 well plate "CD19+21"	29%
Negative control	0%

8.6.2 Screening of initial CD19mutAFc/CD21mutBFc transfectant pools after limiting dilution subcloning

Figure 8.6.2.1 shows the result of a qualitative anti-human-gamma-chain ELISA performed on the supernatant of the 96 well plates on day 21 after transfection (384 well plates were transferred to 96 well plates beforehand) to choose the best producing clone pools. The best clone pool with a titer of 113 ng/ml was 3G4, followed by 9D2 (75.24 ng/ml) and 5D8 (73.08 ng/ml) It is important to note that this ELISA was only aiming at the Fc-part of the CD19/CD21 protein, thus only giving information about the sum of CD19 and CD21 but this assay is not suitable to determine the quantity of CD19. Furthermore, because of the different cell numbers used for the 384 and 96 well plates, titers of pools derived from different plate types cannot be compared with each other.

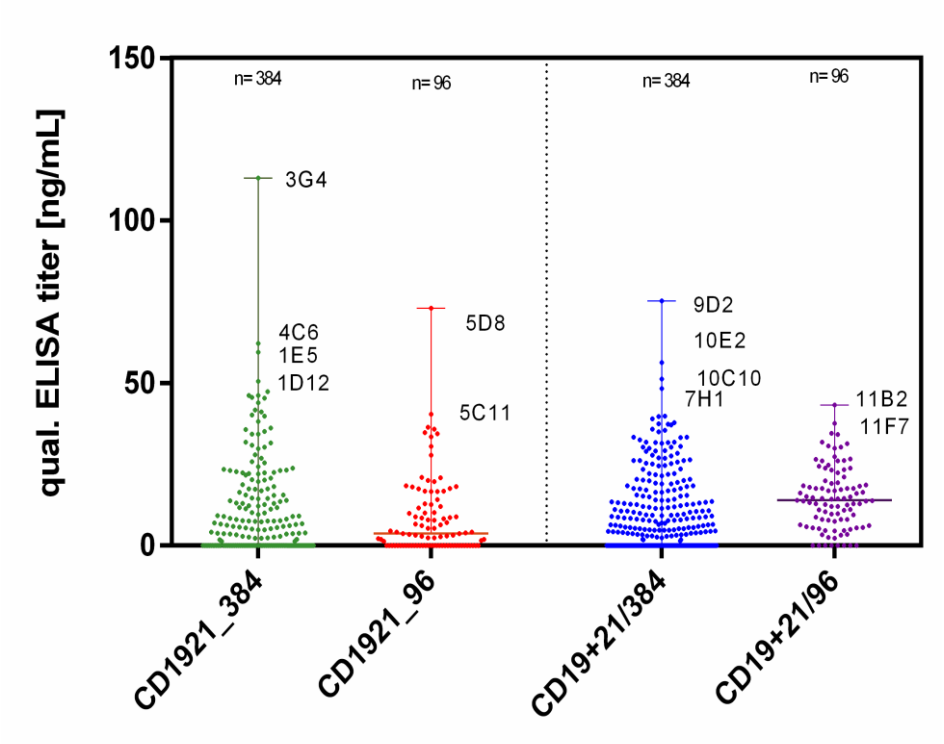

Figure 8.6.2.1. Result of the qualitative anti-human-gamma-chain ELISA for heterodimeric CD19mutAFc/CD21mutBFc cell pools 21 days after transfection. Coating antibody: goat anti-human gamma chain antibody (1:2000). Conjugating antibody: goat anti-human gamma chain HRP antibody (1:2000). Standard: 3D6-scFv-Fc 40 ng/ml, samples diluted 1:4. All clone pools derived from 384-well plates were transferred and grown into 96-well plates before sampling for ELISA.

After screening and expansion, the clone pools were cultivated in cultivation tubes for an extended amount of time by passaging them every 3-4 days into fresh CD-CHO “selection” medium

Figures 8.6.2.2-8.6.2.4 show the results of the viable cell number, growth rates and viabilities of the individual clones during the cultivation.

Viable cell numbers up to $9.33*10^6$ cells/ml could be achieved at the beginning of the cultivation, with an average cell number of $3.66*10^6$ cells/ml between passage 2 and 5. The two clone pools which were chosen for prolonged cultivation (1E5, 10C10) were ranging between $3\text{-}6*10^6$ cells ml after passage 8.

When looking at the specific growth rate in figure 8.6.2.3, most clone pools obtained values between 0.8 and 1.0 d^{-1}. The 10C10 clone pool started out with the lowest growth rate of 0.56 d^{-1}, but could also maintain growth rates between 0.8 and 0.9 d^{-1} throughout the later passages.

During the earlier passages, viabilities never went below 90%, however, from passage 14 to 19, the viability of the 1E5 clone dropped considerably down to 72.3%.

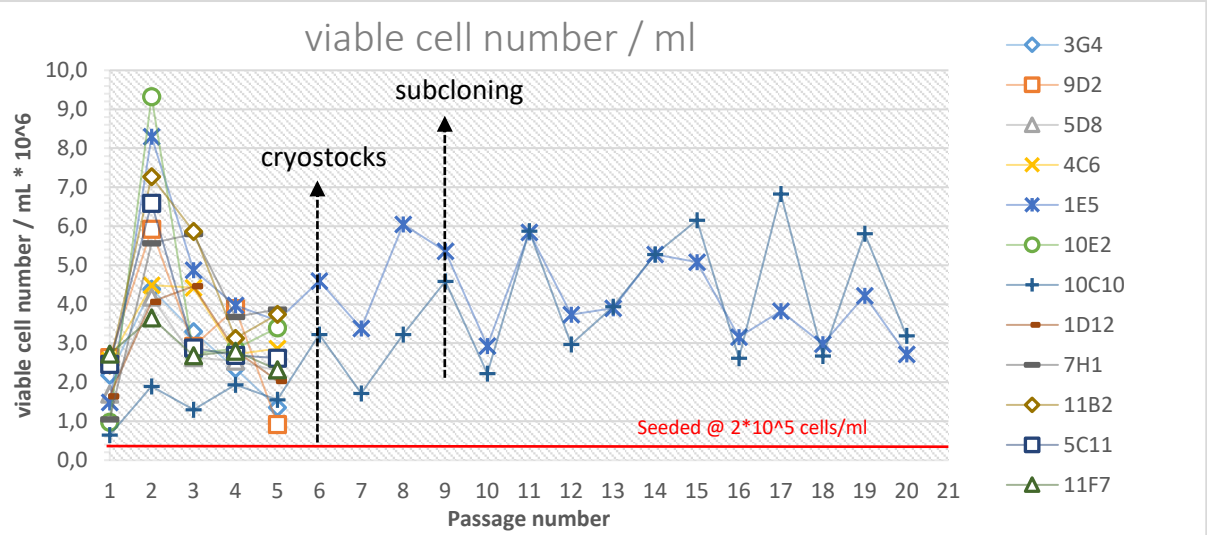

Figure 8.6.2.2.: viable cell numbers of CD19mutAFc/CD21mutBFc producing clone pools cultured in CD-CHO selection medium containing 0.5 mg/mL G418

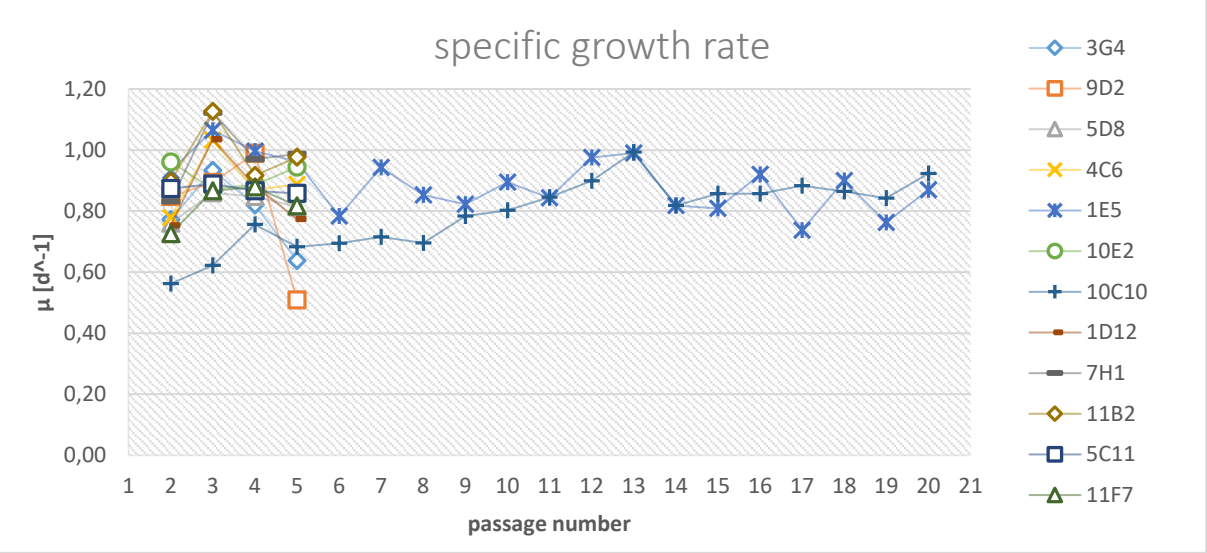

Figure 8.6.2.3.: specific growth rates of CD19mutAFc/CD21mutBFc producing clone pools cultured in CD-CHO selection medium containing 0.5 mg/mL G418

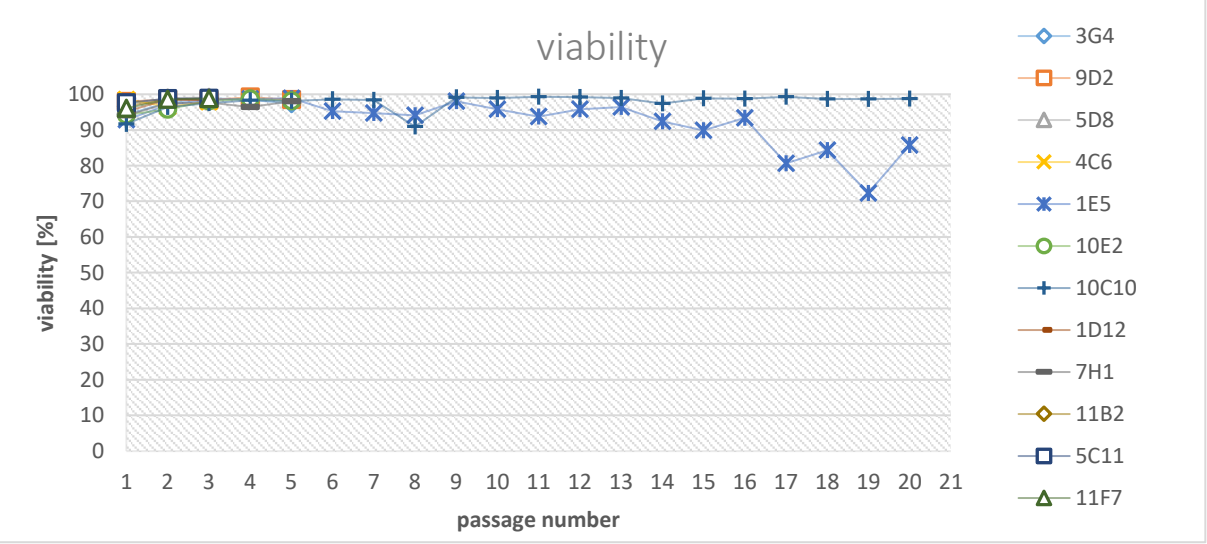

Figure 8.6.2.4.: viabilities of CD19mutAFc/CD21mutBFc producing clone pools cultured in CD-CHO selection medium containing 0.5 mg/mL G418

During the passaging process, samples of the supernatant were taken to determine the concentration of CD19mutAFc/CD21mutBFc via a quantitative anti-gamma-chain ELISA. The determined titers and calculated specific productivities are shown in figure 8.6.2.5 and 8.6.2.6 respectively.

One of the best clone pools (1E5) which was chosen based on the titers and the specific productivity on passage number 5, was able to produce up to 587 ng/ml of CD19mutAFc/CD21mutBFc on passage number 19, with titers generally ranging between 200 and 400 ng/ml. The second-best clone pool (10C10) started out with titers up 482.60 ng/ml, but then settled at about 100 ng/ml throughout passage 10-24, with specific productivities being in the range of 0.02 pg/cell/day. Specific productivities for the 1E5 clone pool were much higher with top values of 0.121 pg/cell/day on passage number 20 and values between 0.04 and 0.06 pg/cell/day on most passage days. However, when looking at the graph it seems that the specific productivies of 1E5 between passage number 19 and 21 are unusually high and might therefore be outliers (the same applies to the 10C10 clone pool on passage number 7).

Figure 8.6.2.7 shows the result of a flow cytometric analysis of the 1E5 and the 10C10 clone pool on passage number 19, which was performed to compare the amount of intracellular CD19mutAFc/CD21mutBFc of both clones with each other as well as to the intracellular CD19-Fc content of a 1G4 clone (which achieved about 50 ng/ml of CD19-Fc in the supernatant). Although the 1E5 clone pool had a titer of 587 ng/ml on passage number 19, the fluorescence signal in the flow cytometer was lower than that of the 10C10 and the 1G4 clones (which both had significantly lower titers in the supernatant). This indicates that either the 1E5 clone pool was exceptionally good in secreting the product into the supernatant, or that the ELISA analysis or the sample taking on this specific passage might have been faulty.

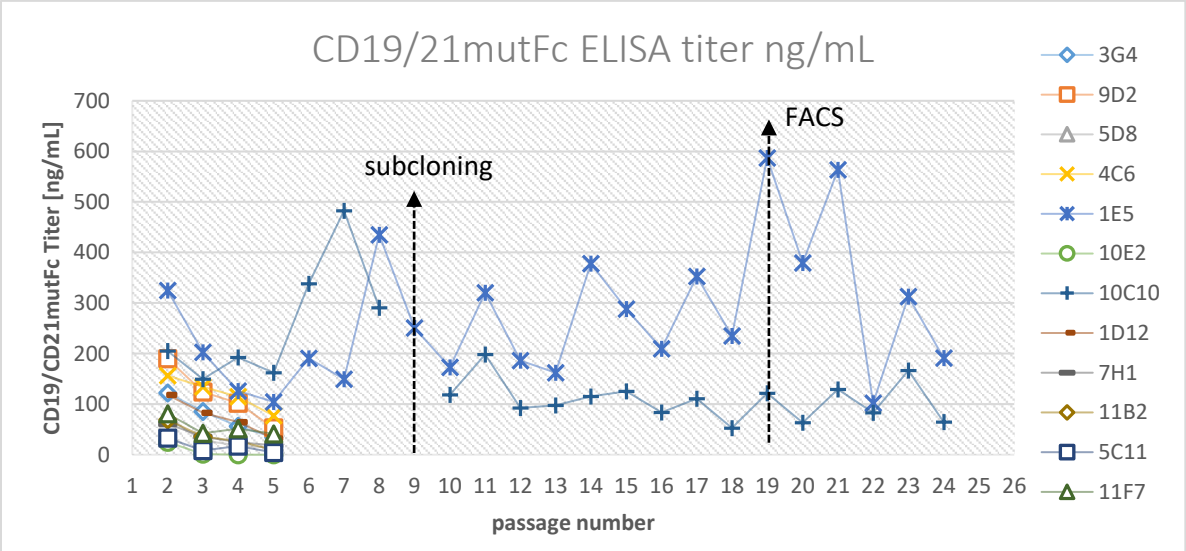

Figure 8.6.2.5.: CD19mutAFc/CD21mutBFc titers from the supernatant of CHO-K1/ CD19mutAFc/CD21mutBFc. Coating antibody: goat anti-human gamma chain antibody (1:2000). Conjugating antibody: goat anti-human gamma chain HRP antibody (1:2000). Standard: 3D6-scFv-Fc 40 ng/ml, samples diluted 1:4

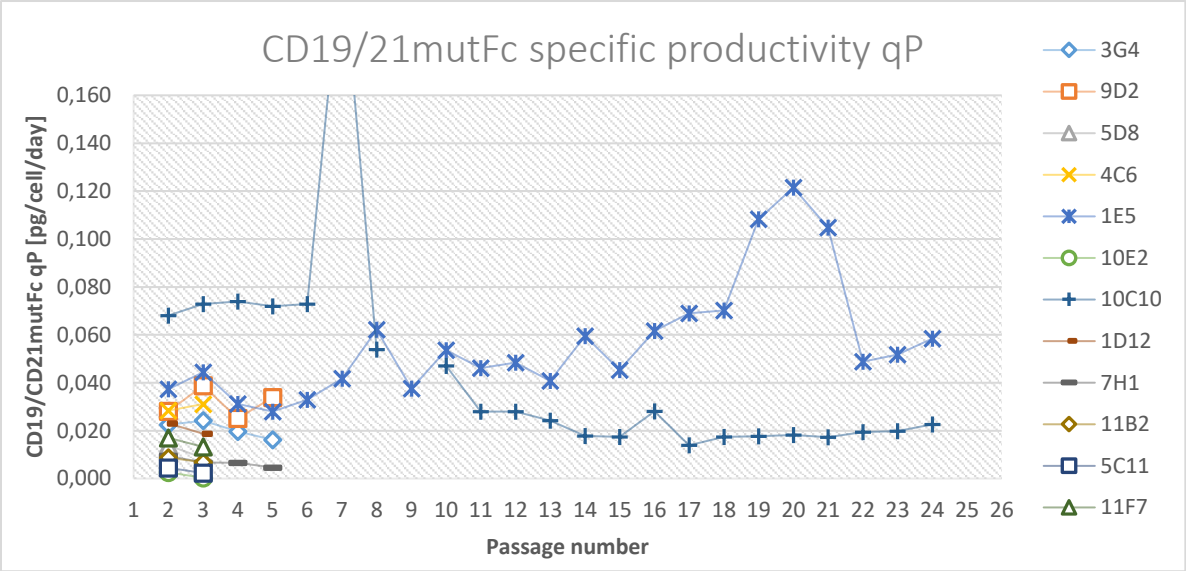

Figure 8.6.2.6.: CD19mutAFc/CD21mutBFc specific productivities.

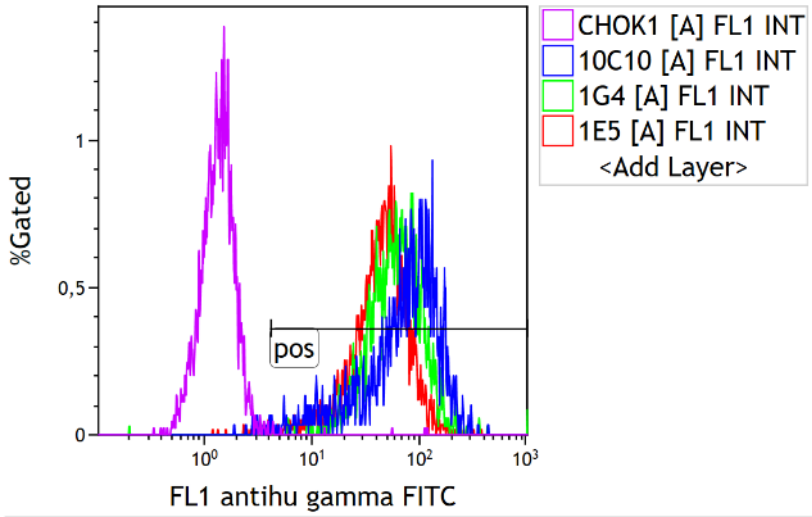

Marker	Number	%Gated	X-Med	X-Mode	X-GMean
All	1.493	100,00	1,35	1,49	1,32
All	1.002	100,00	80,32	130,55	64,18
All	1.179	100,00	61,15	45,58	58,93
All	1.974	100,00	45,77	54,07	42,00
pos	7	0,47	13,11	N/A	19,02
pos	990	98,80	81,29	130,55	66,59
pos	1.178	99,92	61,18	45,58	59,22
pos	1.957	99,14	46,03	54,07	43,01

Figure 8.6.2.7.: Flow cyctometric analysis of 10C10 and 1E5 on passage number 19. 1.5 mio cells fixed with ethanol. Antibody: anti-human-gamma-chain-FITC diluted 1:100.

8.6.3. Single-cell subcloning of CD19mutAFc/CD21mutBFc pools by limiting dilution

On passage number 9, 1E5 and 10C10 of the parental CD19mutAFc/CD21mutBFc were chosen for subcloning based on the product titers in the supernatant as well as the specific productivity. For subcloning a 96 well plate was seeded with 3 cell/well as well as a 384 well plate with 1 cell/well. On day 21 the subcloning efficiency was calculated based on the amount of the yellow wells, which were then transferred into new 96 well plates.

Table 8.6.3.1. subcloning efficiency of CD19mutAFc/CD21mutBFc producing clone pools 1E5 and 10C10

Clone	Plate	yellow wells/transferred wells	subcloning efficiency (day 21)
1E5	96	13	13.5%
1E5	384	40	10.4%
10C10	96	15	15.6%
10C10	384	50	13.0%

The best clone pools of the subcloning procedure were chosen by performing a qualitative anti-human-gamma-chain ELISA on the supernatant of the 96 well plates on day 25 after subcloning. The result of the ELISA as well as the original subcloning plate/parental clone can be seen in table 8.6.3.2.

Table 8.6.3.2.: titers of CD19mutAFc/CD21mutBFc subclones determined via qualitative ELISA: Coating antibody: goat anti-human gamma chain antibody (1:2000). Conjugating antibody: goat anti-human gamma chain HRP antibody (1:2000). Standard: 3D6-scFv-Fc 40 ng/ml, samples diluted 1:4

Subclone	subcloning plate	parental clone	Titer [ng/ml]
1H9	96 well plate	10C10	74,86
2H4	384 well plate	1E5	77,45
2G3	384 well plate	1E5	82,16
2A8	96 well plate	1E5	77,38
1F7	384 well plate	10C10	74,93
2F3	384 well plate	1E5	75,16
1D6	384 well plate	10C10	75,60
1E10	96 well plate	10C10	76,11
1H6	384 well plate	10C10	76,28
2H8	96 well plate	1E5	82,65
1G3	384 well plate	10C10	82,81
2B3	384 well plate	1E5	75,76

8.6.4 Clone expansion and comparison of CHO-K1/CD19/CD21mutFc subclones

After screening and expansion, the clones were cultivated in cultivation tubes for an extended amount of time by passaging them every 3-4 days into fresh CD-CHO “selection” medium.

Figure 8.6.4.1-8.6.4.3 show the results of the viable cell number, growth rates and viabilities of the individual clones during the cultivation.

During passage 3-7, an average viable cell number of $3.35*10^6$ cells/ml and an average growth rate of 0.81 d^{-1} could be obtained, with the 1D6 clone reaching the highest cell number of $6.40*10^6$ on passage number 10 and 2H4 reaching the highest growth rate of 1.1 d^{-1} on passage number 3. Viabilities never dropped below 90% throughout the whole cultivation.

On passage number 4, 1D6, 2H8, 2F3 and 2B3 were chosen for further cultivation based on their product titer, specific productivity and growth rate. 1D6 and 2H8 were chosen to be the main CD19mutAFc/CD21mutBFc producers on passage number 11 and in addition 4 cryostocks were established on passage number 13 of both clones.

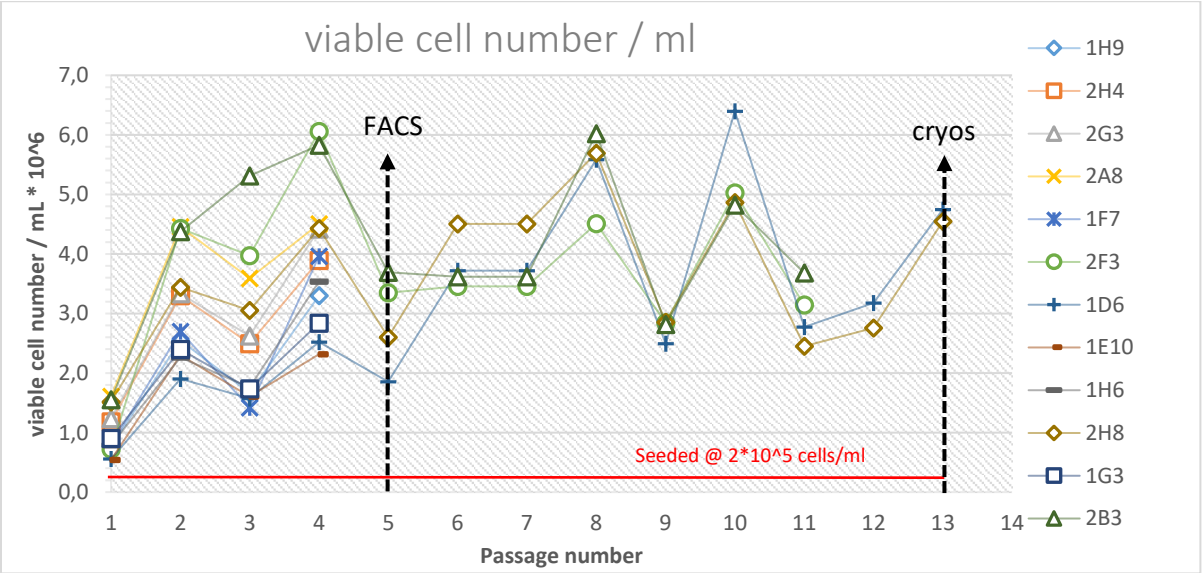

Figure 8.6.4.1.: viable cell numbers of CD19mutAFc/CD21mutBFc producing sub-clones cultured in CD-CHO selection medium containing 0.5 mg/mL G418

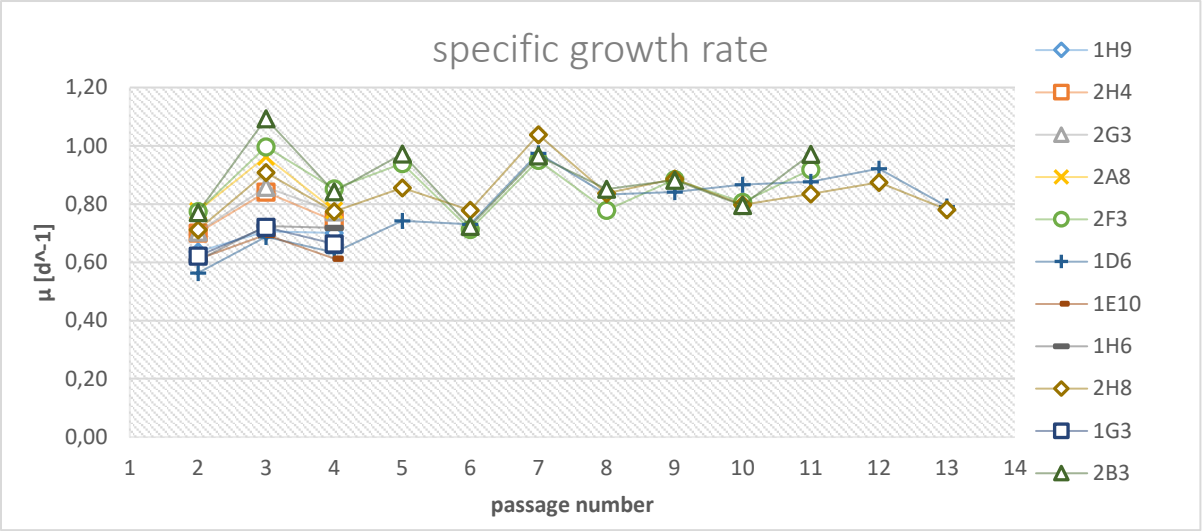

Figure 8.6.4.2.: specific growth rates of CD19mutAFc/CD21mutBFc producing sub-clones cultured in CD-CHO selection medium containing 0.5 mg/mL G418

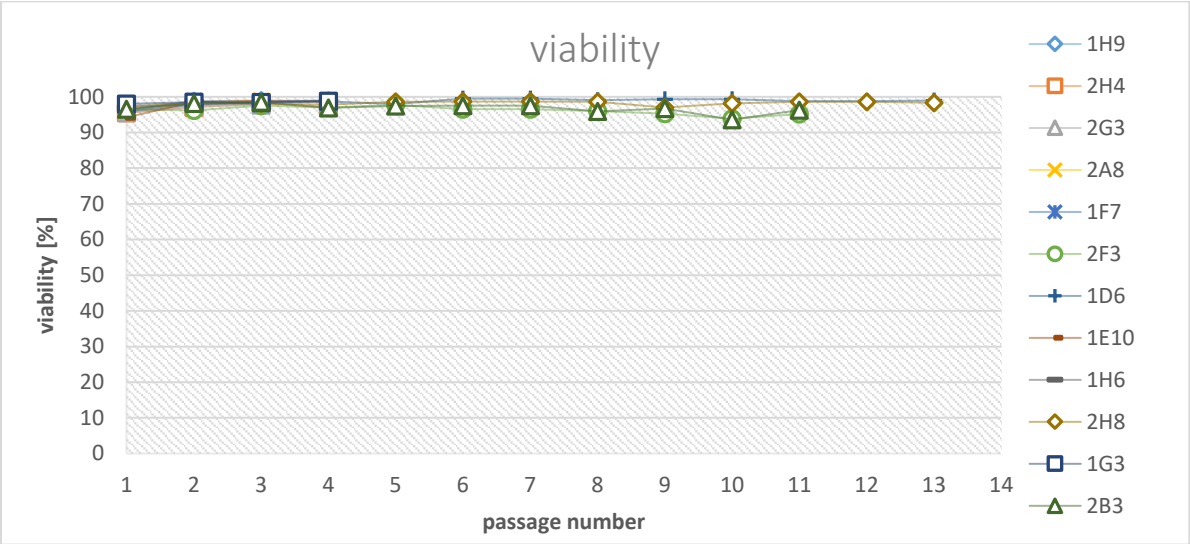

Figure 8.6.4.3.: viabilities of CD19mutAFc/CD21mutBFc producing clones cultured in CD-CHO selection medium containing 0.5 mg/mL G418

During the passaging process, samples of the supernatant were taken to determine the concentration of CD19mutAFc/CD21mutBFc via a quantitative anti-gamma-chain ELISA. The determined titers and calculated specific productivities are shown in figure 8.6.4.4 and 8.6.4.5 respectively.

On passage number 3 all clones except for 2F3, 1D6, 2H8 and 2B3 were removed from culture. After passage 3, these clones achieved titers between 200 and 500 ng/ml, with a highest titer of 526.36 ng/ml for the 2F3 clone on passage number 4. Most clones had specific productivities between 0.06 and 0.08 pg/cell/day, however, 1D6 reached values up to almost 0.14 pg/cell/day on passage number 5 and dropped down to 0.03 pg/cell/day until passage number 13, which can be explained by an increase in growth rate as well as a decrease in product titer.

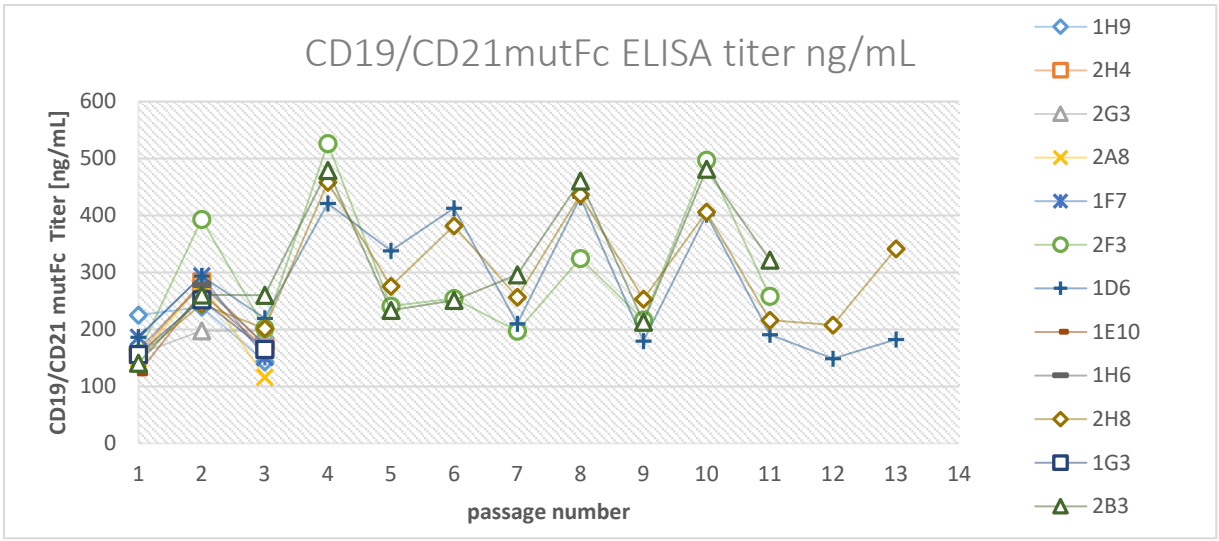

Figure 8.6.4.4.: CD19mutAFc/CD21mutBFc titers from the supernatant of CHO-K1/ CD19mutAFc/CD21mutBFc. Coating antibody: goat anti-human gamma chain antibody (1:2000). Conjugating antibody: goat anti-human gamma chain HRP antibody (1:2000). Standard: 3D6-scFv-Fc 40 ng/ml, samples diluted 1:4

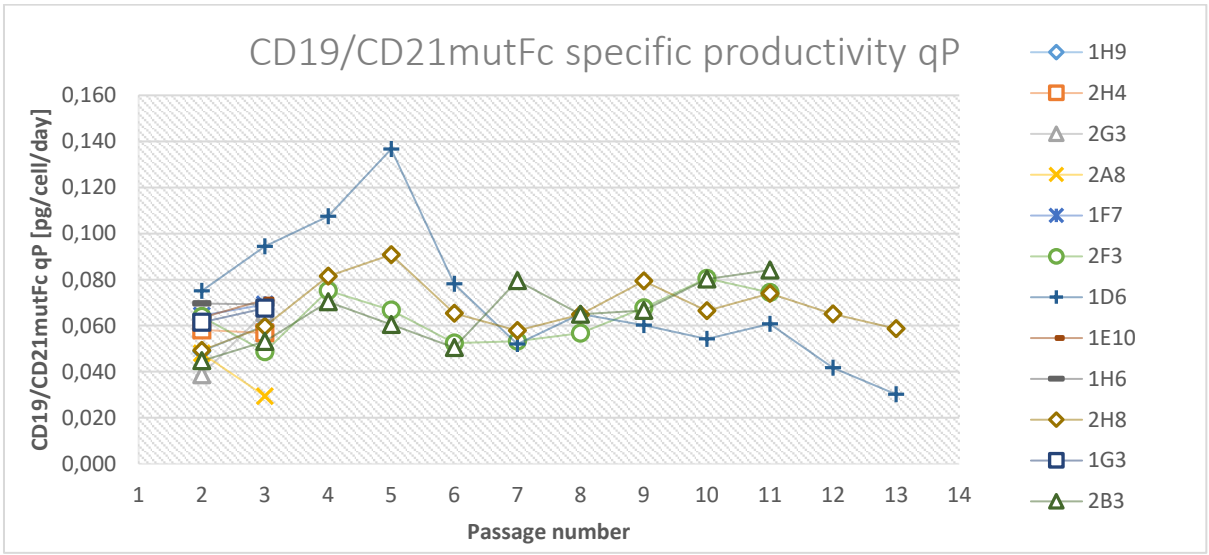

Figure 8.6.4.5.: CD19mutAFc/CD21mutBFc specific productivities.

8.6.5 Intracellular product content of CHOK1/CD19/CD21mutFc clones via flow cytometry with anti-CD19 and anti-CD21 antibodies

Since the previous ELISA analysis only detected the Fc parts of CD19mutAFc/CD21mutBFc and therefore was not able to distinguish between CD19 and CD21, antibodies against these specific domains were tested in a flow cytometric analysis with the parental 3G4 clone pool fixed with ethanol on passage number 5.

Figure 8.6.5.1 shows the result of the cells stained with a rabbit-anti-CD19 antibody as primary antibody and an anti-rabbit-FITC antibody as secondary/labelling antibody detected via the FL1 laser channel. The Peaks in group “C” were not subjected to the FITC labelled antibody at any time of the sample preparation and are therefore displaying the lowest fluorescence signal. Group “B” shows the negative controls (untransfected CHO-K1 and 3G4 without primary antibody) that were treated with the FITC antibody, which was not entirely removed from the samples during the washing steps, resulting in a higher fluorescence signal compared to the samples of group “C”. Finally, group “A” represents the 3G4 clone pool treated with the first and the secondary antibody allowing for detection of CD19. Peaks of this group had a higher fluorescence signal than the negative control, indicating that there has to be at least some CD19mutAFc present within the cell and that the anti-CD19 antibody was able to detect it.

The flow cytometric analysis of figure 8.6.5.2 used the exact same sample as figure 8.6.5.1, only this time the fluorescence signal of the FL2 laser for phycoerythrin was recorded. The phycoerythrin labelled anti-mouse antibody acted as a secondary antibody which bound to the mouse-anti-CD21 antibody, which in turn stained intracellular CD21mutBFc. Unfortunately, the only increased fluorescence signal was obtained by the samples containing the FITC antibody (staining CD19) due to an overlap of the emission spectra of FITC and PE (therefore FITC shows some fluorescence signal even when the FL2 laser channel for phycoerythrin is used). Since the 3G4 clone pool treated with the mouse-anti-CD21 antibody and the anti-mouse-PE antibody did not display peaks with an increased fluorescence intensity, it’s either possible that no CD21 is present within the cell or that the CD21 antibody is not working properly or the antibody dilutions were not appropriate (recommended dilution of 1:2 by the manufacturer for flow cytometry). Because of the missing positive control for CD21, it is not possible to tell which of the aforementioned reasons holds true.

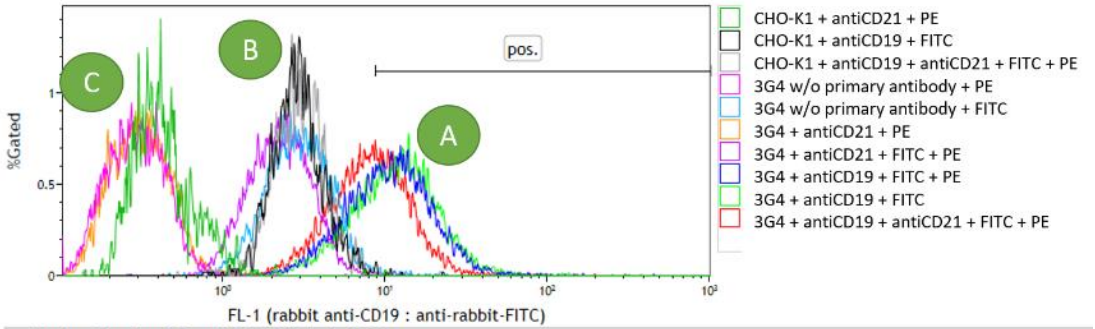

Marker	Number	%Gated	X-Med	X-Mode	X-GMean
All	1,068	100.00	0.41	0.30	0.40
All	1,760	100.00	2.89	2.96	2.86
All	1,565	100.00	2.98	2.68	2.90
All	6,489	100.00	0.29	0.23	0.26
All	4,203	100.00	2.93	2.36	2.82
All	5,351	100.00	0.31	0.35	0.28
All	5,968	100.00	2.25	2.49	2.16
All	6,280	100.00	10.80	12.59	10.08
All	6,944	100.00	11.90	14.03	11.05
All	5,296	100.00	8.22	6.96	7.78
pos.	1	0.09	10.08	N/A	10.08
pos.	9	0.51	10.29	8.87	10.80
pos.	5	0.32	10.76	N/A	15.51
pos.	1	0.02	12.20	N/A	12.20
pos.	36	0.86	12.26	9.36	12.61
pos.	0	0.00	N/A	N/A	N/A
pos.	25	0.42	11.38	11.51	11.23
pos.	3,948	62.87	14.15	12.59	14.89
pos.	4,770	68.69	14.89	14.03	15.54
pos.	2,371	44.77	12.21	10.91	12.92

A 3G4 + anti CD19 + FITC

B Negativ controls with FITC

C Negativ controls without FITC

Figure 8.6.5.1.: flow cytometric result of the CD19/CD21mutFc producing clone pool 3G4 on passage number 2. All antibodies diluted 1:100. "PE" = anti-mouse-phycoerythrin antibody (binding to mouse anti CD21 antibody), "FITC" = anti-rabbit FITC (binding to rabbit anti CD19 antibody). ***Laser channel: "FL1" for FITC excitation.***

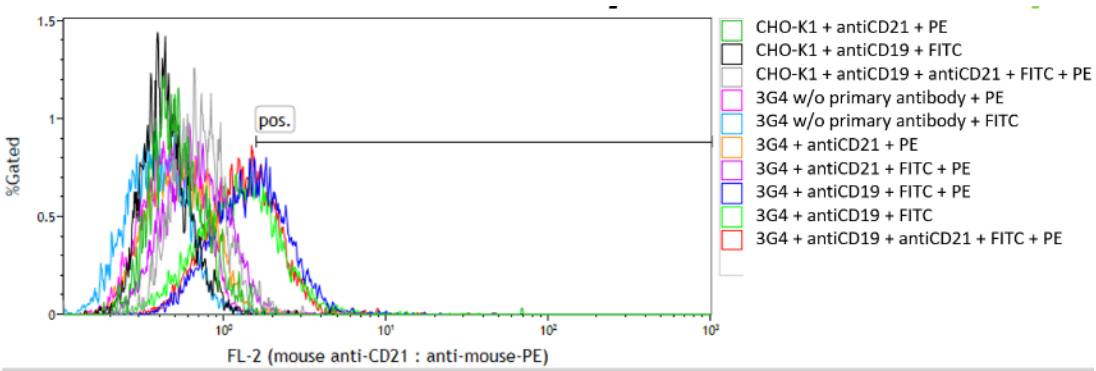

Marker	Number	%Gated	X-Med	X-Mode	X-GMean
All	1,068	100.00	0.51	0.60	0.50
All	1,760	100.00	0.43	0.39	0.42
All	1,565	100.00	0.69	0.66	0.67
All	6,489	100.00	0.49	0.43	0.46
All	4,203	100.00	0.39	0.34	0.36
All	5,351	100.00	0.53	0.47	0.50
All	5,968	100.00	0.67	0.62	0.63
All	6,280	100.00	1.48	1.80	1.38
All	6,944	100.00	1.25	1.02	1.14
All	5,296	100.00	1.32	1.49	1.24
pos.	6	0.56	4.24	N/A	3.76
pos.	4	0.23	2.80	N/A	2.68
pos.	38	2.43	1.78	1.66	1.89
pos.	11	0.17	2.09	N/A	2.29
pos.	9	0.21	2.02	N/A	2.25
pos.	43	0.80	2.17	1.84	2.50
pos.	133	2.23	1.84	1.59	1.99
pos.	2,843	45.27	2.16	1.80	2.26
pos.	2,364	34.04	2.07	1.76	2.21
pos.	1,901	35.90	2.03	1.62	2.13

Figure 8.6.5.2.: flow cytometric result of the CD19/CD21mutFc producing clone pool 3G4 on passage number 2. All antibodies diluted 1:100. "PE" = anti-mouse-phycoerythrin antibody (binding to mouse anti CD21 antibody), "FITC" = anti-rabbit FITC (binding to rabbit anti CD19 antibody). ***Laser channel: "FL2" for phycroerythrin excitation.***

After testing the anti-CD19 antibody for its functionality (figure 8.6.5.2), all CD19/CD21mutFc producing subclones on passage number 5 and the two parental clone pools 1E5/10C10 on passage number 20 were analysed via flow cytometry to screen them for intracellular CD19, which can be seen in figure 8.6.8.3. The CD19-Fc producing clone 1G4 acted as a positive control (dark blue curve), since it can only contain CD19, which has already been proven by the anti-human-gamma-chain ELISA. An untransfected CHO-K1 clone was used as negative control, which can be seen as the light blue curve. Additionally, the 1E5 clone pool without a primary antibody provided a second negative control which is represented by the light green peak. Since the CD19/CD21mutFc producing clones did not display a significantly higher fluorescence signal than the negative control, it is possible that these clones contained very little (if any) intracellular CD19. Furthermore, if the intracellular presence of CD19 is taken as an indicator of CD19 in the supernatant, the supernatant titer determined by the ELISA targeting the Fc part might be predominantly derived from CD21.

In addition to the analysis with the anti-CD19 antibody, all clones were treated with an anti-human-gamma-chain-FITC antibody to analyse the Fc part of both CD19mutAFc and CD21mutBFc simultaneously. The result of the flow cytometric analysis is shown in figure 8.6.8.4. The untransfected negative control can be seen in dark green and compared to the use of the anti-CD19 antibody, all clones were able to deliver a significantly higher fluorescence signal than the negative control, showing that at least in term of intracellular Fc, the CD19/CD21mutFc presented a positive result.

Furthermore, all the peaks except for 10C10 in red had a very symmetrical shape, indicating the absence of different sub-populations within one clone which is also indicated by similar mode, geometric mean and median values. The peak of the CD19-Fc producer 1G4 had the same fluorescence intensity as most of the CD19/CD21mutFc clones which demonstrates equal levels of intracellular product, however, in terms of product titer in the supernatant, the 1G4 clone performed 4-6 times worse than the CD19/CD21mutFc clones (60 ng/ml of CD19-Fc compared to 240-340 ng/ml of CD19/CD21mutFc), which could be explained by an increased secretion capability of the CD19/CD21mutFc clones.

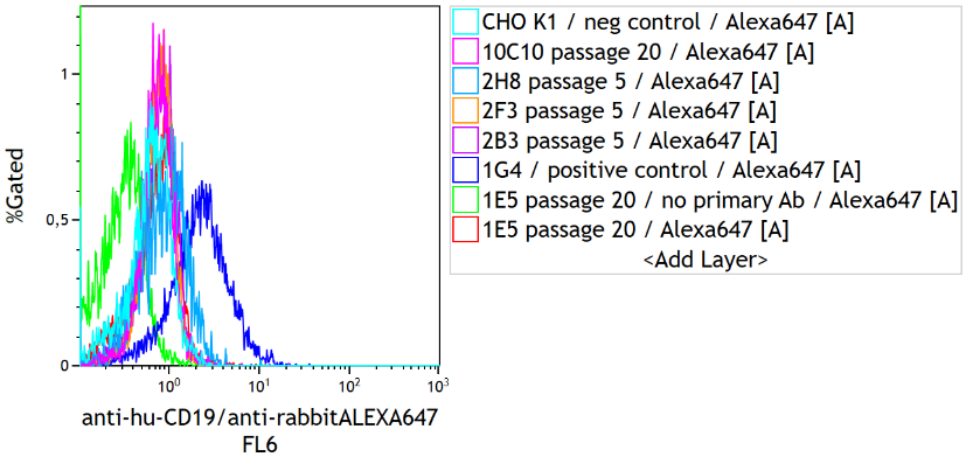

Marker	Number	%Gated	X-Med	X-Mode	X-GMean
All	3.300	100,00	0,65	0,60	0,60
All	4.480	100,00	0,75	0,65	0,72
All	1.695	100,00	0,87	0,50	0,82
All	6.378	100,00	0,78	0,66	0,75
All	6.316	100,00	0,81	1,04	0,76
All	5.507	100,00	2,23	1,80	2,11
All	4.902	100,00	0,31	0,10	0,29
All	6.178	100,00	0,75	0,86	0,68

Figure 8.6.8.3.: flow cytometric result of the CD19/CD21mutFc producing subclones on passage number 5. Antibodies: rabbit anti-human-CD19 (1:100), anti-rabbit-Alexa647 (1:100). ***Laser channel: FL6 for Alexa647***

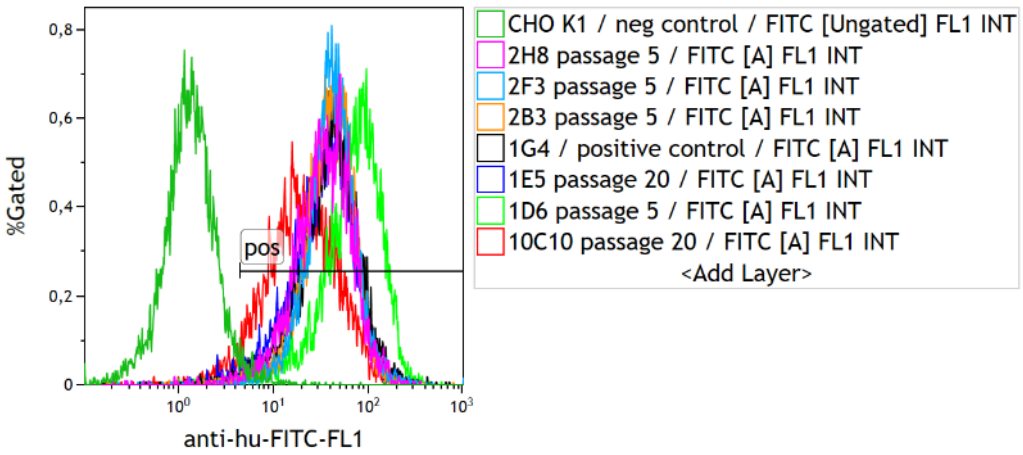

Marker	Number	%Gated	X-Med	X-Mode	X-GMean
All	6.285	100,00	1,33	1,37	1,32
All	3.625	100,00	35,56	31,24	33,12
All	6.518	100,00	41,47	45,17	39,96
All	6.593	100,00	40,41	35,11	37,68
All	5.449	100,00	40,65	38,42	36,94
All	5.910	100,00	35,95	56,56	32,04
All	5.155	100,00	75,49	95,29	67,08
All	5.363	100,00	20,00	15,63	19,40
pos	187	2,98	6,13	6,02	7,26
pos	3.574	98,59	35,98	31,24	34,45
pos	6.478	99,39	41,62	45,17	40,75
pos	6.539	99,18	40,62	35,11	38,56
pos	5.353	98,24	41,22	38,42	38,82
pos	5.776	97,73	36,77	56,56	33,89
pos	5.111	99,15	75,90	95,29	69,27
pos	5.107	95,23	21,06	15,63	21,49

Figure 8.6.8.4.: flow cytometric result of the CD19/CD21mutFc producing subclones on passage number 5. Antibodies: anti-human-gamm-chain-FITC (1:100). ***Laser channel: FL1 for FITC***

8.7 Product characterization by SDS-PAGE and Western Blot analysis of CD19 constructs

Figure 8.7.1 shows the result of a non-reducing SDS-PAGE and subsequent western blot of CD19Fc, CD19HSAD2 and CD19mutAFc products. Both blots were run on the same gel and had the same samples applied. The left plot was aiming at the CD19 part of the different constructs and labelled with alkaline phosphatase (colorimetric detection) of the secondary antibody. The right blot was using an anti-human-gamma-chain antibody targeting the Fc part of the CD19-Fc and the CD19mutAFc construct. The antibody was labelled with horse-radish peroxidase (HRP) and detected via enhanced chemiluminescence.

The CD19-Fc product (in blue) in lane 1 appears on both blots at about 140 kDa which correlates with the size of the heterodimer (136 kDa). The bands above 140 kDa are probably the result of some form of aggregation of the CD19-Fc. Another band that can be seen at about 55 kDa on the anti-gamma-chain blot could be caused by the cleavage of the Fc part (2x CH2&CH3 domain) from CD19, which also explains why this specific band is not present on the CD19 blot.

CD19-HSAD2 in lane 2 is only visible on the CD19 blot since is does not contain any Fc part. Again, a large smear above 65 kDa indicates an aggregation of the product, with a small band appearing at 65 kDa which could be explained by the monomer of CD19-HSAD2.

Lane 3 was used for a positive control with a 3D6 scFv-Fc, which can only be seen on the anti-gamma-chain blot because of the missing CD19 portion. The band appears at approximately 115 kDa and can also be seen to a small extend in band 4 and 5 due to some unintended sample transfer during the sample loading into the wells.

The CD19mutAFc in lane 4 and 5 can be seen on both blots as a band at 68 kDa, which represents the monomer of the construct. Due to the higher sensibility of the enhanced chemiluminescence on the anti-gamma-chain blot, two additional band can be seen. The first band between 115 kDa and 140 kDa is probably the result of an unwanted homodimer formation of two CD19mutAFc, since the mutation in the Fc part should prevent such occurrences. The second band at 30 kDa might again be caused by the cleavage of CD19 from Fc, however, this time only half of the Fc part can be seen (1x CH2 & CH3 domain) because of the mutation preventing the connection of two CH_3 domains.

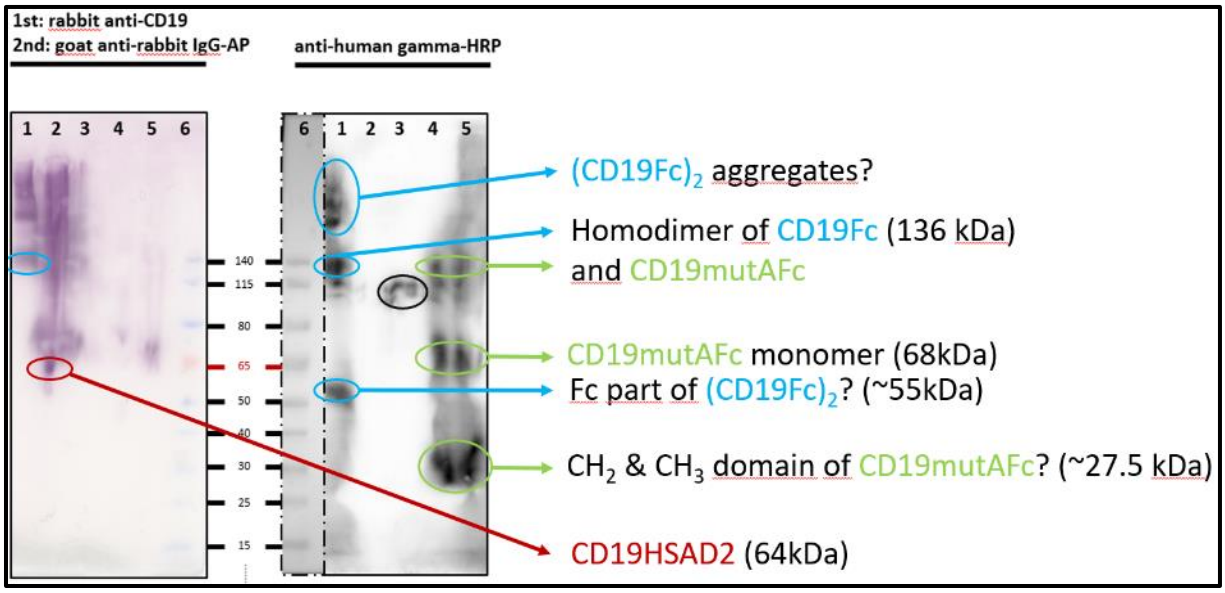

Figure 8.7.1.: Western Blot of CD19-Fc, CD19HSAD2 and CD19mutAFc. Left: rabbit anti-CD19 antibody + anti-rabbit-AP antibody. Right: anti-human-gamma-chain antibody labelled with HRP. Lanes: (1) CD19-Fc 64ng, protein A purified (2) CD19-HSAD2, concentration unknown, supernatant concentrated 1:35 at 10 kDA (3) 3D6 scFv-Fc 64ng (4) CD19mutAFc, 46ng concentrated from supernatant (5) CD19mutAFc, 59ng concentrated from supernatant (6) PageRuler prestained protein ladder. SDSPAGE conditions: non-reducing, NuPAGE™ Novex™ 4-12% Bis-Tris 1.0 mm 12-well gel, MOPS buffer (200 V, 1h).

In figure 8.7.2 a silver-staining of an SDS-PAGE gel was performed with samples of CD19-Fc purified via IMAC or protein A chromatography. All the samples were applied twice, once in non-reduced form and once in reduced form to break up disulfide bonds. In Lane 1, the IMAC purified CD19-Fc was applied but since the CD19-Fc was still in elution buffer, which contained high amounts of imidazole, no clear band could be obtained from that sample. Lane 2 and 3 shows CD19-Fc purified with protein A chromatography with the sample being in PBS buffer (lane 2) and protein A elution buffer (lane 3) respectively. The protein ladder in lane "L" was not intended for the use in a combination with Tris/Acetate buffer and the 4-12% BIS/TRIS gel, therefore, the indicated kDa values can only be taken as approximations.

The application of the reducing agents and heat resulting in the destruction of disulfide bonds, inhibited the formation of heterodimers of CD19-Fc which can be seen on the "reduced" part of the gel in lane 2 and 3 at about 70 kDa (monomer size = 68 kDa). However, there are still some residual homodimers which can be seen between 130 and 180 kDa and are probably the result of an incomplete disulfide bond dissolution. Furthermore, there is a small band in lane 3 below the 35 kDa marker which could represent the CH2 and CH3 domain of the Fc-Part of CD19-Fc, again displaying the phenomenon of the Fc cleavage from CD19 (see also figure 8.7.1).

In lane 2 and 3 of the non-reduced half of the gel, the homodimer of CD19-Fc can be seen between the 130 and 180 kDa marker, with a band of unknown origin slightly above 100 kDa in lane 3. Moreover, the cleaved off Fc part can be seen again in lane 3 at about 55 kDa.

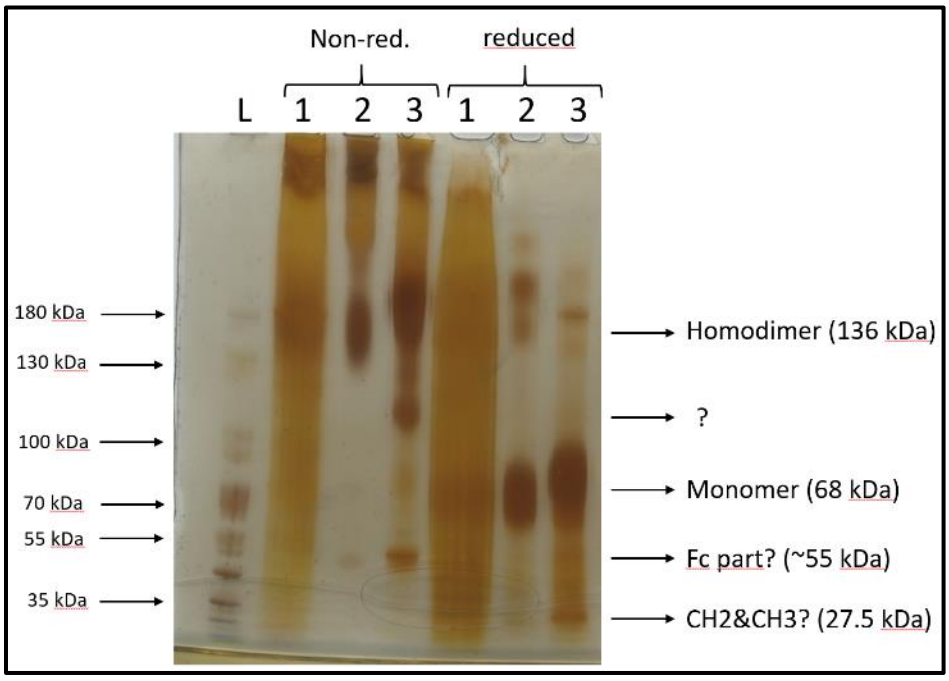

Figure 8.7.2.: Silver stained SDS-PAGE gel of CD19Fc. (1) CD19-Fc 260 ng IMAC purified in elution buffer (2) CD19-Fc 530 ng protein A purified in PBS (3) CD19-Fc 570 ng protein A purified in elution buffer (L) PageRuler prestained protein ladder. SDS-PAGE conditions: 4-12% BIS/TRIS gel – 10 well, NuPage Tris-Acetate running buffer, Sample reduction: 50 mM DTT, 95°C

Figure 8.7.3 shows the result of a western blot using different antibodies targeting CD19, CD21, Fc, and the His-tag of the CD19/CD21 subclones 2H8 and 1D6. Unfortunately, none of the CD19/CD21 clones revealed any bands on any of the blots. The only bands that can be seen are obtained by the positive controls: 3D6-scFv-Fc in lane 6 at 115 kDa and CD19-Fc in lane 4 and 8. However, the bands of the CD19-Fc blot appear in close proximity to the 50 and 185 kDa marker and it is therefore not certain whether those bands are caused by the CD19-Fc monomer (68 kDa) and homodimer (136 kDa) respectively. Additionally, it is not entirely clear, as to why the CD19/CD21mutFc clones did not reveal any bands, however, in contrast to the positive controls, which were purified products, the CD19/CD21mutFc was simply applied form concentrated supernatant of the clones, which might have had an impact on the SDS-PAGE and/or western blot as well.
Furthermore, before the overnight incubation with the primary antibody, the blots have already been incubated for 1h with the primary and secondary antibody and analysed via ECL. However, the blot did not reveal any bands which is why the blots were again incubated with the primary antibodies o/n at 4°C and the secondary antibodies for 3h at room temperature. This first ECL analysis, as well as the "off-protocol" incubation might have influenced the result as well.

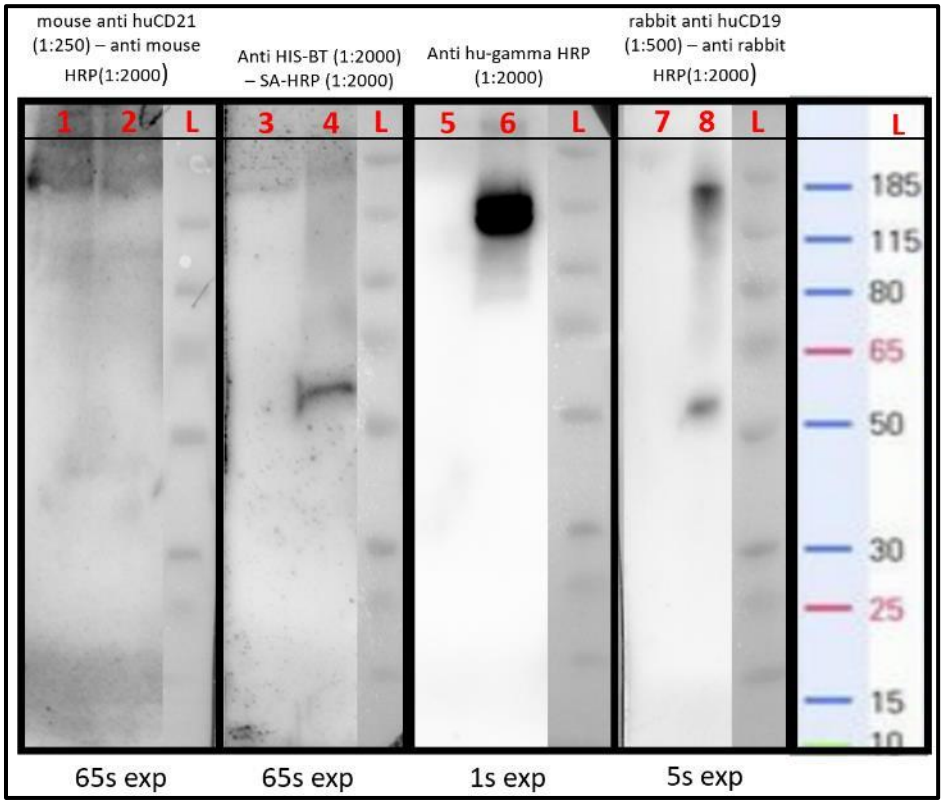

Figure 8.7.3.: Western Blot of CD19/CD21mutFc concentrated from culture supernatant to 100ng/well (subclone 1D6 and 2H8 on passage number 11) with different detection antibodies. Different exposure times for the enhances chemiluminescence were employed which can be seen below the blots. Lanes: (1) 2H8 (2) 1D6 (3) 1D6 (4) CD19-Fc protein A purified (5) 1D6 (6) 3D6scFv-Fc (7) 1D6 (8) CD19Fc (L) PageRuler prestained Protein Ladder. SDS-PAGE conditions: NuPAGE™ Novex™ 4-12% Bis-Tris Protein Gels, 1.0 mm, 12-well, MOPS buffer (200 V, 1h), LDS loading buffer, 6 µL Ladder, non-reducing (no DTT, no heat). Primary antibody incubation: o/n 4°C. Secondary antibody incubation: 3h/RT

8.8 His-tag targeting flow cytometric analysis

In order to find a staining procedure that can be applied for the CD19-Fc and the CD19-HSAD2 constructs in parallel, a flow cytometric analysis aiming at the His-tag of the respective proteins was performed. An untransfected CHO-K1 clone acted as a negative control, which can be seen in blue. For the CD19-HSAD2 (green), the subclone 2C12 of passage number 6 was used which achieved a titer of 120 ng/ml in the supernatant on that day. The subclone 1G4 was used for analyzing CD19-Fc, which was fixed on passage number 29 (CD19-Fc titer of 35 ng/ml). Both constructs show similar fluorescence intensities, with CD19-HSAD2 being slightly higher which correlates with the higher products titer in the supernatant on that day. Other than that, the flow cytometric analysis targeting the His-Tag seems to work for both constructs.

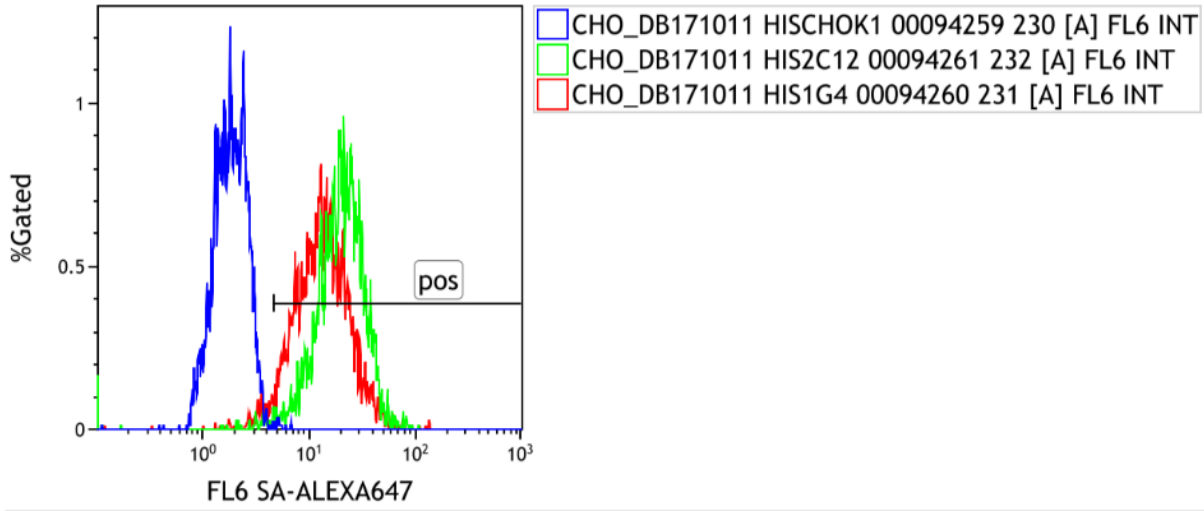

Marker	Number	%Gated	X-Med	X-Mode	X-GMean
All	2,671	100.00	1.84	1.80	1.77
All	2,394	100.00	20.32	21.03	17.59
All	3,361	100.00	13.14	13.90	11.90
pos	13	0.49	5.23	4.81	5.39
pos	2,351	98.20	20.55	21.03	19.51
pos	3,216	95.69	13.64	13.90	13.41

Figure 8.8.1.: Flow cytometric analysis using anti-His-tag-biotin antibody (1:100) coupled with a strept-avidin-Alexa647 antibody (1:100). Negative control in blue, CD19HSAD2 subclone 2C12 in green, CD19-Fc subclone 1G4 in red.

8.9 Cell-based assay for evaluation of CAR-T cell interaction with CD19-Fc by flow cytometry

To test the binding of the recombinantly produced CD19-Fc to anti-CD19 CAR-T cells, the purified CD19-Fc constructs (see 8.5) were used in a flow cytometric analysis in combination with anti-CD19 CAR-T cells. The CD19-Fc itself was additionally labelled with anti-His-biotin and strept-avidin-Alexa647 to render it detectable via fluorescence.
Figure 8.10.1 shows the result of the flow cytometric analysis with CD19-Fc samples from three different chromatography purifications: 2x protein A (dark green and red) and 1x His-Tag (moss-green). The black curve represents the CAR-T negative control incubated with anti-HIS antibody and Alexa647 conjugate, but without CD19-Fc product. CAR-T cells alone were also measured which can be seen in light green. In order to indirectly test for the presence of CAR molecules on the surface of T cells, co-expression of tEGRF (truncated epidermal growth factor receptor) was detected via an anti-EGFR antibody labelled with biotin and strept-avidin-Alexa647 (dark blue curve). This indirect confirmation of the CAR presence is made possible by the fact that both receptors are transcribed as a bicistronic mRNA, with a ribosomal skip element separating the two proteins.
The red curve (CD19-Fc purified by protein A chromatography) displays the only sample that delivered a higher fluorescence signal than the negative control which therefore indicates the successful binding of CD19-Fc to the anti-CD19 CAR T-cell. Unfortunately, the other two tested samples did not display a positive signal, however, the positive sample was only about three months old (18 µg/ml CD19-Fc), whereas the other two samples were about 5.5 months (His-tag purified CD19-Fc, 23 µg/ml CD19-Fc, moss green curve) and 7 months (protein A purified CD19,26 µg/ml CD19-Fc, dark green curve) old, which could have had an impact on the protein quality and therefore on the binding capacity.

To compare the protein quality of the used samples a SDS-PAGE or size-exclusion-chromatography could have been performed to check whether there has been some proteolytic cleavage of the CD19-Fc construct. A silver stained SDS-PAGE was performed on the exact same samples seven weeks prior to the CAR-T cell assay which can be seen in figure 8.7.2, where some possible proteolytic cleavage of the CD19 from the Fc part already occured in both protein A purified samples. Unfortunately, it was not possible to evaluate the IMAC purified sample due to the absence of bands on the gel.

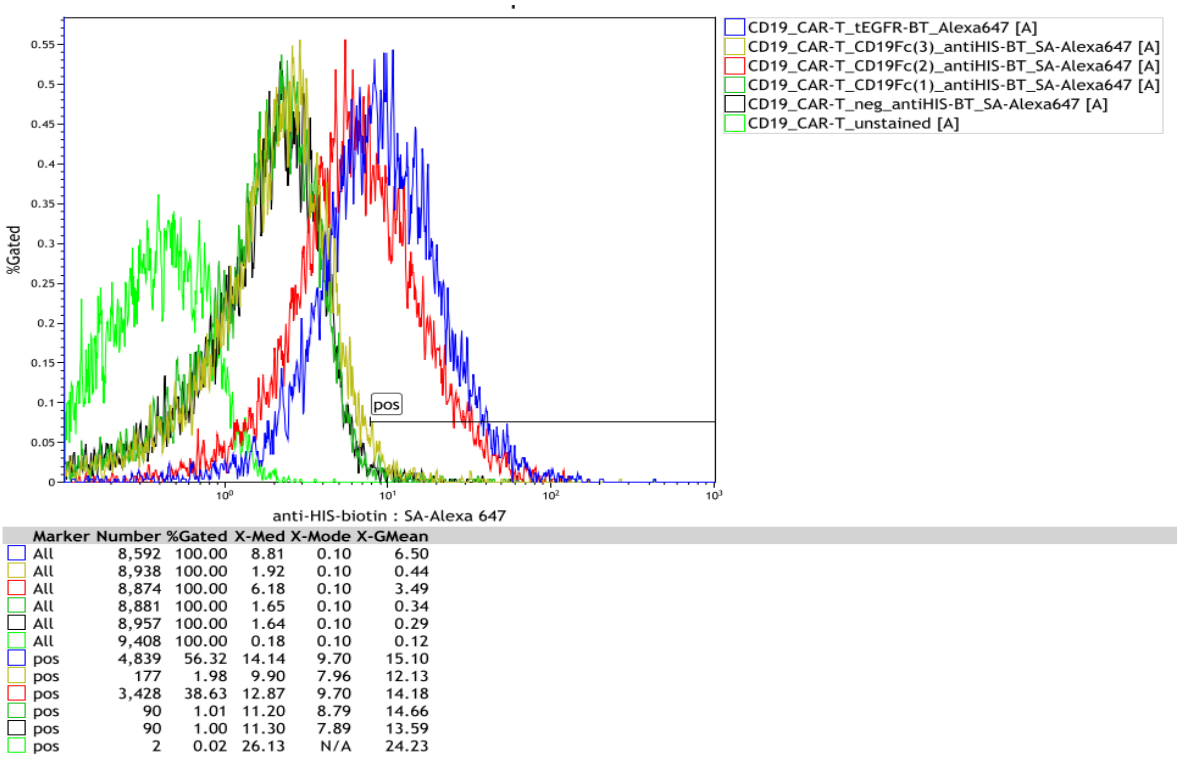

Marker	Number	%Gated	X-Med	X-Mode	X-GMean
All	8,592	100.00	8.81	0.10	6.50
All	8,938	100.00	1.92	0.10	0.44
All	8,874	100.00	6.18	0.10	3.49
All	8,881	100.00	1.65	0.10	0.34
All	8,957	100.00	1.64	0.10	0.29
All	9,408	100.00	0.18	0.10	0.12
pos	4,839	56.32	14.14	9.70	15.10
pos	177	1.98	9.90	7.96	12.13
pos	3,428	38.63	12.87	9.70	14.18
pos	90	1.01	11.20	8.79	14.66
pos	90	1.00	11.30	7.89	13.59
pos	2	0.02	26.13	N/A	24.23

Figure 8.10.1.: Result of the flow cytometric analysis of CD19-Fc with anti-CD19 CAR-T cells. Detection of CD19 with anti-His-biotin antibody (1:100) coupled with strept-avidin-Alexa647 (1:100). Positive control: dark blue, sample with positive signal: red, negative control: black, CAR-T cells without CD19-Fc and antibodies: light green.

In addition to the CAR itself, the CAR-T cells also carry GFP on the surface which was measured during the flow cytometric analysis and correlated with the signal of Alexa647 (and therefore binding of CD19-Fc to the CAR). This correlation can be seen in figure 8.10.2.: (1) non-CAR-T cells without GFP (2) CAR-T cells without antibodies or CD19-Fc (3) CAR-T cells with antibodies but without CD19-Fc (negative control) (4) CAR-T cells stained for tEGFR (positive control) (5) CAR-T cells with CD19-Fc and antibodies (positive sample).

Compared to the negative control (3), it can clearly be seen that the addition of CD19-Fc (5) causes cells with high GFP fluorescence signals to display higher signals of Alexa647 which can be seen in a shift to the right on the x-axis. This means that predominantly, cells with GFP on their surface possess an anti-CD19 CAR receptor which allows for binding of the CD19-Fc product and fluorescence detection via Alexa647.

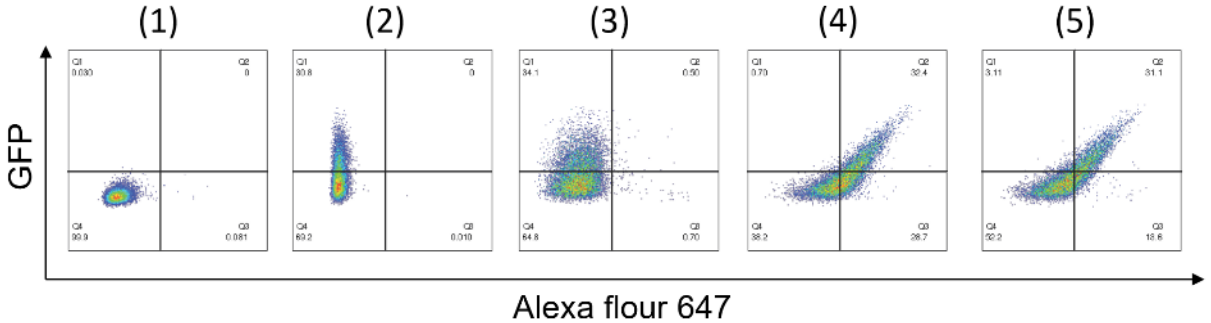

Figure 8.10.2.: Correlation of GFP and Alexa647 signals of the CD19-Fc/CAR-T interaction. (1) non-CAR-T cells without GFP (2) CAR-T cells without antibodies or CD19-Fc (3) CAR-T cells with antibodies but without CD19-Fc (negative control) (4) CAR-T cells stained for tEGFR (positive control) (5) CAR-T cells with CD19-Fc and antibodies (positive sample)

9. Discussion

9.1 Transfection of CHO-K1 with pL_CD19-HSAD2 and pL_CD19mutAFc pL_CD21mutBFc

For the transfection of CHO-K1 cells, the polyplex forming agent PEIMAX (polyethylenimine) was used in combination with the desired plasmid (pL_CD19-HSAD2 or pL_CD19mutAFc and pL_CD21mutBFc). The positively charged PEIMAX binds the negatively charged DNA and therefore allows the uptake by the slightly negatively charged cell surface. As a negative control, CHO-K1 without a transfected plasmid was cultivated under the same conditions to check whether the applied G418 selection marker works as intended. G418 is an aminoglycoside which interferes with the function of 80S ribosomes and protein synthesis in eukaryotic cells. Since the plasmids used for transfection carry a neoR gene (for neomycin phosphotransferase), which confers resistance to G418 by phosphorylating the aminoglycoside, successfully transfected cells can be selected [24,25].
About three weeks after transfection, the transfection efficiency was determined based on the number of acidified (yellow) wells. Negative controls had transfection efficiencies of 0%, meaning that the applied selection pressure performed as intended and did not allow non-transfected cells to grow. For the transfection with pL_CD19-HSAD2, high transfection efficiencies of 82-94% could be achieved, which increases the likelihood of having more than one transfected clone in one well, potentially leading to an inhomogeneous cell population in one clone pool. The twelve clone pools chosen for cultivation were therefore analysed via flow cytometry during cultivation in tubes, which revealed that half of the clone pools consisted of a very heterogenic population. The reason for the high transfection efficiency was probably the high seeding number of 2500 cells/well for the 384 well plate and 10000 cells/well for 96 well plate, which is why only half of that was used for the next transfection with pL_CD19mutAFc and pL_CD21mutBFc.
Due to the fact, that two plasmids needed to be transfected for the CD19/CD21mutFc construct, two approaches of co-transfection were tested: 1) Polyplex formation with PEIMAX and both plasmids at once using 4 µg of each plasmid (=”CD1921”) and 16 µg of PEIMAX and 2) Polyplex formation with PEIMAX and only one plasmid at a time using 8 µg of each plasmid and 16 µg of PEIMAX (=”CD19+21”). This means a total of 16 µg of plasmid DNA and 32 µg of PEIMAX was added to the cells in this approach. For “CD1921”, transfection efficiencies of 60% for the 96 well plate seeded with 5000 cells/well and 17% for the 384 well plate seeded with 1250 cells/well were determined, showing the effect of the lower seeding number on the transfection efficiency. The “CD19+21” approach led to transfection efficiencies of 92% (96 well plate) and 29% (384 well plate), which is probably owed to the use of twice the amount of plasmid DNA in the transfection. The use of twice as much PEI – which is toxic to the cells – did not seem to lower transfection efficiencies, probably because the cells were subjected to PEI for only 4 hours. Unfortunately, no flow cytometric analysis was performed on the twelve clone pools coming from the CD19/CD21mutFc transfection and it is therefore not possible to speculate if the use of lower seeding numbers led to more homogenous clone pools compared to the CD19HSAD2 transfection.

The screening process after transfection which was performed via qualitative ELISA revealed, that CHOK1/CD19-HSAD2/J16 was the clone pool with the highest titer (39.48 ng/ml) in the supernatant of the 384 well plate. J16 was also the clone pools which performed best during the cultivation in tubes and was therefore chosen for subcloning, which gave rise to the subclone 2C12, which was ultimately found to be the best and final producer of CD19-HSAD2. The screening of the CD19/CD21mutFc transfectants showed 3G4 with a titer of 113 ng/ml as the best clone pool, however it was outperformed by 1E5 and 10C10 (which only had titer between 50 and 60 ng/ml in the qualitative

ELISA) during the cultivation in tubes and therefore not chosen for subcloning and establishment of a final producing clone. Since a qualitative ELISA only measures one well per clone pool, it is very susceptible to displaying outliers as the best clone pools, which can be caused by handling errors during the analysis.

9.2 Performance of CHO-K1 expressing different CD19 constructs

CD19-HSAD2:

During the routine cultivation with cell passaging every 3-4 days, the twelve cultivated clone pools of CHOK1/CD19HSAD2 were able to reach an average of $6*10^6$ viable cells/ml with an average growth rate of 0.9 d^{-1} during passage 4 to 9. From these twelve clones, J16 could achieve the highest viable cell number and specific growth rate with values of $8*10^6$ cells/ml and 1.14 d^{-1} respectively. In combination with its CD19-HSAD2 expression capabilities, leading to average titers between 100-200 ng/ml (max. 600 ng/ml) and specific productivities between 0.02-0.03 pg/cell/day (max 0.07 pg/cell/day), J16 was the best clone pool after transfection, which could already be seen during the screening of transfectants via qualitative ELISA, where J16 was also the best clone pool of the 384 and 96 well plates. In the flow cytometric analysis J16 displayed the highest intracellular product content as well, which indicates the correlation between intracellular product and titer in the supernatant. However, the flow cytometric analysis also showed a more heterogenous cell population of J16 compared to other clone pools. During the later phases of the cultivation, J16 was again observed via flow cytometry and compared to its subclones and this time a homogenous cell population could be seen, which means that the homogeneity increased over time.

Due to its performance, J16 was chosen along 3 other partenal clone pools for subcloning via limiting dilution. During the screening of subclones, CHOK1/CD19-HSAD2/J16/2F7 displayed the highest titer in the qualitative ELISA with 30 ng/ml. Additionally, 11 other clones were chosen and during the routine cultivation and the subclone CHOK1/CD19-HSAD2/J16/2C12 (with a titer of only 13 ng/ml during screening) turned out to be the best producing clone with titers up to almost 450 ng/ml on passage number 2 which then settled around 100 ng/ml with specific productivities of about 0.02 pg/cell/day throughout passage number 8 to 12. An average viable cell number of $5*10^6$ and an average growth rate of 0.94 d^{-1} could be obtained by 2C12 during passage 2-12, which is almost the same as the average values of its parental clone pool J16 ($5*10^6$ cell/ml and $0.92*d^{-1}$).
In the flow cytometric analysis, the subclones as well as the partental clone J16 displayed a very homogenous cell population and about the same intracellular product content. To summarize the effect of subcloning: growth of the 2C12 subclone was similar to that of the parental clone J16 which in turn could achieve slightly higher CD19-HSAD2 titers. 2C12 was still chosen to be the final producing clone, since subcloning decreases the chance of drifting to a more heterogenous, less producing cell population during longer episodes of cultivation (i.e. weeks and months of passaging). Another important factor for the evaluation of CD19-HSAD2 titer via ELISA is that the anti HSA ELISA was not optimized. We are not definitely sure if the measured values are accurate – for details see the result part 8.2. Furthermore, the standard used in the ELISA was HSA, whereas the samples only consist of the D2 (domain 2) part of HSA. Therefore, the titers of the samples calculated based on the absorption of the standard might differ from the real values since the polyclonal antibodies have more binding sites on the HSA standard compared to the CD19-HSAD2 construct.

CD19-Fc:

Clone pools expressing CD19-Fc were growing to average viable cell numbers of $4*10^6$ cells/ml with average growth rates of 0.8 d^{-1}, which is considerably lower than what the CD19-HSAD2 clones were capable of. However, maximum cell number of $8*10^6$ and maximum specific growth rates of 1.06 d^{-1} could be obtained by the N9 clone pool which are similar maximum numbers as the ones achieved by CHOK1/CD19HSAD2/J16. The untransfected CHO-K1 clone showed similar growth behaviour as the compared to the (on average) best growing clone pool H21, however, the average viable cell number of $5*10^6$ cells/ml and average growth rate of 0.94 d^{-1} were still higher than the average of the other transfected clone pools, probably due to the lack of stress induced by the recombinant protein production resulting in enhanced growth. Titers were ranging between 30-60 ng/ml with a specific productivity of about 0.01 pg/cell/day, which is about half than was produced by the CD19-HSAD2 clones. However, it should again be noted that 1) the ELISA for HSA was not optimized for a lot of the measurments of the titer and 2) the standard of the ELISA for both CD19 constructs is not the same as the sample (i.e. 3D6sc-FvFc for CD19-Fc and HSA for CD19-HSAD2). Therefore, the titers calculated based on the absorption of the standard which is different from the sample might not be entirely correct. Both reasons should be kept in mind when comparing titers of the two different CD19 constructs.

The subclones 1G4 and 1C9 had similar growth as their parental clone pool H21 with specific growth rates between 0.8-1.0 d^{-1} and viable cell numbers up to $7*10^6$ cells/ml. However, 1G4 had titers settling in the range of 50-100 ng/ml during later passages, whereas H21 never managed to produce more than 58 ng/ml. The better CD19Fc production capabilities can also be seen in terms of specific productivity, where 1G4 was achieving between 0.01-0.02 pg/cell/day and H21 could only reach productivities up to 0.01 pg/cell/day. 1C9 could accomplish even higher titers between 100-150 ng/ml, however, due to a drop in viability, 1G4 was chosen to be the final producing clone of CD19-Fc. In terms of cell population homogeneity determined via flow cytometry, the parental as well as the subclones had a very symmetrical peak, indicating the absence of subpopulations. Intracellular product content was a little bit lower of H21 on one passage, again showing the correlation between the amount of product in the cell and the titer in the supernatant. Compared to CHOK1/CD19-HSAD2, the subcloning procedure seemed to have a greater impact on the CD19 production, which can be seen when comparing titers of H21 with those of its subclones 1G4 and 1C9. Cell population homogeneity and growth performance however, were not influenced that much.

Another phenomenon that was observed with some CD19-Fc producing clones/clone pools, was a slow decrease in viability over several passages accompanied by a very steep increase in product titer. A possible explanation for this correlation between CD19-Fc titer and viability might be that either upon cell-death, intracellular CD19-Fc is released or the increased CD19-Fc concentration in the supernatant is toxic to the cells themselves. However, if the second possibility were true, then all the other clones would be affected by the CD19-Fc in supernatant as well and there would be still no explanation why the CD19-Fc titer increased that much in the first place.

CD19/CD21mutFc:

Viable cell numbers of the two best clone pools 1E5 and 10C10 were between 3-$6*10^6$ cell/ml with growth rates being between 0.8-1 d^{-1}. 1E5 had average values of $5*10^6$ cells/ml and 0.92 d^{-1} which is in between CHOK1/CD19-Fc and CHOK1/HSAD2 in terms of growth performance. Maximum titers of 578 ng/ml could be obtained by 1E5 which is similar to what was achieved by CHOK1/CD19HSAD2/J16. However, the maximum titer of 587 ng/ml might be an outlier which is further indicated by the flow cyctometric analysis of the intracellular product content, which was lower than the 1G4 (CD19-Fc producer) and 10C10 clones which had titer between only 50 and 100 ng/ml. Another option might be

that 1E5 has better product secretion capabilities which leads to lower product accumulation in the cell and higher titer in the supernatant.
This can also be seen in the average titers of 1E5 which were between 200 and 400 ng/ml with specific productivities of 0.04-0.06 pg/cell/day. Therefore, production performance of CD19/CD21mutFc was a lot higher compared to CD19-Fc and CD19-HSAD2 clones. However, since the ELISA was only aiming at the Fc part of the construct and cannot distinguish between a monomer and dimer it is not possible to compare these titer with the other constructs, since the titer refers to CD19mutAFc and CD21mutBFc both and it is not possible to know how much of it is actually CD19.

The growth performance of the subclones of 1E5 and 10C10 was similar to CHOK1/CD19-Fc clones, with average cell numbers of $3*10^6$ and average growth rates of 0.81 d^{-1}. Titer between 200-500 ng/ml and specific productivities of 0.06-0.08 pg/cell/day were accomplished which is slightly better than the production performance of the parental clone pools. The subclones 1D6 (parental clone 10C10) and 2H8 (parental clones 1E5) were ultimately chosen to be the final producing CD19/CD21mutFc clones.

The clones producing CD19/CD21mutFc were also analysed with flow cytometry using an anti-CD19 antibody to see whether the transfectants were really producing CD19mutFc and not only CD21mutFc. In the first analysis the anti CD19 antibody was first tested on CHOK1/CD19/21mutFc/3G4 to check if the antibody works for the flow cytometry in the intended way. 3G4 gave a positive result, indicating that 1) the antibody works for the detection of CD19 in a flow cytometric analysis and 2) 3G4 is producing at least some CD19mutFc.
However, using the same staining procedure as with 3G4, no positive signal obtained by the parental clones 10C10, 1E5 and their subclones 2H8, 2F3, 2B3. The positive control CHO-K1/CD19-Fc/H21/1G4 delivered a positive result, indicating the flow cytometric staining and analysis had worked and therefore the only explanation for the negative result of the CHOK1/CD19/CD21mutFc is that only very little or no CD19 is present in them. Furthermore, if the intracellular presence of CD19 is taken as an indicator of CD19 in the supernatant, the supernatant titer determined by the ELISA targeting the Fc part might be predominantly derived from CD21mutBFc, which might also explain the higher titers achieved by the CD19/CD21mutFc clones compared to the other CD19 construct producing clones.

In the flow cytometric analysis targeting the Fc part, CHO-K1/CD19-Fc/H21/1G4 displayed equal levels of intracellular product content compared to the CD19/CD21mutFc clones (which were analysed with the anti-CD19 antibody before), which achieved 4-6 times higher titers in the supernatant. This could be explained by the increased secretion capabilities of CD19/CD21mutFc clones.

Furthermore, the 3G4 clone pool was also stained with an anti-CD21 antibody for the flow cytometric procedure. However, 3G4 treated with the anti-CD21 antibody did not display peaks with an increased fluorescence intensity, it's either possible that no CD21 is present within the cell or that the CD21 antibody is not working properly or the antibody dilutions were not appropriate (recommended dilution of 1:2 by the manufacturer for flow cytometry). Because of the missing positive control for CD21, it is not possible to tell which of the aforementioned reasons holds true.

9.3 Pseudoperfusion cultivation

The aim of the pseudoperfusion cultivation experiments with the established main-producer of CD19-Fc (CHO-K1/CD19-Fc/H21/1G4), was to achieve very high cell numbers by daily media exchange, and in turn to produce higher amounts of CD19-Fc compared to traditional cell passaging every 3-4 days. For the experiment, different media as well as a "cell bleeding" approach were tested. 20% of the cells were removed each day in the bleeding strategy to prevent them from being in a real stationary phase, which may yield higher product titers by maintained productivities.

The pseudoperfusion culture in CDM4-HEK293 base medium was able to achieve viable cell numbers up to $32*10^6$ cells/ml with a corresponding titer of 120 ng/ml at the end of the exponential phase. Cells grown in CD-CHO base medium could reach viable cell numbers of $26*10^6$ cells/ml and a titer of 140 ng/ml. This shows that supplying the cells with fresh medium every day allows for maximum cell numbers up to 5-10 times higher than in a routine culture. Although titers were similar to those of a routine culture, it has to be considered that the pseudoperfusion culture produced these titers within one day, yielding a higher total amount of product in the same time period.

Although the CD-CHO medium was specifically designed for CHO cells, the CDM4-HEK293 got the cells to grow to slightly higher numbers. But despite the lower cell numbers, product titers were higher using the CD-CHO medium. Specific growth rates for both cultivations were approximately 0.5 d^{-1} in the exponential phase and furthermore, a flow cytometric analysis revealed that there was no change in intracellular product content or cell population homogeneity. Another observation was, that after reaching the stationary phase, the cell number decreased slightly from day to day which can be explained by several factors: 1) a loss of cells during medium exchange (i.e. removal of old medium after centrifugation), 2) sample taking for cell number and titer determination 3) dissolution of dead cells which were not analysed by the ViCell cell counter and 4) no re-growth of cells.

In 10 days of peudoperfusion cultivation (excluding the three days of batch culture before), 20 µg of CD19-Fc were produced in the pseudoperfusion culture using CD-CHO as base medium. Assuming, that in this timeframe two regular passages of a routine culture are necessary, and further assuming that 30 ml of routine culture were used with an average titer of 50 ng/ml, only 4.5 µg of CD19-Fc can be produced (in 3x30 ml) when using the regular culture approach with passaging every 3-4 days. Therefore, the pseudoperfusion culture provides a means to produce larger amount of product in the same time. Considering that a pseudoperfusion cultivation requires about 300 ml of medium for a duration of 10 days (about three times as much as the regular cultivation), but produces ~4 times as much product, it is additionally more profitable when it comes to the cost of the media. The downside to this is the increased work load in the laboratory that is necessary.

The cell bleeding approach was tested on pseudoperfusion cultivations using CDM4NS0 and CDM4NS0 + CellBoost 1 and 3 (CB 1/3) as base medium, starting before reaching the assumed stationary phase (at about $25\text{-}30*10^6$ cells/ml). Maximum viable cell numbers for both cultivations were $26.5*10^6$ cells/ml with a specific growth rate between 0.5-0.7 d^{-1} during the exponential phase. As mentioned before, the cells were not able to divide after reaching the stationary phase, and therefore the cell bleeding resulted in a reduction of viable cell number by 20% from day to day. However, an increase in average cell diameter from 16 µm to 19 µm could be seen from day 3 to 14, showing a slight growth in cell size. Although cell numbers decreased after day 7, an increase in CD19-Fc titer from about 50 ng/ml to over 100 ng/ml could be observed from day 9 onward, meaning fewer but larger cells which are not in an exponential phase could produce more CD19-Fc in the supernatant. This can also be seen in terms of specific CD19-Fc production which increased 5-fold to about 0.015 pg/cell/day from day 10 to 14.

In terms of CD19 production the CDM4NS0 medium produced about 24 µg of CD19-Fc in total, whereas the CDM4NS0 + CB1/3 was only able to achieve 15 µg. However, these numbers are still similar to those of CDM4HEK293 and CD-CHO pseudocultivation, although the cell bleeding led to a drastic decrease in cell number over time.

9.4 Purification of CD19-Fc via chromatography

For the purification of CD19-Fc from the culture supernatant (e.g. from the pseudoperfusion cultivation) the supernatants were first concentrated via crossflow filtration and then subjected to either protein A chromatography or Immobilized metal affinity chromatography (IMAC), making use of the Fc-part or the His-tag of the protein, respectively.

During the chromatography steps using protein A affinity, between 50-70% of CD19-Fc were lost with a total of 6-12 µg remaining in the eluate. The "flowthrough", the "wash" and the "clean" fraction did only contain little to no CD19-Fc, and can therefore not be the reason for low yields in the protein A chromatography. Other options might be that not all of the CD19-Fc is eluted from the column, but is only removed when applying the cleaning steps with NaOH, which resulted in a peak of the UV signal, further supporting this theory. Unfortunately, the chromatogram of the cleaning procedure was not saved and is therefore not included in the result part.

During the cross-flow filtration for the IMAC only 25% of the CD19-Fc could be recovered and essentially no concentration of the sample took place. However, the His-tag chromatography yielded 155% of CD-19Fc coming from the retentate of the crossflow filtration, indicating that maybe the quantification of CD19-Fc in the retentate was faulty. Furthermore, only very little CD19-Fc could be found in the permeate, therefore the low yield of the cross-flow filtration cannot be explained by the loss of protein through the membrane. Another reason might be that there was some CD19-Fc left in the TFF device/membrane which could only be removed by the cleaning steps with H_2O and NaOH.

It can be concluded that either protein A affinity chromatography or IMAC are suited for purification of CD19-Fc, however the loss of product seemed to be smaller using IMAC. For a more meaningful comparison of the two chromatography procedures, 1) more IMAC experiments would have to be carried out and 2) aliquots of the same sample should be used for protein A affinity and IMAC. Nonetheless, for purification of CD19-HSAD2, IMAC is the only viable option of the two since no Fc domain is present for protein A affinity purification.

9.5 ELISA optimization for CD19-HSAD2

A major problem of the HSA quantification via quantitative sandwich ELISA was, that the absorption curve of the samples did not behave like the curves of the standard in lower dilutions, which made it impossible to have a reliable quantification of the CD19-HSAD2 construct. These differences between standard and sample probably arise because they are not the same protein: The sample contains the CD19 domain linked to only the D2 domain of HSA, whereas the standard is made of an entire HSA protein. Furthermore, since the coating and conjugation antibodies against HSA were of polyclonal nature, they had more potential binding sites (epitopes) on the standard compared to the sample which only carries one domain of HSA. This has to be considered when evaluating the determined titers of the samples since they were derived from a standard not matching the sample protein. However, it

has no influence when comparing CD19-HSAD2 titers of individual clones with one another, but makes it difficult to compare them to titers of other CD19 constructs.

Because the result of the SDS-PAGE/Western Blot it can be assumed that CD19-HSAD2 tends to form aggregates which could have had an impact on the binding properties in the lower dilutions of the anti-HSA quantitative ELISA. Since the CD19 domain consists of three disulphide bonds, an ELISA incorporating different reducing agents may have been able to decrease aggregate formation by destroying the tertiary structure and in turn deliver a better result. From the different reducing agents used, only DTT in combination with iodoacetamide was able to deliver a minor improvement compared to the non-reduced samples and other reducing agents. This might be due to the fact, that after breaking up the disulphide bonds with DTT, the iodoacetamide alkylated the reduced cysteine residues which inhibited the reformation of disulphide bonds. This also allowed for the use of regular dilution buffer when diluting the samples, therefore the coating antibodies were not exposed to the reducing agents present in dilutions buffers used in combination with either L-cysteine, mercaptoethanol, alpha-MTG or DTT (without iodoacetamide), which may have also been the reason for the better result of the DTT/iodoacetamide combination.
Furthermore, when looking at the samples subjected to alpha-MTG the binding seemed to be even worse than compared to the untreated samples, as seen by the significantly decreased absorption. This effect might be caused by the destruction of the coating antibody during the incubation with the sample in dilution buffer containing alpha-MTG.
For the approach using reducing agents it can be concluded, that if the aggregation of CD19-HSAD2 is the reason for the aforementioned problems, then the dissolutions of disulphide bonds barely has an influence on that – at least not to the extent where reliable results are produced by the ELISA.

Other parameters effecting the outcome of the anti-HSA ELISA, appear to be the coating antibody dilution as well as the initial dilution of the samples in the first well. When comparing the 1:500 with the 1:1000 coating antibody dilution, a significant improvement can be seen when looking at the absorption curve of the samples subjected to 1:500 diluted coating antibody. A reason for this might be that not all of the polyclonal anti-HSA antibodies bind to the domain 2 of CD19-HSAD2 and that coating with too few antibodies, does not provide enough antibodies binding to CD19-HSAD2. The standard however, which consists of an entire HSA, might be able to deal with a lower amount of coating antibody in the 1:1000 dilution since it provides all the binding sites for the antibody.

Furthermore, a higher initial sample dilution (1:20 compared to 1:4) also seemed to be important for a reliable result, which might have to do with decreased aggregation of CD19-HSAD2 in the well during incubation with the coating antibody. Another possibility is that the 1:4 dilution provides too much CD19-HSAD2 which cannot be bound by the coating buffer antibody. Therefore, an even lower dilution (e.g 1:250) of the coating antibody could have been able to deal with the 1:4 dilution since more antibodies are provided.

It should also be noted that the initial standard concentration seemed not to matter all that much, however standard concentrations that approximately match the titer of the highest sample should be chosen to obtain similar absorption curves. Furthermore, the use of PVP instead of BSA in the dilution buffer did not have an influence on the outcome of the ELISA.

9.6 CD19 product analysis

SDS-PAGE/western blotting

The analysis via SDS-PAGES (reduced and non-reduced) as well as western blots revealed a possible cleavage of the CD19-part from the Fc part, which is indicated by the bands appearing at the respective sizes of the fragments. Furthermore, a large amount of the CD19-Fc and CD19-HSAD2 constructs seems to aggregate, leading to unclassified bands/smears above the size of the homodimer of CD19-Fc or monomer in case of CD19-HSAD2. This aggregation might be caused by the natural behaviour of CD19 on the surface of B-Cells where they form clusters in order to modulate the B-cell receptor signalling [1,2].

The incorporation of a mutation in the Fc part of CD19mutAFc seems to prevent unwanted homodimer formation to some extent, however, with the high sensitivity of the ECL detection, there are still some homodimers which can be seen.

Additionally, a Western Blot was tested on CD19/CD21mutFc using anti CD21 antibodies to specifically stain CD21mutBFc. Unfortunately, the test again failed to deliver any results, which might either be caused by an inappropriate staining protocol for the CD21 antibody in terms of dilutions, incubation times, temperatures, secondary antibodies etc. or by the absence of CD21 in the sample. Since no positive control was available it is not possible to tell which one is true. The anti CD19 antibody used for Western Blotting only displayed bands on the positive control (CD19-Fc protein A affinity purified) which again showed that no CD19 might be present in the CD19/CD21mutFc clones.

Cell-based assay for evaluation of CAR-T cell interaction with CD19-Fc by flow cytometry

The recombinantly produced CD19-Fc - which was purified via protein A affinity chromatography from the supernatant of CHOK1/CD19-Fc/H21/1G4 and stored in the respective elution buffer at pH 7 for three months – was able to deliver a positive result compared to the negative control by successful binding to the anti-CD19 CAR of the T-cell. Since this was only a binding study, it only shows if the CD19 is capable to bind to the CAR-T-Cell and might also have the potential to activate it's cytolytic properties. In order to test if the bare binding of CD19 to the T-cell is sufficient for its activation, other assays need to be carried out (e.g. analysis of Ca^{2+} release of the T-Cell).

Unfortunately, the other two tested samples did not display a positive signal, however, the positive sample was only about three months old, whereas the other two samples were about 5.5 months (IMAC purified CD19-Fc, 23 µg/ml CD19-Fc) and 7 months (protein A purified CD19,26 µg/ml CD19-Fc) old, which could have had an impact on the protein quality and therefore on the binding capacity.
To compare the protein quality of the used samples a SDS-PAGE or size-exclusion-chromatography could have been performed to check whether there has been some proteolytic cleavage of the CD19Fc sample, which has already been observed with other samples. A silver stained SDS-PAGE was performed on the exact same samples seven weeks prior to the CAR-T cell assay which can be seen in figure 8.7.2, where some possible proteolytic cleavage of the CD19 from the Fc part already occurred in both protein A purified samples. It might therefore be possible that there is some time dependent proteolytic activity taking place which eventually destroys the CD19-Fc construct and therefore its detectability in the used assay. Unfortunately, it was not possible to evaluate the IMAC purified sample due to the absence of bands on the gel.

10. Conclusion

The preparation of the plasmid expression vector for CD19-HSAD2, which included the amplification of gene of interest from a template vector, the ligation with a pL vector, subsequent transformation of *E. coli* and midi-scale preparation used for stable transfection of CHO-K1 did not exhibit any complications (i.e. impurities of the plasmid solution or mutations in the gene of interest) and allowed for a successful transfection of CHO-K1 cells via PEI. The negative controls of the CD19/CD21mutFc and the CD19-HSAD2 transfection, which did not carry a plasmid were not able to grow in selection medium containing G418, demonstrating the selection pressure was working as intended.

The best CD19-HSAD2 transfectant (J16) was achieving titers in the range of 100-200 ng/ml with specific productivities 0.02-0.03 pg/cell/day, which is only slightly better than its subclone 2C12, which was chosen as the final producing clone since subcloning decreases the chance of having low or non-producers within a cell population.

Among the CHOK1/CD19-Fc clones, a subclone (CHOK1/CD19-Fc/H21/1G4) was found to be the final producer, with titers between 50-100 ng/ml and 0.01-0.02 pg/cell/day, whereas the final producers CHO-K1/CD19/CD21mutFc/10C10/1D6 and CHO-K1/CD19/CD21mutFc/1E5/2H8 had titers of 200-500 ng/ml and 0.06-0.08 pg/cell/day.

For the comparison of titers of different CD19 constructs three caveats have to be considered: 1) the standards for the quantification were not the same as the analysed product, meaning that the actual titers might be different (however it still allows for comparisons within one construct), 2) the quantification of CD19/CD21mutFc via ELISA solely relies on the Fc tag, which makes it impossible to distinguish between the amount of CD19 and CD21. Since no CD19 was found in an anti-CD19 flow cytometry and Western Blot analysis, it can be assumed that indeed no CD19 in present and that the ELISA only determined titers of CD21. 3) The anti-HSA ELISA had to be optimized first, which was only successful during the later stages of the CHOK1/CD19-HSAD2 cultivation.

In terms of cell growth, cells were growing between 4-6*10^6 cells/ml with a specific growth rate of 0.8-1.0 d^{-1} on average, with CHOK1/CD19-HSAD2 being best the growing and CHOK1/CD19-Fc being the worst growing clones.

Pseudoperfusion cultivations of CHOK1/CD19-Fc/H21/1G4 led to maximum cell numbers of about 30*10^6 cells/ml and four times more total production of CD19 in the same amount of time compared to traditional cell passaging every 3-4 days.

The purification of CD19-Fc worked with either protein A affinity chromatography or IMAC, with smaller losses observed in the IMAC.

The product analysis via SDS-Page and Western Blot that there was some proteolytic activity present which resulted in the cleavage of the Fc tag from CD19-Fc and CD19/CD21mutFc. Furthermore, aggregation of CD19-Fc and CD19-HSAD2 could be observed.

Lastly, the cell based assay for evaluation of CAR-T cell interaction with CD19-Fc by flow cytometry performed at the Huppa Lab, Medical University of Vienna, showed that the recombinantly produced and protein A affinity purified CD19-Fc has the ability to bind to anti-CD19 CAR-T cells. Based on this result, further experiments could be conducted, to see whether not only binding but also activation of the CAR-T cells by the recombinant CD19-Fc is possible and do additionaly study the molecular dynamics of the binding event.

11. List of tables and figures

List of figures

List of tables

12. References

[1] Yuekang Xu, “CD19 differentially regulates BCR signalling through the recruitment of PI3K”, Autoimmunity, vol. 47, issue 7, pp 430-437, 2014

[2] Robert H. Carter and Douglas T. Fearon, “CD19: Lowering the Threshold for Antigen Receptor Stimulation of B Lymphocytes”, Science, vol. 256, issue 5053, pp 105-107, April 1992

[3] Alexey Teplyakov, “Crystal structure of B-cell co-receptor CD19 in complex with antibody B43 reveals an unexpected fold”, Proteins: Structure, Function, and Bioinformatics, vol. 86, issue 5, February 2018

[4] Armin Ghobadi, “Chimeric antigen receptor T cell therapy for non-Hodgkin lymphoma”, Current Research in Translational Medicine, article in press at the time of this writing, April 2018

[5] James N. Kochenderfer, “Eradication of B-lineage cells and regression of lymphoma in a patient treated with autologous T cells genetically engineered to recognize CD19”, Blood, vol. 116, issue 20, pp. 4099-4102, 2010

[6] Renier Brentjens, Marco L Davila, Isabelle Riviere, Jae Park, “CD19-targeted T cells rapidly induce molecular remissions in adults with chemotherapy-refractory acute lymphoblastic leukemia”, Science Translational Medicine, vol. 5, issue 177, pp 177ra38, March 2013

[7] Shiqi L, “Treatment of acute lymphoblastic leukaemia with the second generation of CD19 CAR-T containing either CD28 or 4-1BB”, British Journal of Haematology, vol. 181, issue 3, April 2018

[8] Ashok D. Bandaranayake, Steven C. Almo, “Recent advances in mammalian protein production”, FEBS Letters, vol. 588, issue 2, December 2013

[9] Jee Yon Kim, Yeon-Gu Kim, Gyun Min Lee, “CHO cells in biotechnology for production of recombinant proteins: current state and further potential”, Appl. Microbiol. Biotechnol., vol. 93, issue 3, pp 917-930, February 2012

[10] Kishwar Hayat Khan, “Gene Expression in Mammalian Cells and its Applications”, Advanced Pharmaceutical Bulletin, vol. 3, issue 2, pp 257-263, 2013

[11] Tingfeng Lai, “Advances in Mammalian Cell Line Development Technologies for Recombinant Protein Production”, Pharmaceuticals, vol 6, issue 5, pp 579-603, 2013

[12] Britta Krampe, Mohamed Al-Rubeai, “Cell death in mammalian cell culture: molecular mechanisms and cell line engineering strategies”, Cytotechnology, vol. 62, issue 3, pp 175-188, June 2010

[13] Keqin Chen, “Engineering of a Mammalian Cell Line for Reduction of Lactate Formation and High Monoclonal Antibody Production”, Biotechnology and Bioengineering, vol. 72, issue 1, November 2000

[14] Victor V.T. Wong, “Enhancing Production of Recombinant Proteins from Mammalian Cells”, Molecular Engineering of Biological and Chemical Systems, January 2003

[15] D.P. Palermo, “Production of analytical quantities of recombinant proteins in Chinese hamster ovary cells using sodium butyrate to elevate gene expression”, Journal of Biotechnology, vol. 19, issue 1, pp 35-47, June 1991

[16] Robert J. Ferrante, “Histone Deacetylase Inhibition by Sodium Butyrate Chemotherapy Ameliorates the Neurodegenerative Phenotype in Huntington’s Disease Mice”, The Journal of Neuroscience, vol. 23, issue 28, pp 9418-9427, October 2003

[17] Gaurav Backliwal, “Valproic Acid: A Viable Alternative to Sodium Butyrate for Enhancing Protein Expression in Mammalian Cell Cultures”, vol. 101, issue 1, September 2008

[18] Soeren Turan, “Recombinase-Mediated Cassette Exchange (RMCE): Traditional Concepts and Current Challenges”, Journal of Molecular Biology, vol. 407, pp. 193-221, 2011

[19] Lin Zhang, ” Recombinase-Mediated Cassette Exchange (RMCE) for Monoclonal Antibody Expression in the Commercially Relevant CHOK1SV Cell Line”, Cell Culture and Tissue Engineering, September 2015

[20] Leander Blaas, “The Use of Bacterial Artifi cial Chromosomes for Recombinant Protein Production in Mammalian Cell Lines”, Methods in Molecular Biology, vol. 824, pp 581-593, November 2011

[21] P.L. Pham, “Transient Gene Expression in HEK293 Cells: Peptone Addition Posttransfection Improves Recombinant Protein Synthesis”, Biotechnology and Bioengineering, March 2005

[22] Rüdiger Heidemann, “The use of peptones as medium additives for the production of a recombinant therapeutic protein in high density perfusion cultures of mammalian cells”, vol. 32, issue 2, pp 157-167, February 2000

[23] Raphael Reuten, “Maltose-Binding Protein (MBP), a Secretion Enhancing Tag for Mammalian Protein Expression Systems”, Plos One, March 2016

[24] ShoshanaBar-Nun, “G-418, an elongation inhibitor of 80 S ribosomes”, Biochimica et Biophysica Acta (BBA) - Gene Structure and Expression, vol. 741, issue 1, pp 123-127, October 1983

[25] Julian Davies, “A New Selective Agent for Eukaryotic Cloning Vectors”, The American Society of Tropical Medicine and Hygiene, vol. 29, issue 5, pp 1089-1092, September 1980

STATUTORY DECLARATION

I declare that I have authored this thesis independently, that I have not used other than the declared sources / resources, and that I have explicitly marked all material which has been quoted either literally or by content from the used sources.

Vienna, May 2018

Dominik Brunner

EIDESSTATTLICHE ERKLÄRUNG

Ich erkläre an Eides statt, dass ich die vorliegende Arbeit selbstständig verfasst, andere als die angegebenen Quellen/Hilfsmittel nicht benutzt, und die den benutzten Quellen wörtlich und inhaltlich entnommene Stellen als solche kenntlich gemacht habe.

Wien, Mai 2018

Dominik Brunner